

University of Mississippi

eGrove

Electronic Theses and Dissertations

Graduate School

2015

Novel Delivery Systems For Iron Replenishment

Naresh Modepalli

University of Mississippi

Follow this and additional works at: <https://egrove.olemiss.edu/etd>



Part of the [Pharmacy and Pharmaceutical Sciences Commons](#)

Recommended Citation

Modepalli, Naresh, "Novel Delivery Systems For Iron Replenishment" (2015). *Electronic Theses and Dissertations*. 732.

<https://egrove.olemiss.edu/etd/732>

This Dissertation is brought to you for free and open access by the Graduate School at eGrove. It has been accepted for inclusion in Electronic Theses and Dissertations by an authorized administrator of eGrove. For more information, please contact egrove@olemiss.edu.

NOVEL DELIVERY SYSTEMS FOR IRON REPLENISHMENT

A Dissertation
presented in partial fulfillment of requirements
for the degree of Doctor of Philosophy
in the Department of Pharmaceutics and Drug Delivery
The University of Mississippi

by

NARESH MODEPALLI

April 2015

Copyright © 2015 NareshModepalli
ALL RIGHTS RESERVED

ABSTRACT

Iron is an integral part of hemoglobin and essential for the production of red blood cells. Iron deficiency and the resulting anemia are major nutritional deficiency disorders. The majority of patient populations suffering from iron deficiency anemia (IDA) are women of child bearing age and children of all ages. Iron deficiency is a complication of various other chronic conditions.

Oral iron salts or colloidal parenteral iron formulations are treatment options for iron replenishment since several decades, but they are associated with severe side effects along with other patient noncompliance issues. Transdermal delivery of iron could be a potential alternative to treat iron deficiency due to safety and offers more acceptability. Since conventional iron formulations are not suitable for transdermal delivery, quest for an ideal iron compound resulted in identification of soluble Ferric Pyrophosphate (FPP), which was demonstrated to be very stable and safe for parenteral administration.

Passive delivery of FPP was not successful due to its high molecular weight (~745 Da) and low lipid solubility. Transdermal delivery of FPP using chemical permeation enhancers, iontophoresis, microneedle pretreatment and combination of these techniques were evaluated and proved to be successful in delivering iron across the skin. When iontophoresis was combined with microneedle pretreatment, adequate iron could be delivered in anemic rat models to reverse the iron deficiency. Further, a safe and patient friendly iron delivery system was developed by incorporating FPP in soluble microneedles. *In vitro* and *in vivo* studies were carried out to

evaluate the FPP release and dermal kinetic profile of the iron from the soluble microneedles. Safety and toxicity of FPP in human skin cell lines was also investigated.

The feasibility of transdermal delivery of Iron-dextran was also evaluated. Passive delivery of iron dextran is impossible due to its high molecular weight. Microneedle assisted delivery of iron dextran was investigated and soluble microneedle system with iron dextran was developed.

Overall, the results of the project suggest that transdermal delivery of iron could be a potential alternate to treat IDA. Iron replenishment via transdermal route is likely to be more effective and safer than the conventional routes of administration.

DEDICATION

To my parents, family and lovely wife

LIST OF ABBREVIATIONS AND SYMBOLS

ID	Iron deficiency
IDA	Iron deficiency anemia
FPP	Ferric pyrophosphate
Hb	Hemoglobin
Hct	Hematocrit
MCV	Mean corpuscular volume
MCH	Mean corpuscular hemoglobin
MCHC	Mean corpuscular hemoglobin concentration
RDWc	Red blood cell width
SI	Serum iron
TIBC	Total iron binding capacity
%TS	% transferrin saturation
TBARS	Thiobarbituric acid reactive substances
MDA	Malondialdehyde
IBD	Inflammatory bowel syndrome
CKD	Chronic kidney disease
HPMC	Hydroxypropyl methyl cellulose
TEWL	Transepidermal water loss
ESAs	Erythropoietin stimulating agents

ACKNOWLEDGEMENTS

I would like to express my special appreciation and sincere gratitude to my advisor Dr. S. Narasimha Murthy for his countless hours of reflecting, reading, encouraging, and most of all patience throughout the entire process. I would like to thank him for all the support in my research that allowed me to grow as a research scientist. His advice on both research as well as on my career have been priceless.

I am also immensely grateful to my thesis committee members, Dr. Michael A. Repka, Dr. Bonnie Avery and Dr. Samir Ross, who were more than generous with their expertise and precious time and letting my defense be an enjoyable moment with their brilliant suggestions.

I take this opportunity to express gratitude to Dr. Seongbong Jo, Dr. SoumyajitMajumdar, Dr. Christy M Wyandt and Dr. Walter G Chambliss for sharing their expertise and the encouragement extended to me. My special thanks go to Ms. Deborah King for her assistance with administrative activities.

I would like to show appreciation to Dr. Murthy's group past and present members, especially Dr. Siva Ram KiranVaka and Dr. Srinivasa Murthy Sammeta for providing support and guidance in my early days at OleMiss. I also thank my friends and fellow students in the department of pharmaceuticals and in the school of pharmacy for the unceasing encouragement, and support. I would also like to thank all the friends I made at Oxford and my dearest friends ChinniYalamanchili and Rambabu Sankranti for their support all the time.

I wish to express my sincere thanks to Dr. Mohammad K Ashfaq (NCNPR), Dr. Mika B Jekabsons and Dr. Lainy Day (Department of Biology), Dr. John H O'Haver(Department of

Chemical Engineering) and Dr. James V Cizdziel (Department of Chemistry & Biochemistry) for providing access to use their research facilities for my projects. I am grateful to Dr. Ryan F Donnelly (Queen's University Belfast, UK) for soluble microneedles and Dr. Valerie Jones (Ray Biotech, Atlanta, GA) for her support with cytokine assays.

I owe my sincere thanks to Dr. Vijaysankar Raman, Dr. Vamsi Manda, Dr. Radha Krishnan SVS and Mr. RajanishSahu (NCNPR) for their help and contribution to my research projects.

A special thanks to my family. Words cannot express how grateful I am to my family and especially my parents for all of their sacrifices that they have made on my behalf. At the end I would like to express appreciation to my beloved wife Sowjanya, who has been always my support, even in the events of hardship.

In conclusion, I recognize that this research would not have been possible without the financial assistance of Eunice Kennedy Shriver National Institute of Child Health & Human development (NICHD)-Grant # HD061531A, Core-NPN Fellowship and Graduate Student Council Grants.

TABLE OF CONTENTS

ABSTRACT.....	ii
DEDICATION.....	iv
LIST OF ABBREVIATIONS.....	v
ACKNOWLEDGEMENTS.....	vi
LIST OF TABLES.....	x
LIST OF FIGURES.....	xi
CHAPTER 1: INTRODUCTION.....	1
CHAPTER 2: TRANSDERMAL DELIVERY OF IRON-APPLICATION OF PASSIVE AND ACTIVE TECHNIQUES.....	9
INTRODUCTION.....	9
MATERIALS AND METHODS.....	12
RESULTS AND DISCUSSION.....	16
CONCLUSIONS.....	23
CHAPTER 3: MICROPORATION AND 'IRON'TOPHORESIS FOR TREATING IRON DEFICIENCY ANEMIA IN ANEMIC RAT MODEL.....	24
INTRODUCTION.....	25
MATERIALS AND METHODS.....	25
RESULTS AND DISCUSSION.....	31
CONCLUSIONS.....	41

CHAPTER 4: SOLUBLE MICRONEEDLE SYSTEM FOR DELIVERY OF FPP.....	42
INTRODUCTION.....	42
MATERIALS AND METHODS.....	43
RESULTS AND DISCUSSION.....	50
CONCLUSIONS.....	71
CHAPTER 5: MINIMALLY INVASIVE METHOD FOR DELIVERY OF IRON-DEXTRAN VIA TRANSDERMAL ROUTE.....	73
INTRODUCTION.....	74
MATERIALS AND METHODS.....	76
RESULTS AND DISCUSSION.....	85
CONCLUSIONS.....	101
BIBLIOGRAPHY	102
VITA.....	121

LIST OF TABLES

- 1-1. List of oral iron preparations available for clinical use along with their elemental iron content.....6
- 1-2. List of parenteral iron formulations with molecular weight.....8
- 3-1. Observed mean hematological and biochemical parameters in rats at healthy state (prior to iron free diet plan) and at anemic condition.....34
- 3-2. The mean hematologic and biochemical parameters observed at the end of treatment period in rats administered with FPP via different modes of administration.....39
- 4-1. The mean weights of FPP polymer matrix loaded into microneedle molds initially, after drying for 48 hours and final average weight of array after sidewalls removed. The values represented are the average of $n=30 \pm S.D.$50
- 5-1. The mean values of hematological parameters, prior to inducing anemia (healthy), after inducing anemia, after treating with iron dextran in case of microneedle pretreatment and after treating with iron dextran via intraperitoneal route.....92
- 5-2. The mean biochemical parameters measured at different time points. Iron dextran soluble microneedle array (430 μg of iron) was inserted into the rat abdominal skin for 12 hours and blood sample were collected till 24 hours. The values represented are the average of $n= 3 \pm S.D.$95

LIST OF FIGURES

- 1-1. Molecular structure of heme.....3
- 2-1. Transverse section showing different layers of skin and the major drug transport pathways via skin10
- 2-2. Structure of Ferric Pyrophosphate.....12
- 2-3. The cumulative amount of FPP permeated across porcine epidermis in presence of various chemical permeation enhancers. The data points represented are the average of $n= 6 \pm S.D.$17
- 2-4. The cumulative amount of FPP permeated across porcine epidermis after pretreatment with various chemical permeation enhancers. The data points represented are the average of $n= 6 \pm S.D.$18
- 2-5. The cumulative amount of FPP permeated across rat skin with various chemical permeation enhancers along with iontophoresis(IN) (0.3 mA/cm^2). The data points represented are the average of $n= 6 \pm S.D.$20
- 2-6. The cumulative amount of FPP permeated across rat skin in case of passive (◆), iontophoresis (IN) (■), microneedle pretreatment (MN) (▲) and combination of microneedle pretreatment with iontophoresis (MN+IN) (●). Permeation studies were carried out for 6 hours. The data points represented are the average of $n= 6 \pm S.D.$22
- 3-1. VetScan HM2 Hematology system.....28

- 3-2.Histological section of skin treated with microneedles and stained with hematoxylin and eosin stain shown at 10x magnification. The epidermis and dermal layers were shown clearly in this picture.....32
- 3-3.The *In vivo* TEWL measurements after microporation at different time points. The unfilled bar (□) represents the TEWL of intact skin before microporation. The data points represented are the average of $n= 6 \pm S.D$33
- 3-4. Representative pictures of morphology of RBCs (a) RBCs in healthy rats (b) RBCs of anemic rats (Microcytic and hypochromic RBC shown with ↑marks) (c) RBCs in group 3 administered with FPP by iontophoresis (IN) (d) RBCs in rats administered with FPP following microneedle (MN) pretreatment(group 4) (e) RBCs of the rats administered with FPP using combination of iontophoresis and microneedle pretreatment (MN+IN) (group 5) and (f) RBCsof rats received FPP through IP injection (group 6)..... 40
- 4-1.Images of FPP soluble microneedles (a) Microneedle array on the investigators finger. [Pictures were taken using Nikon Digital Camera (Nikon Inc., NY)] (b) SEM images of FPP soluble microneedle arrays containing 121 microneedles (18X magnification) (b) microneedles array visualized at 90X magnification.....51
- 4-2. SEM Images of FPP soluble microneedle arrays (a) Microneedles before insertion into the skin (b) Microneedles inserted into the rat skin and removed at 1 hour time point (c) Microneedles inserted into the rat skin and removed after 3 hours. Arrows indicate the position of individual microneedles.....52

- 4-3. The Cumulative amount of FPP permeated across rat skin from soluble microneedles containing ~5.2 mg of FPP (◆) and ~9.3 mg of FPP (■). The data points represented are the average of $n=3 \pm S.D.$53
- 4-4. Image showing *in vivo* cutaneous microdialysis on the abdominal part of the hairless rat after application of soluble microneedle array.....54
- 4-5. The time course of free FPP in the dermal interstitial fluid following the application of soluble microneedles loaded with (A) ~5.2 mg of FPP and (B) ~9.3 mg of FPP. The data points represented are the average of $n= 4 \pm S.D.$55
- 4-6. Iron disposition and expected pathways of iron disappearance from the skin. Most of the iron from soluble microneedles was rapidly cleared as free iron into the systemic circulation to bind transferrin in other metabolic pools and some iron might be bound to transferrin in interstitial fluid. About one-third of transferrin bound iron in interstitial pool was entering into skin cells. From the literature, interstitial fluid in the skin acts as an exchange pool for iron between the skin cells and other metabolic pools.....59
- 4-7. The mitochondrial activity (MTS activity) of (A) HEK and (B) HDF cells after 24 h exposure to 100 μ l of FPP (250-7.8 mg/ml) and digitonin [D] (60 μ g/ml-1.87 μ g/ml). Results are combined from three independent exposures and expressed as mean ($\pm S.D.$).....61
- 4-8. Standard calibration curve for 2', 7'-dichlorodihydrofluorescein (DCF) assay in HEK and HDF media.....63

- 4-9. Induction of reactive oxygen species (ROS) by FPP (250-7.8 mg/ml) or hydrogen peroxide (HP) in (A) HEK and (B) HDF cells after 24 hours exposure. Results are combined from three independent exposures and expressed as mean (\pm S.D.).....64
- 4-10. Scheme of DCF assay.....65
- 4-11. An overview of the amount of cytokines detected in HEK and HDF cell line after treating them with FPP at different concentrations (31.2-250 mg/ml), H₂O₂ (1000 μ M) and digitonin (30 μ g/ml). Results are combined from three independent exposures and expressed as mean (\pm S.D.).....67
- 4-12. Presence of cytokines in (A) HEK and (B) HDF cells after 24 h exposure to 100 μ l of FPP (31.25-250 mg/ml) and hydrogen peroxide (1000 μ M) and digitonin (30 μ g/ml). Results are combined from three independent exposures and expressed as mean (\pm S.D.).....68
- 4-13.Descriptive image to show the floor map of standard glass slide uses in Quantibody[®] array along with the detection mechanism of cytokines (With kind permission from RayBiotech, Atlanta, GA).....69
- 4-14.Experimental procedure (work flow) with Quantibody[®] array for detection of cytokines.....70
- 5-1. *In vitro* permeation studies of Iron dextran across the (■) intact hairless rat skin (control) and (▲) skin pretreated with microneedles.....87
- 5-2.The mean values of all biochemical parameters, prior to inducing anemia (Normal), after inducing anemia (Anemic), after treating with iron dextran (microneedle pretreatment (ID-MN)) and treatment with intraperitoneal injection of iron dextran (ID-IP).....90

- 5-3. Representative pictures of morphology of RBCs (a) RBCs in healthy rats (b) RBCs of anemic rats (arrow marks point the microcytic and hypochromic RBC) (c) RBCs of rats treated with iron dextran following microneedle pretreatment and (d) RBC of rats received iron dextran through intraperitoneal injection.....92
- 5-4. SEM images of iron dextran soluble microneedle arrays. (a) microneedles array containing 121 microneedles (18X magnification) (b) microneedles array visualized at 75X magnification.....93
- 5-5. The cumulative amount of iron dextran permeated across rat skin from soluble microneedles with ~260 µg of iron (◆) and with ~ 430 µg of iron (■). The data points represented are the average of $n= 6 \pm S.D.$94
- 5-6. The mitochondrial activity (MTS activity) of (A) HEK and (B) HDF cells after 24 h exposure to 100 µl of iron dextran (10-0.31 mg/ml) and digitonin (60 µg/ml-1.87 µg/ml). Results are combined from three independent exposures and expressed as mean (\pm S.D.).....97
- 5-7. Induction of reactive oxygen species (ROS) by iron dextran (10-0.31 mg/ml) or hydrogen peroxide in (A) HEK and (B) HDF cells after 24 h exposure. Results are combined from three independent exposures and expressed as mean (\pm S.D.).....98
- 5-8. An overview of the amount of cytokines detected in HEK and HDF cell line after treating them with iron dextran at different concentrations (1.25-10 mg/ml), H₂O₂ (1000 µM) and digitonin (30 µg/ml). Results are combined from three independent exposures and expressed as mean (\pm S.D.).....99

- 5-9. Presence of cytokines in (A) HEK and (B) HDF cells after 24 h exposure to 100 μ l of iron dextran (1.25-10 mg/ml) and hydrogen peroxide (1000 μ M) and digitonin (30 μ g/ml). Results are combined from three independent exposures and expressed as mean (\pm S.D.).....100

CHAPTER 1

INTRODUCTION

1.1. Brief history and role of iron in early life

Iron is a ubiquitous transition metal and is the fourth most abundant element present in the earth's crust. Life on earth started about 3.5 billion years ago in a relatively oxygen-free atmosphere on the mineral surfaces, such as iron pyrites (FeS_2) [1-3]. Nearly three billion years ago, abundant soluble ferrous iron was available for early life forms, before the introduction of oxygen in the atmosphere by cyanobacteria via photosynthesis. In the next ~1.5 billion years, the atmospheric oxygen content increased to approximately 21 % which became toxic to organisms that were not adapted to oxygen environment. This increase in oxygen resulted in a great enhancement in the metabolic efficiency (~18 folds) of oxygen-adapted organisms compared to anaerobic fermentation. The increased oceanic oxygen oxidized soluble ferrous iron to virtually insoluble ferric iron form. This enormous transformation in the atmospheric oxygen and its oxidization of ferrous iron made all oxygen respiratory organisms to struggle for acquiring and storing this valuable metal, iron [1].

1.2. Iron- precious metal for survival

Iron can be considered as the most valuable metal for life on Earth. The typical adult human body contains an average of 3.5 g of iron (approximately 4 g for males and 3 g for females). Iron is found in the human body in two forms, as functional iron (iron that serves a metabolic function) and as storage iron. Iron homeostasis in the system is closely regulated via intestinal absorption from diet and by recycling of iron from the senescence of aged red blood

cells. There is no physiologic mechanism for iron excretion from the body. Only 1 mg of iron is lost per day by males and 2 mg by menstruating females (through blood and mucosal epithelial cell loss) [4].

Iron is an essential trace element for cell growth and is the key nutrition element required for all living organisms [5]. Iron is an integral part of heme and hemoglobin (figure 1-1) and functions as carrier of oxygen from lungs to tissues. Iron is also present in myoglobin (an intracellular store of oxygen), in the cytochrome enzymes of the mitochondrial electron transport chain and in cytochrome P-450, which is involved in the metabolism of drugs and other foreign materials [6].

Iron can readily accept or donate electrons and this capacity to participate readily in redox reactions makes, iron a valuable player as catalyst in various biological processes which participates in oxidation and reduction reactions. Iron is also present in catalase and peroxidase, which prevents free radical-mediated cell damage; and in a number of other enzymes involved in energy metabolism, such as reduced nicotinamide adenine dinucleotidephosphate dehydrogenase. Iron participates in the biosynthesis of DNA and RNA [7] and it is a constituent of a number of important macromolecules, including those involved in respiration, oxidative phosphorylation, and xenobiotic metabolism. Iron helps in the production of connective tissues and neurotransmitters in brain and useful for neural development [8, 9]. Excess iron accumulation in the system is harmful and causes organ dysfunction through the production of reactive oxygen species (ROS).

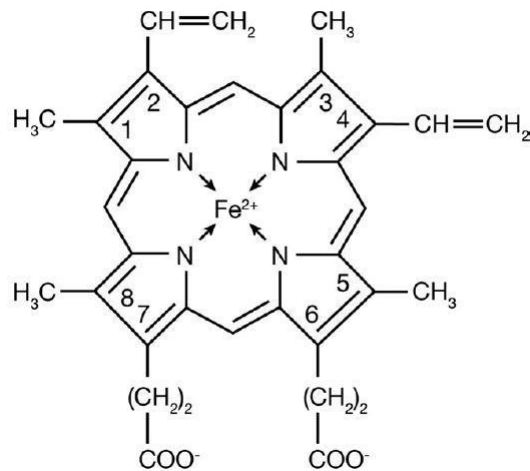


Figure 1-1. Molecular structure of heme

1.3. Iron deficiency and anemia

Iron deficiency (ID) develops when body iron (functional iron) is not adequate to meet the physiological needs for growth and development. As the iron depletion progresses, iron stores in the system will also get affected and the hemoglobin concentration in red blood cells falls below the normal range which is referred as iron deficiency anemia (IDA). Iron deficiency can exist with or without anemia [10, 11]. Iron deficiency anemia is caused by dietary deprivation and/or poor absorption of iron or may occur due to chronic blood loss. Iron deficiency is one of the most prevalent and serious health issues among people all over the world. Iron deficiency anemia is the major contributing factor among all other anemia disorders. An estimated 2 billion people are suffering from iron deficiency and IDA worldwide with the majority from developing countries [12, 13 &14]. IDA can affect the length and quality of life in patients and can increase morbidity and mortality.

IDA is the most common prevalent nutritional deficiency disease among children especially in premature or low birth weight babies and in menstruating, pregnant and lactating women. IDA is associated with growth retardation and cognitive development in children. IDA, if

uncorrected leads to psycho neurological problems in children of all ages and diminished work productivity and behavioral problems in adults [15, 16]. Patients with IDA have a higher risk of psychiatric disorders, including unipolar depressive disorder, anxiety disorder, attention hyperactivity disorder, delayed development and mental retardation [17]. Iron is essential for normal development of the immune system and IDA can be aggravated by presence of infectious diseases and vice versa [18, 19 & 20].

Menstruating women lose ~1–2.5 mg of iron per day on an average through menstrual blood loss and a loss of 1-ml blood would translate to a loss of 0.5 mg of iron. The demand for iron increases several folds in pregnant women to meet the requirements of red blood cell mass expansion and unidirectional transfer of iron from mother to developing fetus [21, 22]. The WHO estimates that 39% of children younger than 5 years, 48% of children between 5 and 14 years, 42% of all women, and 52% of pregnant women in developing countries are anemic with half of them having iron deficiency anemia [22]. According to the WHO, the frequency of iron deficiency in developing countries is about 2.5 times that of anemia [23].

1.4. IDA and comorbidities

Iron deficiency is a complication of other chronic conditions like renal failure, chronic kidney disease (CKD), inflammatory bowel disease (IBD), Parkinson's disease and rheumatoid disease. Iron deficiency is a common problem in patients with end stage renal disease (ESRD), particularly in those treated by dialysis, because of impairment in gastrointestinal absorption, ongoing blood losses and sometimes due to an impaired capacity to mobilize iron from its stores. The anemia associated with end-stage renal disease is corrected with recombinant human erythropoietin and administration of erythropoietin leads to rapid utilization of iron for erythropoiesis. Therefore most dialysis patients require iron supplementation in order to maintain

responsiveness to erythropoietin stimulating agents (ESAs) [24]. Parenteral iron therapy is the only option so far for these patients to sustain adequate treatment with erythropoietin-stimulating agents[25]. Prevalence of IDA in patients with IBD ranged from 9% to 74% [26] and in patients suffering with Crohn's disease the IDA prevalence ranged from 6% to 74% [27].

Iron deficiency coincided with sympathetic activation, left ventricular hypertrophy, dilatation, compromised hemodynamics and symptomatic heart failure [28, 29, 30 & 31]. A large meta-analysis of major heart failure trials has shown that the prevalence of anemia was around 37% in all patients with heart failure [32]. Approximately 20% of patients with colon cancer experience gastrointestinal bleeding, eventually leading to cause iron deficiency anemia (IDA) [33]. A recent study by Gupta *et al* showed that iron deficiency anemia might be a factor for the co-morbidity of migraine and restless leg syndrome [34]. Iron deficiency anemia is also common in patients with menstrual migraine [35].

1.5. Iron for therapeutic purposes

The use of iron for therapeutic purposes has been in practice from ancient times. Ancient Greeks used iron salts in the diet to treat muscular weakness in wounded warriors [36]. Nicholas Monarde, a 16th century physician used iron for a large number of unrelated ailments including gout, acne and alopecia [37]. In the second half of the seventeenth century, Thomas Sydenham, suggested iron as a treatment option for chlorosis in young woman, which they used to refer as a "hysterical disease" or Virgin's disease [38].

1.6. Treatment Options for Iron deficiency anemia

Hydrophilic oral iron salts or colloidal parenteral iron complexes are the treatment options for body iron replenishment since several decades. The existing treatment with oral and

parenteral iron formulations is associated with severe side effects along with various other patient noncompliance issues.

1.7. Oral iron therapy

Oral iron formulations are the choice of first line therapy to replenish body iron stores. Oral iron salts that are widely used in clinical practice are listed in table 1. All iron salts differ in their elemental iron content and the usual treatment regimen with oral iron salts ranges from three to six months.

Formulation	%Elemental Iron(w/w)
Carbonyl Iron(U.S Only)	100
Ferric Ammonium citrate	18
Ferrous bisglycinate (U.S Only)	20
Ferrous fumarate	33
Ferrous gluconate	12
Ferrous sulfate	20
Ferrous sulfate, dried	30
Heme-iron polypeptide	100
Polysaccharide-iron complex	100

Table 1-1. List of oral iron preparations available for clinical use along with their elemental iron content.

Iron is absorbed mostly from the proximal part of the small intestine and only a fraction of the total oral dose is bioavailable due to the carrier mediated absorption mechanism. Moreover, bioavailability of iron from oral administration is regulated by the total iron stores in the body [39]. Until most of the iron stores are exhausted, iron absorption from gut is not increased. Although oral iron therapy is convenient, gastric intolerance and poor adherence of the oral therapy due to unpleasant taste and odor of iron salts are the common disadvantages associated with it [40]. An increase in the dose of oral iron in an effort to increase absorption will

only result in increased gastrointestinal toxicity. Moreover, oral iron supplements have limitations in IDA treatment in case of chronic intestinal bleeding, hemodialysis, malabsorption syndrome, Crohn's disease, inflammatory bowel disease, and chronic bowel obstruction. The most common side effects with iron salts include heartburn, nausea and vomiting, upper gastric discomfort, diarrhea, and constipation. Gastrointestinal symptoms related to oral iron therapy range in frequency from 15% to 40% depending on dose and other factors [41, 42].

Oral iron salts are generally ineffective in the immediate post-surgical settings due to post-surgical inflammation in the gastrointestinal system. Oral salts should be preferably taken on an empty stomach or between meals to facilitate absorption, but epigastric pain is a common complaint among patients if iron is administered in the fasted state. For such patients, it was advised to take oral iron salts along with the meal, but absorption get dampens with food [43]. Oral iron absorption reduces by phytates and other foods rich in polyphenols which form large insoluble complexes with iron salts. Hepcidin, a hepatic peptide hormone play a huge role in regulating the absorption of iron from the gastrointestinal tract and any hepcidin related disorders have indirect effect on iron absorption from the intestine.

1.8. Parenteral iron therapy

Due to limitations and side effects associated with oral delivery, parenteral administration of iron is often preferred or inevitable in some cases. Soluble iron salts used in oral therapy are not suitable for parenteral delivery due to liberation of free iron which in turn leads to lipid peroxidation and oxidative stress. A few heavy iron colloid complexes are in use for parenteral delivery but they are not well tolerated among various patient groups. Parenteral iron formulations that are approved for parenteral therapy are summarized here in table 1-2.

	Type I	Type II	Type III	Type IV
Example	Ferric carboxymaltose Iron dextran Ferumoxytol	Iron sucrose	Sodium ferric gluconate Iron(III)-citrate Iron(III)-sorbitol	Iron(III)-citrate+iron(III)-sorbitol+iron dextrin Sodium ferric gluconate+iron sucrose
Characteristics	Robust Strong	Semi-robust Moderately strong	Labile Weak	Mixtures containing at least two different iron complexes
Molecular weight(Daltons)	>100,000	30,000-100,000	<50,000	<50,000

Table 1-2. List of parenteral iron formulations with molecular weights.
(*Modified from Geisser *et al.* *Pharmaceutics* 2011, 3, 12-33)

Usually, intravenous bolus iron injection is indicated in patients with intestinal malabsorption and they are also considered to be superior to replenish large quantities of iron where the ongoing iron losses exceed the absorptive capacity of oral iron. Intravenous bolus iron therapy is also associated with significant side effects like hypotension, arthralgias, and severe allergies and may cause anaphylactic reactions in case of iron overload [44]. Therefore, intravenous infusions are preferred over frequent bolus injections. However, intravenous infusion is invasive and associated with high treatment cost. Parenteral iron therapy is usually recommended only in severe anemic conditions due to its invasiveness and systemic side effects due to colloidal nature of the parenteral iron products. Moreover, the iron overload with parenteral formulations was reported to cause anaphylactic reactions and rarely even mortality [45, 46]. The colloidal iron is processed by reticuloendothelial system (RES) to liberate iron which binds to transferrin eventually and delivered to bone marrow for erythropoiesis [47, 48].

CHAPTER 2

TRANSDERMAL DELIVERY OF IRON-APPLICATION OF PASSIVE AND ACTIVE TECHNIQUES

2.1. INTRODUCTION

2.1.1. Skin and drug delivery pathways in the skin

Skin is the largest organ of the body and plays a vital role as a defense system to protect the body from external assaults and prevents evaporation of moisture from the body to the external environment [49]. Skin is composed of three main layers; epidermis, dermis and hypodermis (subcutaneous adipose tissues) [figure 2-1]. Each layer in the skin is known to represent different levels of cellular or epidermal differentiation and the barrier function of the skin reflects through its multilayered structure.

The top or uppermost layer of the skin, known as the stratum corneum is the rate limiting barrier for passive delivery of drugs [50]. The stratum corneum is comprised of dead cells (corneocytes) dispersed within a lipid rich matrix. The closely packed keratinocytes as well as the intercellular lipid bilayers in the stratum corneum offer resistance for permeation of polar drugs. Moderately lipophilic drugs are relatively more permeable than extremely hydrophilic and extremely lipophilic molecules. Moreover, the molecular weight of the drugs should be <500 Da to be permeable across the skin. When the drug possesses all these properties, it would be ideal for transdermal delivery provided the dose required is not impractical. In general, drug molecules that are in contact with the skin surface can penetrate by three potential pathways: through the lipids in the stratum corneum (intercellular pathway), through both the lipids and the

keratinocytes-directly across stratum corneum (transcellular pathway), through the sweat ducts, via the hair follicles and sebaceous glands (The shunt or transappendageal route) [51].

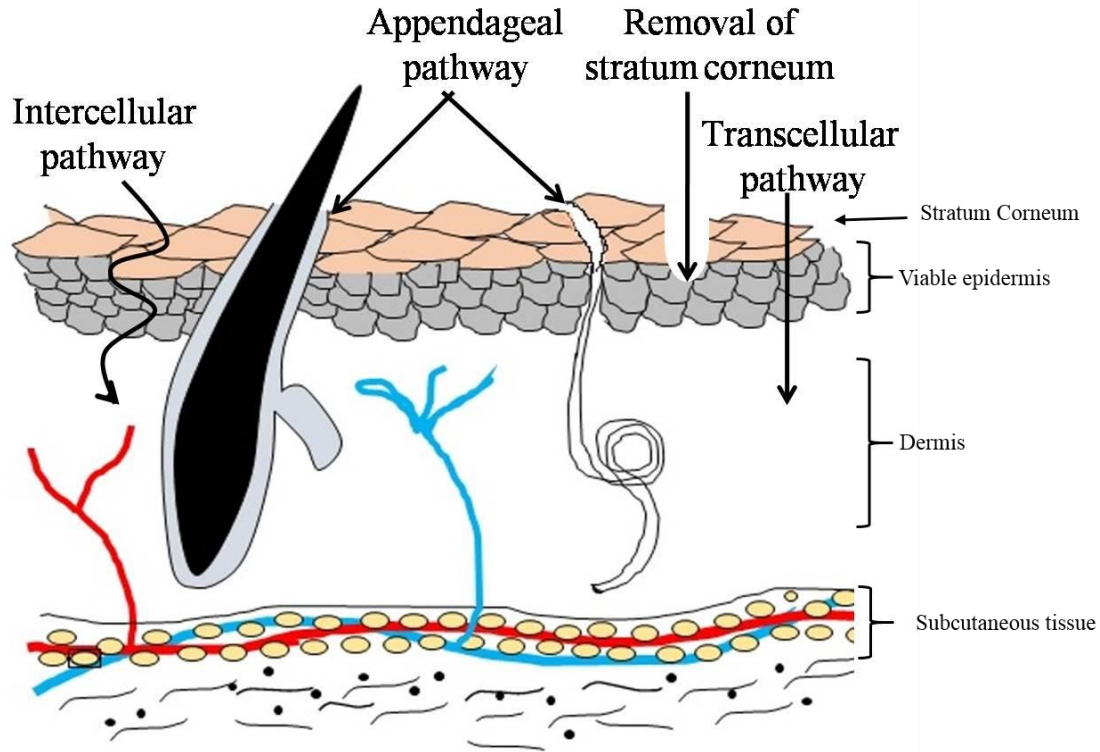


Figure 2-1. Transverse section showing different layers of skin and the major drug transport pathways via skin.

2.1.2 Need for transdermal iron delivery

Delivering therapeutically adequate amounts of iron to treat iron deficiency anemia (IDA) still remains a challenge due to the adverse effects associated with oral and parenteral iron preparations especially in children and pregnant women. Therefore, there is an indispensable need for the development of an alternative and safe mode of administration of iron products. Transdermal delivery of iron could be a potential method of treating iron deficiency due to safety and patient compliance that this route could offer. Transdermal delivery of iron would be

attractive to patients due to the fact that transdermal route could overcome the potential gastric and systemic side effects associated with oral and parenteral formulations respectively. The plausibility of slow and controlled delivery of iron across the skin is possible with transdermal delivery. Slow and prolonged delivery of iron has been reported to be relatively safer than rapid infusion and bolus injections of iron as the former would reduce the likeliness of oversaturation of transferrin [52, 53]. Transdermal delivery allows administration of drugs over long durations simulating slow intravenous infusion. In case of transdermal iron delivery, the choice of iron salts is challenging because all the iron salts used in oral iron therapy are hydrophilic in nature and the products approved for parenteral therapy are huge in size due to their colloidal nature. Not all iron salts could be administered parenterally and, not suitable to transdermal delivery, as there is risk of potential oxidative stress due to free radical formation.

2.1.3 Ferric Pyrophosphate

Therefore, to develop a successful transdermal therapeutic system of iron, there is a need to identify low molecular weight iron compounds, which are safe. In a recent study by Gupta *et al.*, Ferric pyrophosphate (FPP) demonstrated superior safety in maintenance hemodialysis patients without any evidence of toxicity and proved to support erythropoiesis and maintain hemoglobin levels [54]. FPP is a combination of ferric form of iron and pyrophosphate salt and has a high stability constant ($\log K_{stab} 22.3$). Due to this high stability, FPP does not dissociate and liberate free iron in the physiological fluids unlike other soluble salts [55]. Iron derived from FPP was proved to be taken up directly and rapidly by circulating apo-transferrin within minutes of exposure [56]. Moreover, FPP can trigger the direct transfer of iron between transferrin and ferritin and transferrin [55, 57]. In addition, pyrophosphate was also proved to be a potent antioxidant [58]. From all these scientific evidences from Gupta *et al.* and others, FPP was

thought to be a suitable candidate for transdermal delivery for iron replenishment therapy. In the current project, the possibility of delivering soluble FPP via transdermal route was explored using various passive and active techniques.

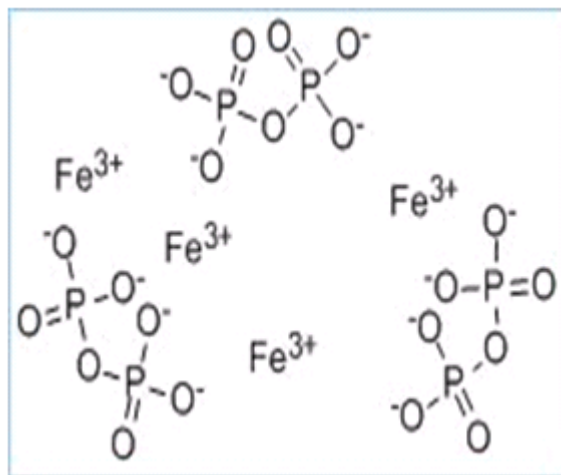


Figure 2-2. Structure of Ferric Pyrophosphate

2.2. MATERIALS AND METHODS

2.2.1. Chemicals

Soluble Ferric pyrophosphate was obtained from Sigma-Aldrich Inc (St. Louis, MO). Phosphate buffered saline (PBS, pH 7.4) premixed powder was obtained from EMD Chemicals (Gibbstown, NJ). Ferrover® iron was purchased from Hach Company (Loveland, OH). All other chemicals and solvents used were of pure grade obtained from Fischer scientific (Fairway, NJ).

2.2.2. Preparation of rat skin/porcine epidermis

FPP permeation studies were carried out using both rat skin and porcine epidermis. For the preparation of rat skin, the animals [Male hairless rats (Charles River, Wilmington, MA, USA)] were asphyxiated with CO₂ and the abdominal skin was excised, subcutaneous fat was removed and the obtained skin pieces were cleaned carefully with normal saline. The rat skin

was used either on the same day or stored at -20 °C for further use. The animal studies were approved by the Institutional Animal Care and Use Committee (IACUC) at the University of Mississippi (Protocol # 10-013). Porcine full thickness skin was obtained from a local abattoir and epidermis was peeled off from full thickness skin after heat treatment at 60 °C for 2 minutes.

2.2.3. General experimental set up

Vertical Franz diffusion cell (PermeGear Inc., Hellertown, PA) set up was used to investigate the permeation of FPP across rat skin or porcine epidermis. The tissue (either rat skin or porcine epidermis) was sandwiched between the donor and receiver compartment of Franz diffusion cell in such a way that dermal side of tissue was in contact with receiver compartment and stratum corneum was facing the donor compartment of the cell. The active diffusion area was 0.64 cm². Electrical resistance across the tissue was used to check the integrity of the barrier. For this set up, Ag/AgCl wires (Alfa-Aesar, Ward hill, MA) made in the form of circular rings and arranged at a distance of 2 mm from the tissue in both donor and receiver compartment. The donor and receiver compartments were filled with 0.5 ml and 5 ml of PBS having a pH of 7.4 and allowed to equilibrate for one hour. The AC electrical resistance of the skin (R_s) was measured by placing a load resistor R_L (100 k Ω) in series with the tissue as reported previously [59]. The voltage drop across the whole circuit (V_0) and across the skin (V_s) was measured using an electrical set up consisting of a wave form generator and a digital multimeter (Agilent Technologies, Santa Clara, CA). Skin resistance was measured by applying a voltage of 100 mV at 10 Hz in the electric setup. Tissues maintaining a resistance of ≥ 20 k Ω /cm² were only considered for permeation studies.

2.2.4. *In vitro* permeation studies

2.2.4.1. Passive permeation

After measuring electrical resistance of the tissue, the PBS in the donor compartment of the Franz diffusion cell was replaced with 0.5 ml of FPP aqueous solution (50 mg/ml, pH-5) and receiver compartment was filled with 5 ml of PBS adjusted to pH-5 using 1 N hydrochloric acid. During *in vitro* permeation studies, the temperature of receiver compartment was maintained at $37\pm 1^{\circ}\text{C}$ by water circulation. Permeation studies were carried out for 6 hours when rat skin was used and all porcine epidermis permeation studies were carried out for 24 hours. One ml of sample was withdrawn from receiver compartment at every hour time point and replaced with fresh buffer solution. The amount of FPP permeated was analyzed using Ferrover® iron reagent, using Lambda EZ201 UV spectrophotometer (Perkin Elmer, Waltham, MA) at 510 nm.

2.2.4.2. Passive permeation studies across porcine epidermis using chemical permeation enhancers

Various transdermal chemical permeation enhancers (CPEs) belongs to different chemical classification such as sulfoxides, fatty acids, fatty acid esters, amides and surfactants were selected in order to study the effect of enhancer on permeation of FPP, *in vitro*. The following chemical permeation enhancers at given concentrations were used for the study; 10 % v/v dimethyl sulfoxide, 1% w/v N-vinyl 2- pyrrolidone, 10 % v/v Transcutol, 20 % v/v Transcutol, 20 % v/v polyethylene glycol (PEG) 400, 20% v/v- Tween 80, 20% v/v Tween 20, 10% w/v urea, 20 % v/v (SLS), cetyltrimethylammonium bromide (CTAB) 20% v/v, 10% v/v isopropyl myristate (IPM) and 20% w/v sodium laurylsulfate (SLS). In few other experiments the following combination of enhancers was also used; Transcutol 25 % v/v + propylene glycol 25 % v/v, Transcutol 10% v/v + propylene glycol 40% v/v. The effect of pretreatment with some chemical permeation enhancers on the permeation FPP was also

investigated. Pretreatment was carried out for 30 minutes and the following enhancers were selected for the study; 1-phenyl piperazine (ashort chain azone), 10 % v/v oleic acid in propylene glycol, 10 % v/v oleic acid, 5 % v/v linoleic acid. After pretreatment with enhancer or combination of enhancers, 0.5 ml of FPP (50 mg/ml) was loaded into the donor chamber and permeation studies were carried out for 24 hours. Samples were withdrawnat regular intervals of time for a period of 24 h from thereceiver compartment and the iron content was measuredat 510 nm by adding Ferrover® iron reagent usingUV spectrophotometer.

2.2.4.3. Iontophoretic delivery

Cathodal iontophoresis was carried out using Phoresor® iontophoresis unit (Iomed, Salt Lake City, UT) at 0.3 mA/cm² for 6 hours across rat skin. When porcine epidermis was used, cathodal iontophoresis was carried out using Phoresor® iontophoresis unit at 0.3 mA/cm² for 24 hours. The electrodes made up of Ag/AgCl were connected with the lead clips from Phoresor® Unit. Donor chamber was filled with 0.5 ml of FPP aqueous solution and receiver with PBS adjusted to pH-5 using 1 N hydrochloric acid. One ml samples were collected at each hour interval and analyzed for FPP.

2.2.4.4. Passive permeation studies across porcine epidermis using chemical permeation enhancers+ iontophoresis

Few selected permeation enhancers that resulted in positive enhancement of FPP in earlier studies were used along with iontophoresis to investigate the effect of combining both the approaches. Cathodal iontophoresis was applied using Phoresor® iontophoresis unit at 0.3 mA/cm² for 24 hours. The electrodes made up of Ag/AgCl were connected with the lead clips from Phoresor® unit. Donor chamber was filled with 0.5 ml of FPP aqueous solution containing enhancer and receiver with PBS adjusted to pH-5 using 1 N hydrochloric acid. One ml samples were collected at each hour interval and analyzed for FPP.

2.2.4.5. Permeation studies after pretreatment with microneedles across rat skin

The rat skin was pretreated with microneedles [AdminPen 600 stainless steel microneedles (nanoBioScience LLC, Alameda, CA)] for 2 minutes. The microporated skin was mounted carefully on Franz diffusion cell and continued with either passive permeation studies or iontophoretic mediated delivery (0.3 mA/cm^2) as described in passive permeation and iontophoretic delivery sections respectively. Microneedles were inserted into the skin with the thumb, each time with uniform force by same individual to avoid variability in the depth of skin penetration.

2.3. RESULTS & DISCUSSION

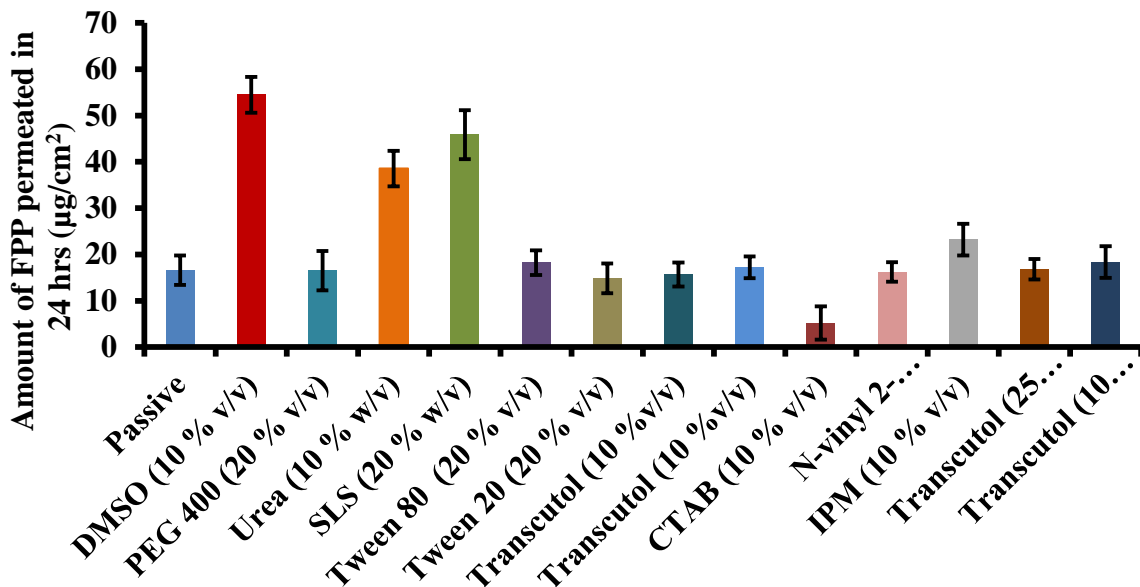
2.3.1. Passive delivery of Iron compounds across skin

Passive delivery of FPP was not successful due to poor permeation properties of FPP because of its high molecular weight ($\sim 745 \text{ Da}$) and low lipid solubility. The amount of FPP delivered across rat skin after 6 hours was only $6.53 \pm 0.45 \mu\text{g/cm}^2$. Even after 24 hours, the amount of FPP delivered across porcine epidermis was only $16.6 \pm 3.16 \mu\text{g/cm}^2$.

2.3.2. Chemical permeation enhancers

For successful delivery of FPP, the effect of chemical permeation enhancers was evaluated in this study. Chemical permeation enhancers act in many different ways; by increasing drug solubility or by disrupting the lipid bilayers in the stratum corneum or by enhancing partitioning of drugs in different layers of the skin and by keratin denaturation [60-63]. Among the permeation enhancers tested, only 10 % v/v DMSO, 10 % w/v urea and 20 % w/v SLS resulted in significant improvement in passive delivery of FPP compared to the control. DMSO at 10 % v/v concentration enhanced the total amount of FPP permeated by ~ 3 folds compared to passive permeation and there was ~ 2.5 fold enhancement in permeation with 10 % w/v urea and ~ 3 fold enhancements in permeation with 20 % w/v SLS.

DMSO was reported to be effective transdermal enhancer and acts by enhancing the diffusion coefficient of drugs by disrupting the lipid bilayer and partitioning of the drug in the skin [64, 65]. Urea might be promoting transdermal permeation by facilitating hydration of the stratum corneum and by the formation of hydrophilic diffusion channels within the stratum corneum barrier by disruption of the lipid packing [66,67]. SLS is an anionic surfactant and it was proved to increase the drug permeation across skin by disrupting the lipid bilayers and by increasing the partition of drug in various layers. SLS was proved to increase the *in vitro* permeation rates of several drugs including naproxen[68] and naloxone [69]. Non-ionic surfactants like Tween 20 and Tween 80 are ineffective for permeation enhancement of FPP. The results of transdermal permeation of FPP with all chemical permeation enhancers and combinations of enhancers are shown in figure 2-3.



Passive, DMSO (10 % w/v), PEG 400 (20 % v/v), Urea (10%w/v), SLS (20% w/v)tween 80 (20% v/v), Tween 20 (20% v/v), Transcutol (10 %v/v and 20 % v/v), CTAB (10 % v/v), N-vinyl-pyrrolidone (1% w/v), IPM (10%v/v), Trancutol (25% v/v)+ Propylene glycol, Trancutol (10% v/v)+ Propylene glycol.

Figure 2-3. The cumulative amount of FPP permeated across porcine epidermis in presence of various chemical permeation enhancers. The data points represented are the average of $n=6 \pm S.D.$

In case of skin pretreatment with chemical permeation enhancers, 10 % oleic acid in propylene glycol resulted in ~2 fold enhancement in the total amount of FPP permeated across porcine epidermis in 24 hours. The other enhancers were not effective and the results are shown in figure 2-4.

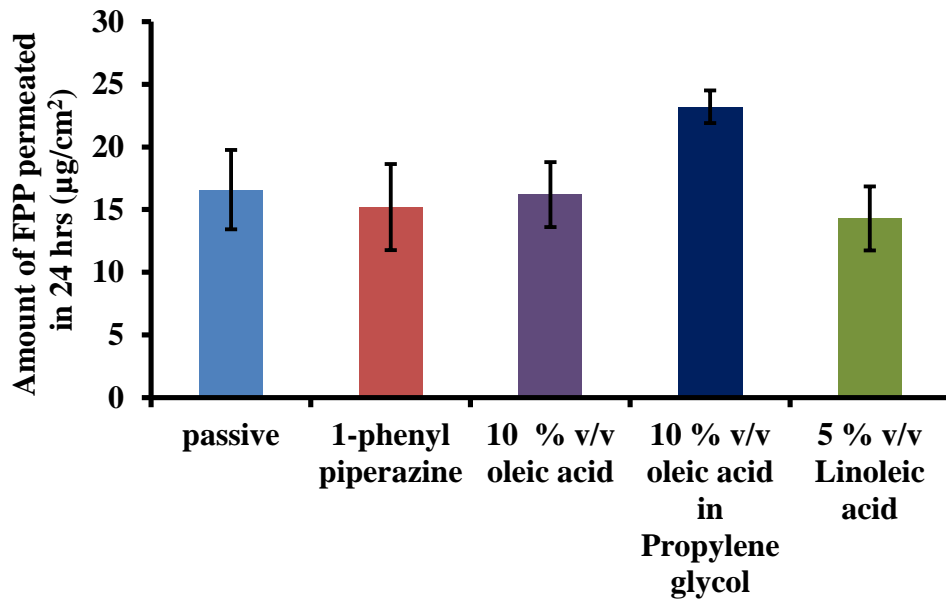


Figure 2-4. The cumulative amount of FPP permeated across porcine epidermis after pretreatment with various chemical permeation enhancers. The data points represented are the average of $n=6 \pm S.D.$

Oleic acid enhancing activity was found to be dependent on the use of a co-solvent, such as propylene glycol, which usually acted synergistically [70,71]. Oleic acid is a monounsaturated fatty acid, exists as heterogeneously dispersed fluid domain in the stratum corneum and enhances the permeation of active by improving diffusion and partition of the drug by fluidization of stratum corneum lipids [72].

2.3.3. Iontophoresis

Iontophoresis is a safe and effective technique to enhance the delivery of drugs across the skin. Iontophoresis utilizes low density electric current and enhances transdermal drug transport via direct electrophoresis, electroosmosis, or by lipid bilayer disordering [73, 74]. The appendageal pathway is the predominant pathway for enhancement of drug delivery by iontophoresis. Iontophoresis can provide programmable delivery of drug across the skin by altering current strength or duration [75].

The *in vitro* flux of FPP with iontophoresis (IN) application after 6 hours was 8.04 ± 0.24 $\mu\text{g}/\text{cm}^2/\text{h}$ which was ~8 fold enhancement compared to the passive flux of FPP across the rat skin. In another study with the use of porcine epidermis there was a ~10 fold enhancement in the permeation flux of FPP with iontophoresis compared to passive delivery. Transdermal iontophoresis was proved to be a useful technique to enhance the delivery of FPP for the treatment of anemia.

2.3.4. Permeation enhancers + Iontophoretic delivery

Combination of several penetration enhancers with iontophoresis has been reported by several authors in the past [76-78]. Greater amounts of drug could be delivered when permeation enhancers were combined with iontophoresis than either technique alone. In the present study, the chemical permeation enhancers that were proved to be effective in enhancing the passive FPP delivery were chosen for iontophoretic delivery of FPP. The results are shown in figure 2-5. When DMSO combined with iontophoresis there was a slight improvement in the amount of FPP delivered, which was not significant compared with iontophoresis alone. In case of iontophoresis + urea (10 % w/v) and iontophoresis + SLS (20 % w/v) combinations, there was no significant difference between the amount of FPP delivered when compared with iontophoresis alone.

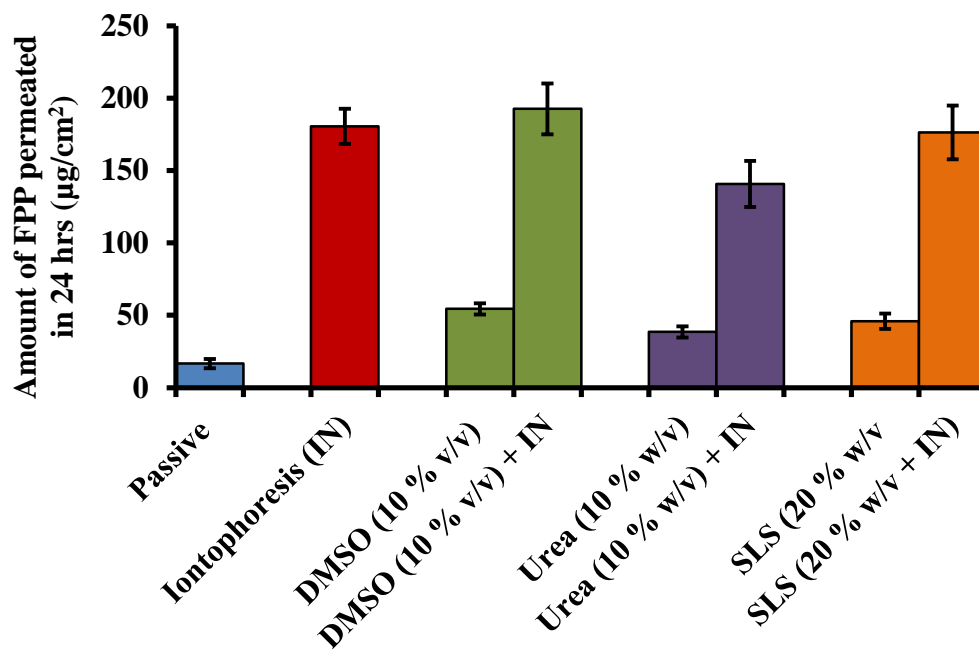


Figure 2-5. The cumulative amount of FPP permeated across rat skin with various chemical permeation enhancers along with iontophoresis(IN) (0.3 mA/cm^2). The data points represented are the average of $n= 6 \pm \text{S.D.}$

2.3.5. Microneedle pretreatment (MN)

Rat skin was pretreated with solid microneedles for 2 minutes and FPP delivery studies were carried out for 6 hours. The *in vitro* flux of FPP after microneedle (MN) pretreatment was $12.36 \pm 0.16 \text{ µg/cm}^2/\text{h}$ which was ~11 fold compared to the passive flux of FPP.

From the above results, it was confirmed that creation of micropores in the skin can improve permeation of FPP across skin. However, microneedle pretreatment alone did not lead to a significant increase (to meet therapeutic requirements in severe anemic cases) in the iron delivery which is likely because of the closing of micropores by physical barrier(property of skin) over a period of time. Here, to make the best use of micropores formed with microneedle pretreatment, two approaches were followed.

Approach I. Transport FPP through micropores created due to microneedle pretreatment.

Approach II. Deliver FPP using soluble microneedles which stay in the pores over prolonged duration without allowing them to close rapidly.

For this purpose, we initially tried approach 1 by combining the iontophoresis(driving force)along with microneedle pretreatment to drive FPP across microperated skin.

2.3.6. Microneedle pretreatment (MN) + Iontophoresis (IN)

In case of the combination of microneedle pretreatment along with cathodal iontophoresis (MN+IN), there was ~44 fold enhancement in the flux ($51.24 \pm 7.55 \mu\text{g}/\text{cm}^2/\text{h}$) over passive permeation in 6 hours. In a separate set of studies, *in vitro* permeation studies of FPP from hydroxyl propyl methyl cellulose(HPMC) gel across rat skin were performed with MN+IN treatment and the resulting flux was almost the same ($\sim 50.45 \pm 5.62 \mu\text{g}/\text{cm}^2/\text{h}$) as with FPP solution. Successful transdermal delivery of certain hydrophilic compounds and high molecular weight peptide drugs using combination of microneedle pretreatment with iontophoresis has been demonstrated by various groups in the past [79,80].

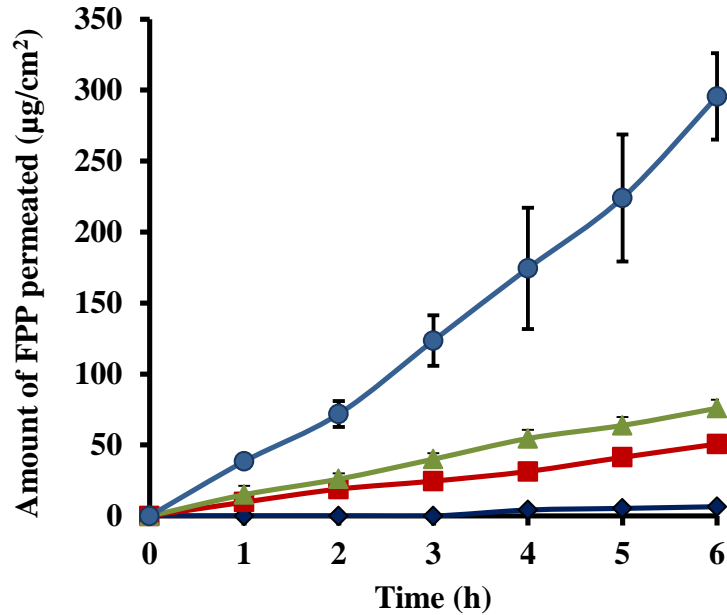


Figure2-6. The cumulative amount of FPP permeated across rat skin in case of passive (◆), iontophoresis (IN) (■), microneedle pretreatment (MN) (▲) and combination of microneedle pretreatment with iontophoresis (MN+IN) (●). Permeation studies were carried out for 6 hours. The data points represented are the average of $n=6 \pm S.D.$

2.4. SUMMARY

From all the *in vitro* permeation experiments of FPP, when iontophoresis applied across porcine epidermis there was ~10 folds enhancement in the permeation flux after 24 hours compared to passive delivery. Among all the permeation enhancers tested only 10 % v/v DMSO, 10 % w/v urea and 20 % w/v SLS showed significant improvement in the permeation compared to passive delivery. When these enhancers combined with iontophoresis there was no significant improvement in the permeation compared to iontophoretic delivery alone. The Passive flux of FPP across hairless rat skin after 6 hours was $1.16 \pm 0.16 \mu\text{g}/\text{cm}^2/\text{h}$. After IN treatment alone there was ~8 folds enhancement in permeation flux compared to passive delivery and after microneedle (MN) pretreatment alone there was ~11 folds enhancement compared to passive flux. Whereas, when iontophoresis was combined with microneedle pretreatment there was ~ 44 folds enhancement in the flux compared with passive permeation and iontophoreis in

combination with microneedle pretreatment was proved to be the most effective technique for transdermal delivery of iron.

2.5. CONCLUSIONS

The results of the study suggest that FPP can be delivered via transdermal route using passive (permeation enhancers) and active techniques (iontophoresis, microneedle pretreatment and iontophoresis in combination with microneedle pretreatment). Even though, the amount of iron delivered was low using chemical permeation enhancers, with iontophoresis alone and with microneedle pretreatment alone; these techniques can find applications in transdermal delivery of iron to treat mild to moderate anemia in patient who cannot tolerate oral iron formulations (especially pregnant women and children). Moreover, these techniques will be of great advantage in terms of non-invasiveness and safety compared to parenteral iron formulations. Successful development of transdermal iron delivery system with the above enhancement techniques will be very useful in patients who are on maintenance therapy for iron deficiency anemia.

CHAPTER 3

MICROPORATION AND 'IRON'TOPHORESIS FOR TREATING IRON DEFICIENCY ANEMIA IN ANEMIC RAT MODEL

ABSTRACT

Purpose: Iontophoretic mediated transdermal delivery of ferric pyrophosphate (FPP) in combination with microneedle pretreatment was investigated as a potential treatment option for iron deficiency anemia (IDA).

Methods: *In vivo* pharmacodynamics studies were performed in hairless anemic rat model. The hematological and biochemical parameters like hemoglobin, hematocrit, mean corpuscular volume and % serum transferrin were monitored in rats at healthy, anemic condition and post treatment conditions. Micropores created by the microneedles were visualized in histological skin sections after staining them with hemotoxylin and eosin. The recovery of micropores was investigated *in vivo* by measuring Transepidermal water loss (TEWL) at different time points.

Results: The passive, microneedle pretreatment and iontophoresis mediated delivery did not lead to significant improvement in hematological and biochemical parameters in anemic rats, when used individually. When iontophoresis (0.15 mA/cm² for 4 hours) was combined with microneedle pretreatment (for 2 minutes), therapeutically adequate amount of FPP was delivered and there was significant recovery in hematological and biochemical parameters in rats indicating this treatment will be effective in treating IDA.

Conclusions: Microneedles pretreatment and iontophoresis mediated delivery of iron via transdermal route could be developed as a potential treatment for IDA. The transdermal controlled delivery of iron could become a potential, safe and effective alternative to parenteral iron therapy.

3.1. INTRODUCTION

Transdermal delivery of iron to treat iron deficiency anemia in anemic animal models was investigated. From our earlier *in vitro* studies, it was evident that iontophoresis, microneedle pretreatment alone and combination of microneedle pretreatment and iontophoresis were able to deliver significant amount of FPP across the skin. In the present study, our aim was to investigate the delivery of iron across skin in anemic animal models using these active techniques to treat iron deficiency anemia. *In vivo* pharmacodynamic studies were carried out to measure various hematologic and biochemical parameters in rats at healthy, anemic and treated conditions. Red blood cell morphology studies were also carried out to show the efficacy of the treatments.

3.2. MATERIALS AND METHODS

3.2.1. Chemicals

Soluble Ferric pyrophosphate was obtained from Sigma-Aldrich Inc (St. Louis, MO). Phosphate buffered saline (PBS, pH 7.4) premixed powder was obtained from EMD Chemicals (Gibbstown, NJ). Hydroxypropyl methyl cellulose (Methocel® E15 premium LV) was obtained from Dow chemical company (Midland, MI). Ferrover® iron was purchased from Hach Chemical Company (Loveland, OH). Serum iron & TIBC kit was procured from Clinia Corporation (San Marcos, CA). Lipid peroxidation assay kit (OXI-TEK TBARS assay) was obtained from Enzo

Life Sciences (Farmingdale, NY). All other chemicals and solvents used were of pure grade obtained from Fischer scientific (Fairway, NJ).

3.2.2. Experimental animals and preparation of skin

Male hairless rats (Charles River, Wilmington, MA, USA) were used *for in vivo* studies. All the animal studies were approved by the Institutional Animal Care and Use Committee (IACUC) at the University of Mississippi (Protocol # 10-013). All the animals were of eight weeks old and weighing between 250-300 g at the time of arrival. The animals were housed in conventional cages and 12 hour day/light cycles were maintained in the facility.

3.2.3. Preparation of hydroxypropyl methyl cellulose (HPMC) gel incorporated with FPP

FPP solution was prepared by dissolving 50 mg of soluble FPP in 1 ml of distilled water and pH was adjusted to 5 using 1 N hydrochloric acid (HCl). HPMC (4% w/v) gel was prepared according to the standard protocol given by the polymer manufacturer; briefly by mixing the hot polymeric aqueous solution to the cold solution of FPP to give a final concentration of 50 mg/ml of FPP in the gel.

3.2.4. Microneedles

AdminPen 600 stainless steel microneedles(nanoBioScience LLC.Alameda, CA) having an area of 1cm²and containing 187 microneedles with a needle height of 500 µm were used in all *ex vivo* and *in vivo* studies.

3.2.5. Visualization of micropores

The depth of penetration of microneedles was visualized by staining the histological section of the microneedle pretreated skin with hematoxylin and eosin. Briefly, freshly excised skin was microporated with the microneedles for 2 minutes. Small skin samples with micropores were fixed in optimum cutting temperature (OCT) medium (Tissue-Tek®) and frozen in dry ice

bath and sectioned at 50 µm on a Leica 1800 cryostat. The obtained skin specimens were stained with hematoxylin and eosin and observed under high resolution light microscope (Axiolab, A1, Carl Zeiss, USA) at 10X magnification to visualize depth of penetration of microneedles into different layers of skin. Images were captured using a Carl Zeiss camera attached to the microscope.

3.2.6. *In vivo* studies

In vivo experimental studies were carried out in hairless rats. The rats were acclimated to vivarium conditions for one week with regular standard diet. Blood samples were drawn from all animals by retro-orbital bleeding and analyzed for hematological and biochemical parameters. Initially 200 µl of blood samples were collected in EDTA (ethylenediaminetetraacetic acid) coated Microvette® tubes (Sarstedt, Newton, NC) and 0.5 ml of blood was collected into 1.5 ml centrifuge tubes (Eppendorf, Hauppauge, NY) from all animals. The blood sample collected into EDTA tubes were analyzed for the hematologic parameters like hemoglobin (Hb), red blood cell (RBC) count, hematocrit (Hct), mean corpuscular volume (MCV), mean corpuscular hemoglobin (MCH), mean corpuscular hemoglobin concentration (MCHC) and red blood cell distribution width (RDWc) using VetScan HM2 hematology system (Abaxis Inc., Union city, CA) (figure 3-1).

Serum was separated from the blood samples collected into centrifuge tubes after centrifugation at 3000 rpm for 10 minutes and analyzed for biochemical parameters. The serum iron, total iron binding capacity of serum and % transferrin saturation (%TS) was calculated using serum iron & TIBC kit (Cliniqa Corporation, San Marcos, CA). Serum lipid peroxidation values were calculated using OXI-TEK TBARS assay kit (Enzo Life Sciences Inc., Farmingdale, NY). The base line values for all of these parameters in the healthy animals were recorded.



Figure 3-1. VetScan HM2 Hematology system (Curtsey: Abaxis Inc., Union city, CA)

3.2.6.1. Induction of iron deficiency anemia

Rats were fed custom made purified low iron diet having iron concentration as low as 2-6 ppm (Harlan laboratories, Madison, WI) till the end of study period. The composition of the diet was in accordance with AIN-76A guidelines with all vitamin and mineral mix except cellulose and iron in it. Rats were allowed free access to this diet and water all the time. The degree of iron deficiency was monitored by measuring the hematologic parameters (hemoglobin and hematocrit) from collected blood samples every week, for 5 weeks. Induction of iron deficiency anemia was confirmed after five weeks by measuring all hematologic parameters and biochemical parameters.

3.2.6.2. *In vivo* delivery of FPP

FPP treatment was initiated, after confirming that the rats were anemic. Rats were divided randomly into the following 6 groups (n=6) and FPP was administered to animals in different groups as described below. All the *in vivo* transdermal studies were carried out on

alternative days for 4 hours under ketamine (80 mg/kg) and xylazine (10mg/kg) anesthesia administered intraperitoneally. Transdermal patch having an area of 10 cm² was applied in all the groups except group 6 as specified below. FPP was administered transdermally for 4 weeks in groups 2, 3, 4 & 5. Group 6 animals were administered with FPP intraperitoneally.

Group 1: Placebo group

A placebo patch (HPMC gel patch with no FPP incorporated) was placed on the rats for 4 hours.

Group 2: FPP-Passive group

In case of passive delivery, a patch containing FPP-HPMC gel (500 mg) was applied on the back of rat. No current was applied and the FPP was allowed to permeate passively.

Group 3: Iontophoresis group (IN)

For iontophoretic delivery, a custom made iontophoretic patch was prepared using an adhesive 3M™ foam tape (3M Drug Delivery Systems, St. Paul, MN) fitted with a snap type Ag/AgCl electrode. FPP-HPMC gel was loaded on to the patch and secured on the back of the rat's body and cathodal iontophoresis was applied at a current strength of 0.15 mA/cm².

Group 4: Microneedle group (MN)

Rats were pretreated with microneedles for 2 minutes using 1 cm² array over a total area of 10 cm². Precautions were taken to avoid overlapping of microporation by marking the already pretreated areas. FPP gel patch was applied immediately after pretreatment and permeation studies were carried out.

Group 5: Microneedle + iontophoresis (MN+IN) group

In the MN + IN group, rats were pretreated with microneedles for 2 minutes and cathodal iontophoresis was applied as described above after applying a custom made iontophoretic patch.

Group 6: Intraperitoneal (IP) group

FPP was dissolved in normal saline to get a concentration of 10 mg/ml. Rats were administered with 0.11 ml of this solution via intraperitoneal route for 3 weeks. This group served a positive control for the study.

Blood samples were withdrawn intermittently and at the end of study period from all animals by retro orbital bleeding and all hematology and biochemical parameters were analyzed.

3.2.7. Recovery of micropores

In a different set of experiment, the TEWL was measured using Vapometer (Delfin Technologies, Kuopio, Finland) *in vivo* on hairless rat skin after pretreatment with microneedles to study the effect of microneedles on skin and the recovery of barrier property. The TEWL of rat skin before and after pretreatment with microneedles was measured at different time points.

3.2.8. Red blood cell Morphology

Visualization of RBC under high resolution microscopy was performed to study the morphology of RBC at healthy, anemic and treated conditions in animals from all groups. Briefly, peripheral blood smear was prepared by wedge slide method using a drop of venous blood collected from animals at healthy, anemic and treated conditions. The dried smears were stained with Wright-Giemsa stain and the red blood cells were visualized under high resolution light microscope (Axiolab A1, Carl Zeiss, USA) at 100x magnification using oil immersion technique. Images were captured using Carl Zeiss camera attached to the microscope.

3.2.9. Statistical analysis

GraphPadInStat 3 software was used for statistical analysis. Unpaired t-test was used to determine the level of significance for correlations between parameters at healthy and anemic conditions and between anemic condition and post treatment condition in all groups. A significance level of $p < 0.05$ was considered as statistically significant.

3.2. RESULTS& DISCUSSION

From the previous studies, the transdermal delivery of FPP by iontophoresis could be significantly enhanced when the stratum corneum barrier is compromised. Based on earlier observations, the present study was planned to investigate the effect of microporation on the passive and iontophoretic delivery of FPP across the skin. Both iontophoresis and microneedle treatment are active transdermal drug delivery techniques that enable drugs to permeate across the skin. Iontophoresis utilizes low density electric current to drive charged drugs across the skin. Microneedles create micropores in the stratum corneum of the skin and allow drugs to permeate into deeper layers [81]. The microneedles used in this study were able to penetrate down to an average depth of $70 \pm 10 \mu\text{m}$ into the skin. The micropores created by microneedles were visualized in the skin sections stained with hematoxylin and eosin which are shown in figure 3-2. The picture clearly indicated that the microneedles penetrated only through the upper layers of the epidermis.

From *in vitro* investigations, when microneedle pretreatment was combined with cathodal iontophoresis (MN+IN), there was ~44 fold enhancement in the permeation flux compared to passive permeation. At this flux, a cumulative dose of ~0.3 mg of FPP would be delivered in six hours. Therefore, in case of *in vivo* studies, cathodal iontophoresis was applied

using a current strength of 0.15 mA/cm^2 for 4 hours after pretreatment with microneedles on alternative days to deliver the required dose of FPP (1.1 mg of FPP $\approx 0.12 \text{ mg}$ of elemental iron).

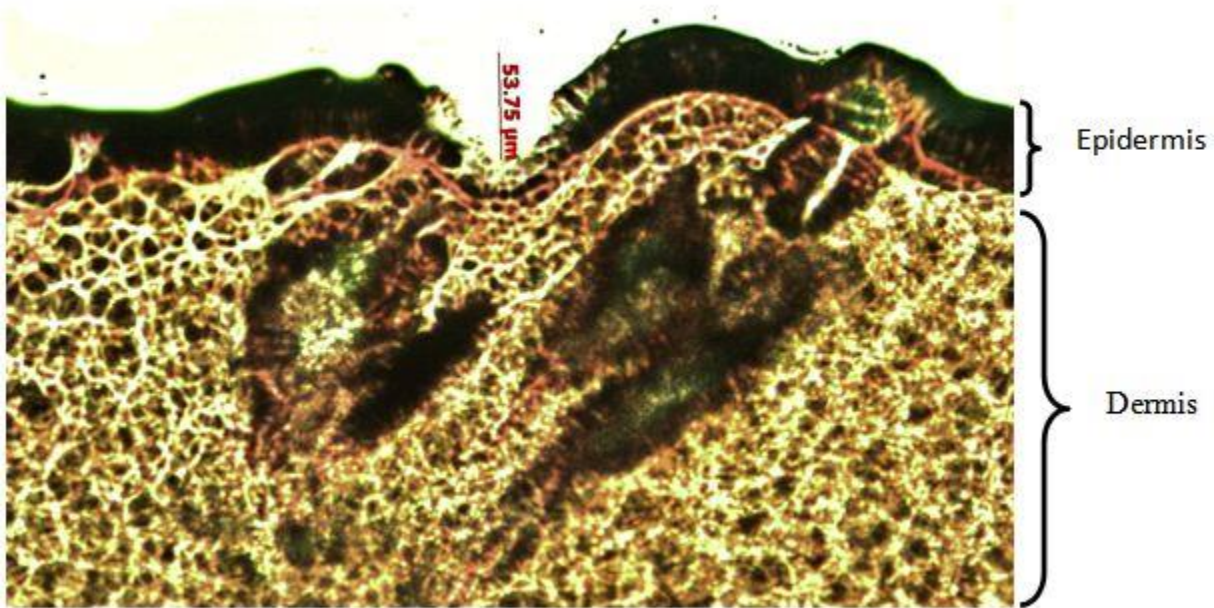


Figure 3-2. Histological section of skin treated with microneedles and stained with hematoxylin and eosin stain shown at 10x magnification. The epidermis and dermal layers were shown clearly in this picture.

3.3.1. *In vivo* studies

3.3.1.1. Recovery of micropores

The duration for the recovery of micropores created with microneedles was investigated by measuring transepidermal water loss (TEWL). Immediately following pretreatment with microneedles, there was an increase in TEWL observed from $13.6 \pm 1.42 \text{ g/m}^2 \cdot \text{h}$ to $28.75 \pm 2.68 \text{ g/m}^2 \cdot \text{h}$ owing to micropore formation. The TEWL values returned to normal ($14.1 \pm 2.22 \text{ g/m}^2 \cdot \text{h}$) within 8-12 hours (figure 3-3). This study suggests that the skin barrier remains compromised for at least 8 hours even in un-occluded condition. On the other hand, the recovery of skin barrier is almost complete within 8-12 hours after removal of the patch/device. From literature, few

earlier studies have clearly shown that the pores reseal relatively faster in case of non-occluded condition than when occluded [82, 83].

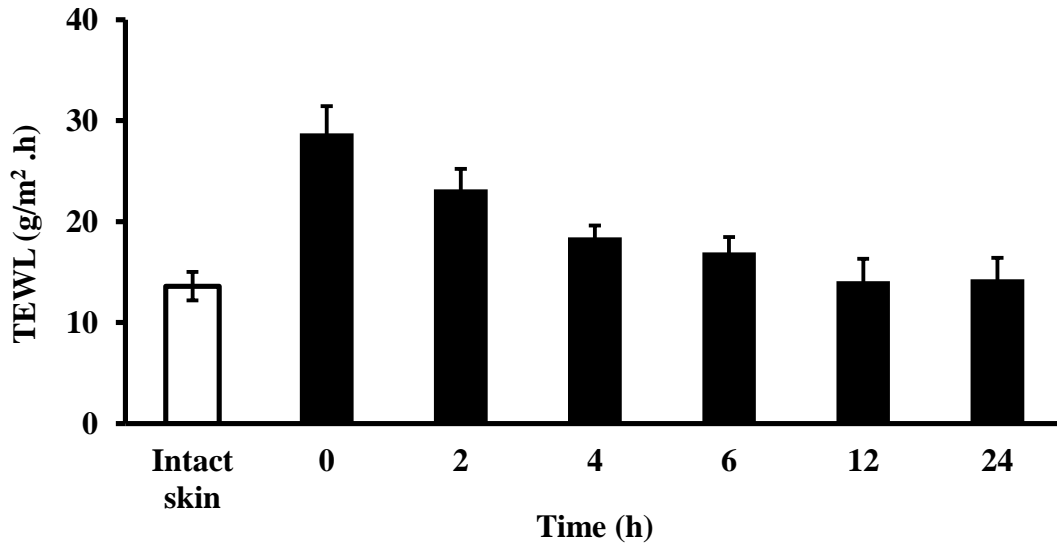


Figure 3-3. The *In vivo* TEWL measurements after microporation at different time points. The unfilled bar (\square) represents the TEWL of intact skin before microporation. The data points represented are the average of $n=6 \pm$ S.D.

3.3.1.2. Induction of anemia and diagnosis

Various conventional laboratory tests are available for successful diagnosis of iron deficiency anemia. In the present work, hematologic and biochemical parameters were assessed to confirm the induction of anemia and recovery from anemia following transdermal FPP administration. The custom made purified low iron diet contains only trace quantities of iron (~ 4 ppm). After 5 weeks on this diet, there was a significant difference in the hematological parameters in rats compared to basal healthy values indicating induction of anemia. There was decrease in hemoglobin concentration and MCV along with other red blood indices. The serum iron and % transferrin saturation were also decreased, whereas the TIBC values were increased

in anemic condition. The observed hematological parameters and biochemical parameters in healthy and anemic rats are shown in table 3-1.

Table 3-1: Observed mean hematological and biochemical parameters in rats at healthy state (prior to iron free diet plan) and at anemic condition

Parameter	Basal values	Anemic condition
<i>Hematological parameters</i>		
Hemoglobin (g/dl)	14.31 ± 2.47	10.58 ± 1.61 [†]
HCT (%)	41.35 ± 8.33	32.4 ± 3.72 [†]
MCV (fl)	56.25 ± 2.12	38 ± 2.86 ^{†††}
MCH (pg)	19.56 ± 1.57	12.4 ± 1.22 ^{†††}
MCHC (g/dl)	34.83 ± 1.61	28.22 ± 2.24 ^{††}
RBC (10 ¹² /l)	8.40 ± 0.83	6.61 ± 0.75 [†]
RDWc (%)	16.71 ± 2.22	28.33 ± 2.73 ^{†††}
<i>Biochemical parameters</i>		
Serum Iron (µg/dl)	179.53 ± 15.84	83.46 ± 17.02 ^{†††}
TIBC ((µg/dl)	374.86 ± 56.33	483.84 ± 57.91 [†]
% TS	46.28 ± 7.04	16.59 ± 2.11 ^{††}
Lipid peroxidation [equivalent to MDA conc (nmol/ml)]	8.58 ± 1.72	14.51 ± 3.92 [†]

*The difference in all parameters in rats between healthy (basal values) and anemic conditions is statistically significant.

[†]p<0.05

^{††}p<0.001

^{†††}p<0.0001

Measurement of hemoglobin concentration and hematocrit are considered to be most appropriate indicators of IDA. Even the most common definitions of anemia by WHO and CDC are based on the levels of hemoglobin present in the blood. The mean basal hemoglobin value of the rats at healthy state was 14.31 ± 2.47 g/dl and decreased to 10.58 ± 1.61 g/dl ($p = 0.01$) at

anemic condition and the mean % hematocrit value was decreased from 41.35 ± 8.33 % at healthy state to 32.4 ± 3.72 % ($p = 0.03$) at anemic condition. A decrease in hemoglobin level implies the decrease in amount of functional iron circulating in the blood. Hematocrit indicates the proportion of whole blood occupied by the red blood cells and depends on the hemoglobin concentration in red blood cells [84]. MCV is the average volume of a single red blood cell and it serves as an important diagnostic tool in the differential diagnosis of anemia. Anemia is classified as macrocytic (increased MCV), normocytic (normal MCV) or microcytic (decreased MCV) on the basis of MCV. Iron deficiency is usually associated with microcytic anemia and decrease in MCV value is one of the specific indicators for iron-deficiency anemia [84]. The MCV values were also decreased after feeding rats with low iron diet and there was a difference in mean MCV about 14.15 ± 0.74 fl from healthy to anemic state.

Red blood cells play a crucial role in the support of tissue metabolism and enough RBCs must be available to maintain tissue oxygenation and sustain a normal acid-base balance in the system [5]. There was a reduction in mean RBC count from $8.4 \pm 0.83 \times 10^{12}/l$ (healthy state) to $6.61 \pm 0.75 \times 10^{12}/l$ ($p = 0.002$) (anemic condition). MCH and MCHC values indicate the average amount and concentration of hemoglobin in red blood cells. MCHC is also an important parameter that indicates the cellular hydration status and the values usually decrease in IDA (hypochromia). There was a 7.16 ± 0.35 pg difference in the mean MCH and 6.61 ± 0.6 g/dl in the mean MCHC between healthy and anemic conditions in rats. The RDWc measures the variation in red blood cell size and the mean values at healthy condition were $16.71 \pm 2.22\%$, which were increased to 28.33 ± 2.73 % at anemic condition ($p < 0.0001$), might be due to the production of increased number of smaller RBCs (under developed) due to iron deficiency. The increase in RDWc along with decrease in MCV is a precise diagnostic characteristic of iron

deficiency anemia [85]. In this study a peripheral smear with microcytic and hypochromic erythrocytes shown in figure 3-4b clearly confirms the presence of anemia in rats.

Among the biochemical parameters, the serum iron concentration values decreased from $179.53 \pm 15.84 \mu\text{g/dl}$ to $83.46 \pm 17.02 \mu\text{g/dl}$ ($p < 0.0001$) and TIBC values increased from $374.86 \pm 56.33 \mu\text{g/dl}$ to $483.84 \pm 57.91 \mu\text{g/dl}$ ($p = 0.008$) after feeding the rats with custom made low iron diet. Serum iron concentration is a measure of the total amount of iron in the serum bound to transferrin. Transferrin is an iron transport protein, which carries iron to the bone marrow. Iron readily bounds to unsaturated transferrin in the system. Measurement of serum iron concentration alone might not be a useful indicator in the diagnosis of IDA because of its low sensitivity. Moreover, many factors could affect the serum iron concentration such as a meal, presence of infections or inflammations and existence of diurnal variations. TIBC measures the total amount of iron needed to saturate serum transferrin. %TS is a ratio of serum iron concentration and TIBC. TIBC and transferrin saturation (% TS) reflects the extent of vacant iron-binding sites on transferrin. In the present experiment, the mean %TS value in rats at healthy state was 46.28 ± 7.04 , which were decreased to 16.59 ± 2.11 ($p < 0.001$) in anemic condition.

Oxidative stress arises due to an imbalance between the formation and neutralization of pro-oxidants which in turn leads to lipid peroxidation. Previously some researchers reported higher lipid peroxide levels in anemic condition and, there are some conflicting reports as well which showed lower or unchanged lipid peroxide levels in anemic condition [86-89]. In the present study, the lipid peroxide level in anemic and treated animals were determined using an *in vitro* diagnostic kit, which measures the increase in thiobarbituric acid reactive substances (TBARS) which is an indicator of oxidative stress. In this test TBARS are expressed in terms of

malondialdehyde (MDA) equivalents and the mean concentration of MDA in blood was 8.58 ± 1.72 nmol/ml at healthy condition. There was a significant increase ($p=0.0068$) in MDA concentration to 14.51 ± 3.92 nmol/ml at anemic condition, which agrees with reports that explain the generation of lipid peroxides in case of IDA.

According to numerous scientific reports, various physiological mechanisms might be responsible for the development of oxidative stress and lipid peroxidation in anemic animal models [90-92]. The main reason for this observation was speculated to be due to accumulation of free copper in liver cells or increase in the triglycerides concentration and increased fragility of mitochondrial membranes [89, 93]. Balagopalakrishna *et al*[94] and Nagababu *et al*[95] demonstrated that the increase in oxidative stress of RBC might be due to decrease in the oxygenation of hemoglobin and resultant increase in auto-oxidation of hemoglobin, which further causes the generation of methemoglobin and superoxides.

3.3.1.3. Transdermal delivery of FPP *in vivo*

The anemic rats were segregated into different groups based on the mode of delivery and the FPP was administered for four weeks. The hemoglobin and hematocrit were measured intermittently during the treatment to assess the improvement in hematological parameters. There was no significant improvement in the hematologic parameters in case of placebo group and passive treatment groups (group 1 and 2 respectively). Rats in both of these groups had rather turned more anemic likely because of negligible iron supplementation. Inevitably, the treatment was terminated after two weeks in case of group 1 and 2. *In vitro*, cathodal iontophoresis and microneedles alone were found to enhance the delivery of FPP considerably. However, *in vivo*, there was no significant improvement in hematologic parameters (Table 3-2) or morphology of

RBC in iontophoresis alone and microneedle pretreatment alone groups (figure 3-4c, 3-4d), again indicating that the amount of FPP delivered in these groups was sub-therapeutic dose.

The amount of iron required to restore the levels in IDA was calculated by different investigators using different approaches based on the body weight and hemoglobin deficit. Various mathematical relationships were derived based on the required hemoglobin to replenish iron using oral and parenteral formulations [96, 5]. In the case of oral iron formulations the daily required dose was calculated based on the amount of elemental iron present in these formulations. According to CDC guidelines, for adults with anemia an oral iron dosage containing 60 mg of elemental iron, one to two times a day is recommended assuming that at least about 10 % will be absorbed from gastrointestinal system. For rats weighing ~250-300 gm, an oral dose about 0.3 mg elemental iron per day is required.

In the current study, we targeted to deliver a cumulative amount of 0.12 mg of elemental iron on alternate days (about ~ 60 µg on daily basis), using 10 cm² iontophoretic patch and a current strength of 0.15 mA/cm² for 4 hours transdermally. The FPP used in this study contains ~11.7 % elemental iron. The combination of microneedle pretreatment along with iontophoresis resulted in significant improvement in the hematologic and biochemical parameters within four weeks. There was an improvement in the mean hemoglobin concentration by ~2.5 g/dl from anemic condition to post treatment. It has been reported that, a successful iron replenishment therapy would result in improving hemoglobin concentration to 1-2 gm % in 2-3 weeks. Here, in rats received iron via iontophoresis after microneedle pretreatment (group 5), the mean RBC count increased from $6.61 \pm 0.75 \times 10^{12}/l$ (in anemic condition) to $7.72 \pm 0.5 \times 10^{12}/l$ ($p=0.013$) after treatment, indicating that the delivered iron was sufficient to meet the requirements for regeneration of red blood cells. The mean hematocrit values also increased from 32.4 ± 3.72 %

to 40.18 ± 4.24 % ($p=0.0068$) after treatment. Similarly, significant improvement in MCV, MCH and MCHC were observed after four weeks of treatment in this group. A decrease in the RDWc was also observed after treatment indicating a significant reduction in the abnormal size and shaped RBCs owing to transdermal delivery of FPP in group 5 (Figure 3-4e).

The serum iron concentration and % TS and TIBC values in the treated rats in group 5 provided validity to the fact that adequate amount of iron was delivered when iontophoresis was combined with microneedle pretreatment. The difference in lipid peroxidation after treatment was not significantly different from that of anemic condition in the same rats, indicating that FPP is not likely to increase the oxidative stress.

Table 3-2. The mean hematologic and biochemical parameters observed at the end of treatment period in rats administered with FPP via different modes of administration.

Parameter	IN	MN	MN+IN*	IP
<i>Hematological parameters</i>				
Hemoglobin (g/dl)	10.42 ± 1.11	10.55 ± 0.9	$13.12 \pm 0.6^{\dagger}$	$14.37 \pm 0.41^{\dagger}$
HCT (%)	34.62 ± 2.45	28.67 ± 1.52	$40.18 \pm 4.24^{\dagger}$	$42.0 \pm 1.30^{\dagger\dagger}$
MCV (fl)	39.2 ± 1.93	40.2 ± 1.4	$46.45 \pm 4.39^{\dagger}$	$46 \pm 1.73^{\dagger\dagger}$
MCH (pg)	11.1 ± 1.16	13.14 ± 2.21	$15.32 \pm 2.51^{\dagger}$	$15.8 \pm 0.62^{\dagger}$
MCHC (g/dl)	30 ± 1.21	30.8 ± 2.44	$32.9 \pm 1.39^{\dagger}$	$34.3 \pm 0.43^{\dagger}$
RBC ($10^{12}/l$)	7.05 ± 1.01	6.99 ± 1.10	$7.72 \pm 0.3^{\dagger}$	$9.11 \pm 0.15^{\dagger}$
RDWc (%)	25.73 ± 2.24	24.71 ± 3.43	$22.58 \pm 2.9^{\dagger}$	$19.47 \pm 2.23^{\dagger\dagger}$
<i>Biochemical parameters</i>				
Serum Iron ($\mu\text{g}/\text{dl}$)	$102.74 \pm 10.22^{\dagger}$	$109.52 \pm 14.2^{\dagger}$	$124.7 \pm 8.8^{\dagger\dagger}$	$139.53 \pm 13.6^{\dagger\dagger\dagger}$
TIBC ($\mu\text{g}/\text{dl}$)	$405.43 \pm 21.67^{\dagger}$	$399.5 \pm 32.7^{\dagger}$	$393.22 \pm 25.3^{\dagger}$	$354.81 \pm 36.3^{\dagger\dagger}$
% TS	$25.3 \pm 3.71^{\dagger\dagger}$	$29.47 \pm 4.82^{\dagger\dagger}$	$31.86 \pm 3.4^{\dagger\dagger\dagger}$	$39.37 \pm 2.2^{\dagger\dagger\dagger}$
Lipid Peroxidation [equivalent to MDA conc. (nmol/ml)] [¶]	13.13 ± 1.32	12.32 ± 2.54	12.42 ± 1.8	11.37 ± 2.2

*The difference in all parameters (except lipid peroxidation) in MN+IN group animals after treatment is significantly different from those before treatment.

† Not significant- There was no significant difference between lipid peroxidation levels at anemic condition and post treatment in all groups.

IN- Iontophoretic treatment group, MN-Microneedle treatment group, MN+IN- Iontophoresis combined with microneedle pretreatment and IP- FPP administered as intraperitoneal injection.

†p<0.05

††p<0.001

†††p<0.0001

3.3.1.4. Intraperitoneal delivery of FPP

FPP was administered intraperitoneally to rats for 2 weeks (positive control). There was a significant improvement in all hematological and biochemical parameters in these animals at end of treatment period. The improvement in the morphology of RBC in this group of animals is evident in figure 3-4f.

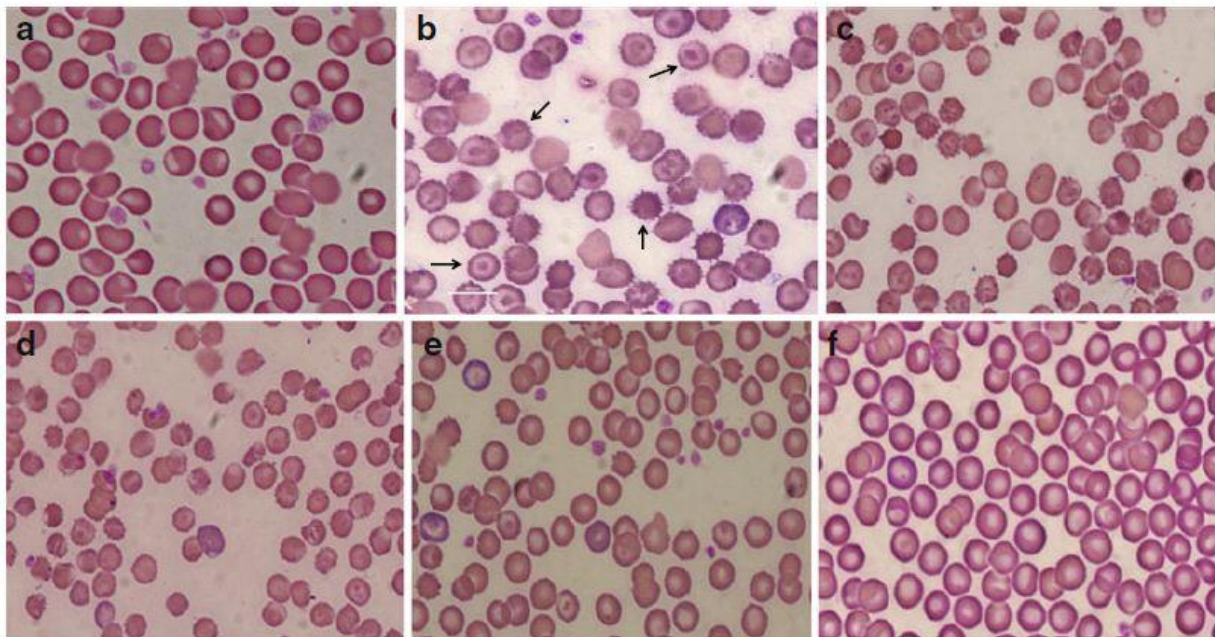


Figure3-4. Representative pictures of morphology of RBCs (a) RBCs in healthy rats (b) RBCs of anemic rats (Microcytic and hypochromic RBC shown with ↑marks) (c) RBCs in group 3 administered with FPP by iontophoresis (IN) (d) RBCs in rats administered with FPP following microneedle (MN) pretreatment(group 4) (e) RBCs of the rats administered with FPP using

combination of iontophoresis and microneedle pretreatment (MN+IN) (group 5) and (f) RBCs of rats received FPP through IP injection (group 6).

3.4. CONCLUSIONS

FPP can be delivered via transdermal route using iontophoresis in combination with microneedle pretreatment. The results of the study suggest that microneedle and iontophoresis mediated delivery of iron via transdermal route could be developed as a potential treatment for IDA. The transdermal controlled delivery of iron could become a potential, safe and effective alternative to parenteral iron therapy.

CHAPTER 4

SOLUBLE MICRONEEDLE SYSTEM FOR DELIVERY OF FPP

4.1. OBJECTIVES

1. Development and optimization of soluble microneedle systems for FPP using poly(methylvinylether/maelic acid) (PMVE/MA) polymers.
2. Kinetic profiling for the FPP released from polymeric microneedle system in the skin.
3. Evaluation of safety and toxicity of FPP in human epidermal keratinocyte (HEK) and dermal fibroblast (HDF) cell lines with the help of cell proliferation, viability, reactive oxygen species, cytokines expression assays.

4.2. INTRODUCTION

Our main aim in this study was to develop a soluble microneedle system incorporated with ferric pyrophosphate (FPP) to deliver iron with an objective to meet higher iron demand in case of moderate and severe anemic conditions. Soluble microneedle systems consist of an array of microneedles prepared using water soluble polymers loaded with the therapeutic agent (FPP) and FPP would be released into the dermal fluids upon penetration of the microneedles. Development of a successful patient friendly, self-administrable dissolvable microneedle array system for iron delivery can offer great advantages over oral and parenteral modes of administration. From the previous study, the possibility of delivering iron in significant amounts leading to reversal of iron deficiency anemia has been demonstrated in iron deficient rat model [97].

Ferric pyrophosphate (FPP) was incorporated into soluble microneedle arrays and morphology of the prepared microneedles was evaluated. The microneedle system was subjected to *in vitro* drug permeation studies across the hairless rat skin. *In vivo* cutaneous microdialysis studies were also carried out in hairless rats after insertion of soluble microneedles prepared with FPP at two different concentrations. The safety of administered iron compound was evaluated using human epidermal keratinocytes (HEK) and human dermal fibroblasts (HDF) cell lines. Cell proliferation/viability, reactive oxygen species generation assays and pro-inflammatory cytokines assay were performed after exposing the cells with FPP at different concentrations. Successful development of safe and effective soluble iron microneedle systems will be of a great advantage in poor economic settings with minimum risk of contamination issues and less discontinuation of iron therapy.

4.3. MATERIALS AND METHODS

4.3.1. Materials

Soluble Ferric pyrophosphate was obtained from Sigma-Aldrich Inc (St. Louis, MO). Phosphate buffered saline (PBS, pH 7.4) premixed powder was obtained from EMD Chemicals (Gibbstown, NJ). Ferrover® iron was purchased from Hach Company (Loveland, OH). Serum iron & TIBC kit was procured from Clinia Corporation (San Marcos, CA). All other chemicals and solvents used were of pure grade obtained from Fischer scientific (Fairway, NJ).

4.3.2. Methods

4.3.2.1. Preparation of soluble microneedles

Soluble microneedles containing FPP were prepared using water soluble polymers. Aqueous blends containing 15% w/w poly (methylvinylether/maelic acid (PMVE/MA) (Gantrez®AN-139, Ashland, Kidderminster, UK) and the relevant concentration of the FPP (143

mg FPP/g formulation) were prepared and used to fabricate microneedle arrays using laser engineered silicone micromold templates. The arrays were composed of 121 (11x11) needles perpendicular to the base, of conical shape ranging in height between 450 and 600 μm with base widths about $\sim 300 \mu\text{m}$. 300 or 600 mg of FPP and polymer mixture was added into the laser-engineered silicon microneedle molds and subjected to centrifugation at 550 g for 15 min followed by drying at room temperature for 48 h. Upon removal from the molds, the sidewalls of the microneedle arrays were removed using a heated scalpel blade. An accurate measurement of the final percentage of active compound in the device was determined based on mass loss calculations following water evaporation from the arrays [Soluble microneedles were prepared at Dr. Ryan Donnelly research lab facility, Queen's University Belfast, UK].

4.3.2.2. Morphology of soluble microneedles after insertion in the tissue

The disappearance/solubilization of microneedles was assessed by investigating the change in morphology of the microneedles after insertion into the skin tissue. Scanning Electron Microscopy (SEM) was used to obtain microneedles pictures to observe the change in morphology. Microneedle arrays were inserted into rat skin with mild force using thumb. The array was removed carefully after 1 hour and 3 hours and, SEM pictures were obtained. For SEM, the microneedle array was fixed on aluminum stubs using glued carbon tapes and coated with gold using Hummer 6.2 sputter coater (Anatech USA, Union City, California). The sputter coating chamber was supplied with argon gas throughout the coating process. Photomicrographs of the microneedle arrays were acquired using a model JSM-5600 scanning electron microscopy (JEOL Ltd., Tokyo, Japan).

4.3.2.3 *In vitro* transdermal permeation of FPP

In vitro permeation studies were carried out across the hairless rat skin using Franz diffusion cell set up. PBS adjusted to pH 5 using 1 N hydrochloric acid (HCl) was used as receiver phase. The electrical resistance was measured to confirm the skin integrity as described earlier. Briefly, a load resistor R_L (100 k Ω) was loaded in series with skin and the voltage drop across the whole circuit and skin was measured with a voltage of 100 mV applied at 10 Hz to obtain skin resistance in k Ω . After insertion of microneedles into the rat skin FPP permeation studies were carried out for 24 hours. The amount of FPP permeated over time across the rat skin was measured using inductively coupled plasma mass spectrometry (ICP-MS) [Thermo Fisher Scientific, Waltham, MA].

4.3.2.4. *In vivo* cutaneous microdialysis studies

All animal studies were approved by the Institutional Animal Care and Use Committee (IACUC) at the University of Mississippi (Protocol # 11-016). Linear microdialysis probe (BASi, WestLafayette IN) with 5 mm length and 30 kDa cut-off molecular weight was used to perform dermal microdialysis studies. A 30G needle was inserted intradermally parallel to the stratum corneum surface, through a distance of 1 cm. The microdialysis probe was inserted through this needle and the needle was withdrawn leaving the probe implanted in the dermal tissue. The inlet tube was connected to an injection pump (BASi, WestLafayette, IN) and the outlet was placed in a sample collection vial.

4.3.2.4.1. Microdialysis probe recovery

Microdialysis probe recovery studies were performed *in vivo* using retrodialysis method. A flow rate of 2 μ L/min was chosen for the entire study. Microdialysis probe was equilibrated with

PBS (pH-5) for 30 minutes and later, known concentration of drug was perfused and dialysate was collected at different time points. The recovery was calculated using the following formula:

$$\text{Recovery}(\%) = 100 - \left(\frac{\text{concentration of dialysate}}{\text{concentration of Perfusate}} \times 100 \right)$$

4.3.2.4.2. Cutaneous microdialysis studies

The microneedle array (with 43 mg and 86 mg of FPP) was applied on the rat abdominal skin by firmly pressing them against the rat skin using thumb and the array was secured with the help of a surgical tape. Dialysate fluid was collected every hour and the array was removed after 3 hours and microdialysis sampling was continued till 10 hours. The microdialysis samples were analyzed using inductively coupled plasma mass spectrometry (ICP-MS).

4.3.2.5. Skin content analysis

Amount of FPP retained in the rat skin after 10 hours was analyzed by taking a biopsy section of microneedle array application area. Skin surface was washed thoroughly with de-ionized water and wiped with alcohol swab to remove adhered FPP on the skin surface. The biopsy section of the skin was minced into small pieces and the tissue was dissolved in 1 N sodium hydroxide for 12 hours and homogenized to extract FPP into solution. The amount of FPP presented in sodium hydroxide was measured using ICP-MS.

4.3.2.6. Evaluation of safety and toxicity of FPP in human skin cell lines

The safety studies were carried out using human epidermal keratinocyte (HEK) [HEK001 (ATCC[®] CRL-2404[™])] continuous cell lines and human skin fibroblast (HDF) [CCD1093Sk (ATCC[®] CRL2115[™])] cell lines [ATCC, Manassas, VA].

4.3.2.6.1. Cell culture

HEK cells were grown in Keratinocyte Serum Free Medium (GIBCO-BRL 17005042) with 5 ng/ml human recombinant epidermal growth factor (EGF) and 2mM L-glutamine (without bovine pituitary extract and serum) in cell culture flasks (75 cm²) to approximately 80% confluence in 5% CO₂ environment incubator maintained at 37 °C. HDF cells were grown in Eagle's Minimum Essential Medium (EMEM) (ATCC-302003) with 10 % FBS in cell culture flasks (75 cm²) to approximately 80% confluence in a 37°C, humidified 5% CO₂ incubator. Both the cell media were supplemented with penicillin (10000 units) and streptomycin (10 mg/mL) solution. The cells were seeded into clear/black wall 96-well microplates at a density of 200,000 cells/ml (200 µL) and cell proliferation/viability assay, reactive oxygen species (ROS) measurement assay and cytokines assays were performed. Cell count was obtained with Bio-Rad automatic cell counter (Bio-Rad, Hercules, CA) after staining a 10 µl aliquot of cell suspension with 10 µl of Trypan blue stain (0.4 %) [Life Technologies, Grand Island, NY]. The passage number 78 was used for HEK cell lines, and passage number 6 for HDF cell lines in all the experiments.

4.3.2.6.2. Cell viability/proliferation assay

Cell proliferation assay was carried out using the CellTiter 96[®] AQueous one solution reagent (Promega, Madison, WI) which can be used to measure the number of viable cells by colorimetric method. After reaching approximately 80% confluence of the cells in microplates, the media in all the wells for both HEK and HDF cell lines was replaced with 100 µL of fresh medium (without serum and penicillin streptomycin solution) and cell lines were exposed to 100 µL of either basal medium (control) or serial dilutions of FPP prepared at different concentrations (250, 125, 62.5, 31.25, 15.62 and 7.81 mg/ml) or digitonin (positive control)

[Promega, Madison, WI] prepared at different concentrations (60 µg/ml-1.87 µg/ml) with serial dilutions for 24 hours. FPP solutions were prepared using basal medium and digitonin solutions were prepared from a stock of 20 mg/ml using cell culture grade dimethylsulfoxide (DMSO) [ATCC, Manassas, VA]. Untreated cells served as control in this study.

The CellTiter 96[®]AQueous one solution reagent was completely thawed in water bath at 37°C for 10 minutes before use and 40 µl of the this reagent was added to each well in the 96 well plate containing the cells and the plate was incubated at 37 °C in a humidified, 5 % CO₂ atmosphere for 4 hours. After incubation the absorbance at 490 nm was recorded using microplate Reader (SpectraMax[®] M5, Molecular Devices, LLC. Sunnyvale, CA). Testing at each concentration of the FPP and positive standard was performed in triplicates.

4.3.2.6.3. Measurement of Reactive Oxygen Species (ROS) activity/oxidative stress markers

Possible generation of reactive oxygen species (ROS) and the intracellular ROS activity upon treating both HEK and HDF cell lines with FPP at different concentrations were measured using Oxiselect[™] intracellular ROS assay Kit (Cell Biolabs, San Diego, CA). After reaching approximately 80% confluence in 96-well microplates, both the cell lines was treated with cell permeable fluorogenic probe 2',7'-dichlorodihydrofluorescein diacetate (DCFH-DA). Cells loaded with DCFH-DA were washed gently with Dulbecco's Phosphate-Buffered saline (D-PBS) (Sigma Aldrich, St. Louis, MO) 2-3 times and 100µL of fresh medium was added to all the wells along with 100µL of FPP prepared at different concentrations (250, 125, 62.5, 31.25, 15.62 and 7.81 mg/ml) or H₂O₂ (positive control) prepared at different concentrations (2000-62.5 µM) for 24 Hours. Later cells were washed 2-3 times with again with D-PBS and 100 µL of fresh medium and 100µL of 2X cell lysis buffer was added. After 5 minutes of incubation, 150 µL of this medium was transferred to a black wall 96-well plate and fluorescence was measured.

Untreated cells served as control in this study. All the studies were performed in triplicates. The results obtained were compared using a standard calibration curve plotted for 2', 7'-dichlorodihydrofluorescein (DCF) from 0.01 nM to 10 μ M using both media.

4.3.2.6.4. Measurement of cytokines as inflammatory response

Levels of various pro-inflammatory cytokines generated in HEK and HDF cell lines after addition of FPP at different concentrations for 24 hours was assayed using Quantibody[®] Human Inflammation Array 1 kit (RayBiotech, Inc. Atlanta, GA). Quantibody[®] array uses the multiplexed sandwich ELISA-based technology which can determine the concentration of multiple cytokines simultaneously and accurately. In the present study, 10 human cytokines, IL-1 α , IL-1 β , IL-4, IL-6, IL-8, IL-10, IL-13, MCP-1, IFN γ and TNF α levels expressed in both the cells were measured after cells were treated with FPP for 24 hours. Digitonin (30 μ g/ml) and hydrogen peroxide (H₂O₂) [1000 μ M] were used as positive controls. After reaching approximately 80% confluence of the cells in microplates, the media in all the wells for both HEK and HDF cell lines was replaced with 100 μ L of fresh medium (without serum and penicillin streptomycin solution). Cells were exposed to 100 μ L of either basal medium (control) or serial dilutions of FPP prepared at different concentrations (250, 125, 62.5 and 31.25 mg/ml) for 24 hours. Untreated cells served as control in this study. The standard glass slide provided as Quantibody[®] array was spotted with 16 wells of identical cytokine antibodies arrayed in quadruplicates. Cell supernatant from each well of 96 microplates treated with samples or standard were loaded into each well of the glass slide. After proper wash steps with the wash buffers, detection antibody cocktail was added to each well and incubated for overnight. Later, detection antibody cocktail was discarded and after proper wash steps Cy3 equivalent dye-conjugated streptavidin was added to each well and the glass slide was incubated in dark for

overnight again. Glass slide was washed again and completely air dried and the signals were visualized through use of a laser scanner equipped with a Cy3 wavelength (Axon GenePix) and data was extracted. Quantitative data analysis was performed using Quantibody® Q-Analyzer software (RayBiotech, Inc. Atlanta, GA).

4.4. RESULTS AND DISCUSSION

4.4.1. Soluble microneedles of FPP

Soluble microneedle arrays incorporating two different FPP loads (with 43 mg and 86 mg of initial FPP) were prepared successfully using aqueous blends of 15% w/w poly (methylvinylether/maelic acid) (PMVE/MA) via laser-engineered silicone micromold templates as described by Donnelly *et al* (2011) previously [98]. In case of microneedle arrays with 43 mg FPP, final weight of the arrays was 36.2 ± 6.7 mg and for microneedle arrays loaded with FPP at 86 mg, the final weight of the arrays was 67.6 ± 20.6 mg. The final amount of FPP presented in the arrays was estimated to be $\sim 5.16 \pm 1.1$ mg and $\sim 9.31 \pm 1.93$ respectively.

Amount of FPP (g)	Weight of polymer and FPP matrix loaded into mold (g)	Weight after drying (g)	Final weight of the array after sidewalls removed (g)
0.043	0.308 ± 0.010	0.11 ± 0.006	0.036 ± 0.006
0.086	0.590 ± 0.004	0.185 ± 0.036	0.0676 ± 0.020

Table 4-1. The mean weights of FPP polymer matrix loaded into microneedle molds initially, after drying for 48 hours and final average weight of array after sidewalls removed. The values represented are the average of $n=30 \pm$ S.D.

4.4.2. Morphology of soluble microneedles

Morphology of the soluble microneedle array was investigated using scanning electron microscope (SEM) and the prepared microneedles had an average height $\sim 540 \pm 50 \mu\text{m}$ with an average base radius of $250 \pm 5 \mu\text{m}$ and an average tip radius of $25 \pm 5 \mu\text{m}$.

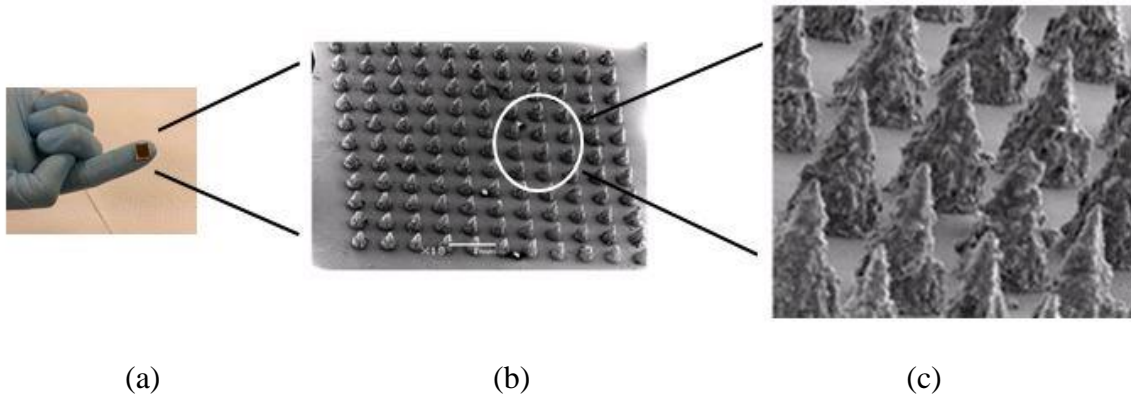


Figure 4-1. Images of FPP soluble microneedles (a) Microneedle array on the investigators finger. [Pictures were taken using Nikon Digital Camera (Nikon Inc., NY)] (b) SEM images of FPP soluble microneedle arrays containing 121 microneedles (18X magnification) (b) microneedles array visualized at 90X magnification.

4.4.3. Soluble microneedles in the skin

Microneedle arrays with FPP were inserted in the rat skin (each array in a different rat). The time required for disappearance of microneedles in the array was visualized with the help of SEM images. Few microneedle arrays were removed at 1 hour time point after insertion and few other microneedle arrays after 3 hours and 4 hours. The removed arrays were sputter coated with gold in argon supplied chamber and SEM photomicrographs were obtained. The morphology of microneedles after 1 hour and 3 hours are shown in the figure 4-2. The microneedles were found to be dissolved/disappeared in $\sim 3-4$ hours in the skin tissue fluid.

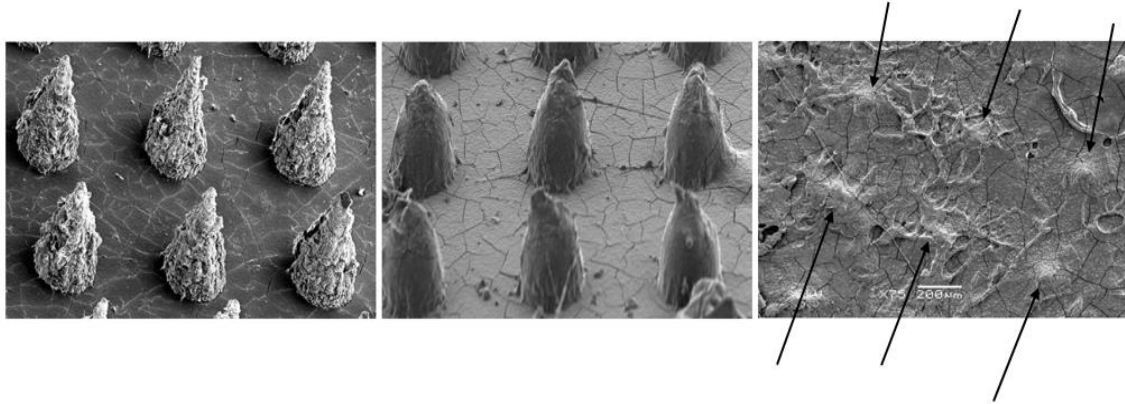


Figure4-2*. SEM Images of FPP soluble microneedle arrays (a) Microneedles before insertion into the skin (b) Microneedles inserted into the rat skin and removed at 1 hour time point (c) Microneedles inserted into the rat skin and removed after 3 hours. Arrows indicate the position of individual microneedles.

*All the mages were taken at 75X magnification and only 6 microneedles were focused to show the time dependent disappearance of microneedles in the rat skin after insertion.

4.4.4. *In vitro* permeation studies of FPP

From the *in vitro* studies, a cumulative amount of $101.66 \pm 6.9\mu\text{g}$ of FPP permeated in 24 hours across the rat skin from microneedle array (0.5 cm^2) having $\sim 5.16 \pm 1.1 \text{ mg}$ of FPP and $120.95 \pm 16.2\mu\text{g}$ permeated from microneedle array (0.5 cm^2) having $\sim 9.31 \pm 1.93 \text{ mg}$ of FPP. The amount of FPP permeated across rat skin was evaluated using inductively coupled plasma mass spectrometry. There was no significant difference between the amounts of FPP permeated across rat skin from the arrays with different FPP loads. The amount of FPP retained in the skin at the site of microneedle array application was found to be $5.63 \pm 2.36 \mu\text{g}/\text{mg}$ and $8.64 \mu\text{g}/\text{mg}$ respectively.

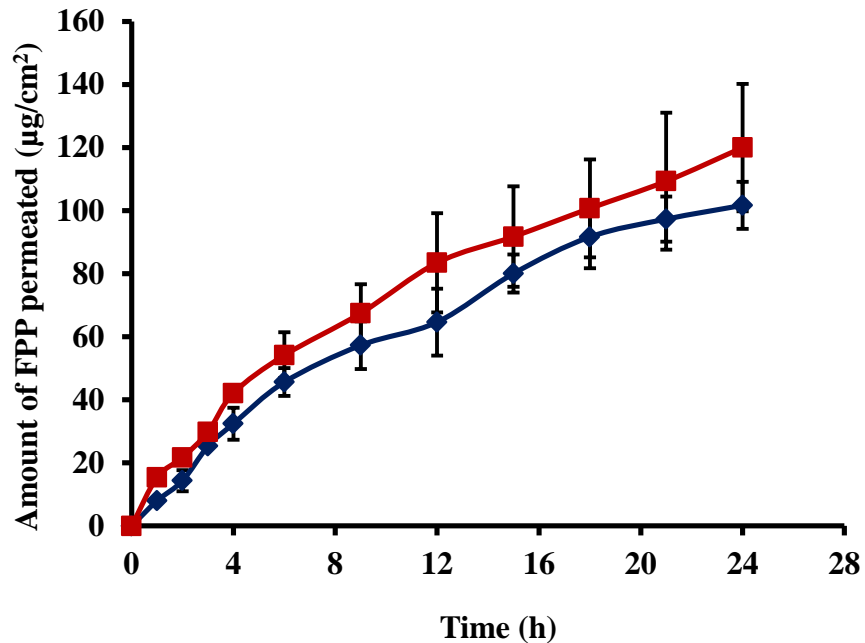


Figure 4-3. The Cumulative amount of FPP permeated across rat skin from soluble microneedles containing ~5.2 mg of FPP (◆) and ~9.3 mg of FPP (■). The data points represented are the average of $n=3 \pm$ S.D.

4.4.5. ICP-MS

Inductively Coupled Plasma Mass Spectrometry or ICP-MS is a popular analytical technique used for elemental determinations due to its superior detection capabilities. ICP-MS combines a high-temperature ICP (Inductively Coupled Plasma) source with a mass spectrometer. The sample is typically introduced into the ICP plasma as an aerosol and the ICP source converts the atoms of the elements in the sample to ions. Once the ions enter the mass spectrometer, they are separated by their mass-to-charge ratio by the quadrupole system and detected by the mass spectrometer. The ions formed by the ICP discharge are typically positive ions which is suitable and highly precise technique which can measure as less aspicomolar concentrations of iron present in the sample.

4.4.6. Cutaneous microdialysis studies

The recovery of FPP by the microdialysis probe in the cutaneous tissue was found to be $58.2 \pm 4.6 \%$. The amount of free iron present at the active application site in the skin was measured as concentration in the dialysate fluid from cutaneous microdialysis studies. When the microneedles were inserted for 3 hours, a gradual increase in the concentration of free iron was observed up to 4 hours and the free iron concentration declined slowly in the next 6 hours. When microneedle array loaded with ~ 5.2 mg of FPP (final amount), $\sim 11 \mu\text{g}$ of FPP was observed at 4 hours in the interstitial fluid, in case of microneedle array loaded with ~ 9.3 mg of FPP (final amount), $\sim 17 \mu\text{g}$ was observed at 4 hours in the interstitial fluid. The amount of FPP retained in the rat skin at the active application site was $6.48 \pm 0.72 \mu\text{g}/\text{mg}$ and $7.89 \pm 0.58 \mu\text{g}/\text{mg}$ respectively with the two FPP loads.



Figure4-4. Image showing *in vivo* cutaneous microdialysis on the abdominal part of the hairless rat after application of soluble microneedle array.

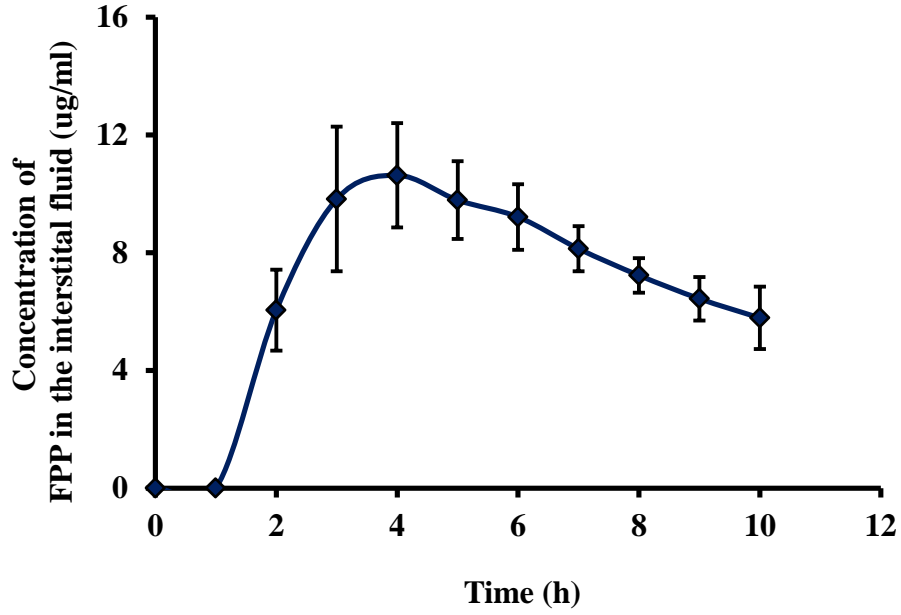


Figure4-5A.

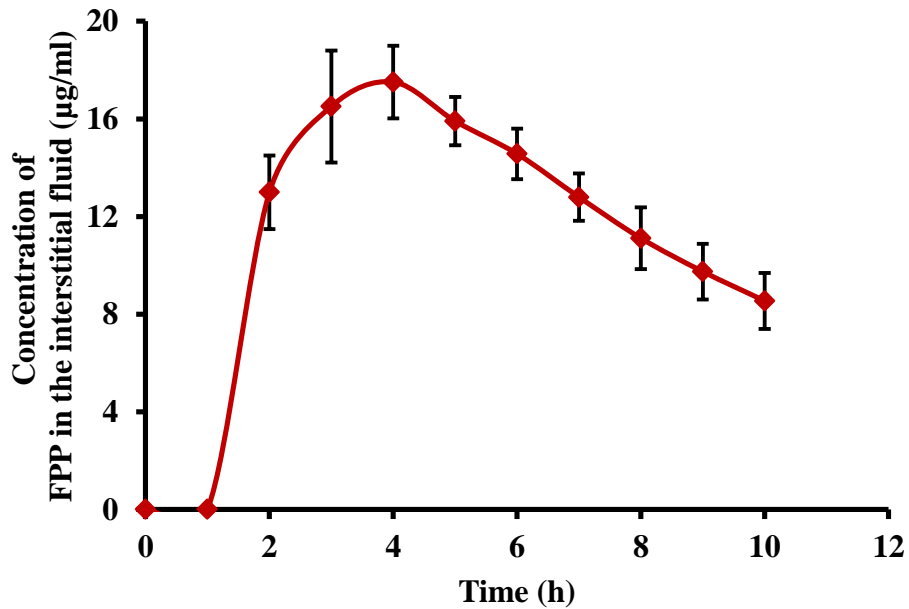


Figure4-5B.

Figure4-5. The time course of free FPP in the dermal interstitial fluid following the application of soluble microneedles loaded with (A) ~5.2 mg of FPP and (B) ~9.3 mg of FPP. The data points represented are the average of $n=4 \pm$ S.D.

4.4.7. Dermal kinetics of Iron

Omnipresence of iron in the physiological system offers a great challenge to quantify and distinguish between the iron present in various metabolic pools. Once introduced into the system, iron readily binds to transferrin protein and circulates as bound iron throughout the body until it reaches bone marrow or reticuloendothelial pool.

Iron kinetics in the skin was extensively studied by various research groups in the past and has been well documented in the literature [99-106]. The aim of these studies was to measure iron disposition and kinetics in the skin that was injected intradermally/intravenously after coupling the iron source with detectable radioactive species. In their earlier studies, Weintraub *et al* estimated that significant quantities of iron get excreted through the skin when Ferrous⁵⁹ citrate was injected as iron source intravenously in healthy volunteers [99]. The whole body scintillation measurements were made after intravenous injection of radioactive iron and 25% loss in total radioactivity through whole body counts was reported. There was a net radioactivity loss of 8.5 % through feces and urine alone. From the results, authors concluded that the observed greater loss in whole body counts other than the radioactivity loss in feces and urine (25 % vs 8.5 %) might be through the skin and speculated that skin might be acting as an active excretory organ for iron. To support the hypothesis, Ferrous⁵⁹ citrate was injected via sub-dermal route in another 6 healthy volunteers, and radio autographs prepared from the skin sections of active application site. A selective localization of radioactivity in the epithelial cells of the epidermis, sweat glands, sebaceous glands and hair follicles was observed. A significant radioactivity was also observed in heat stimulated sweat collections and keratinocytes after scotch tape stripping of the forearm at the injected site in these volunteers. No radioactivity was found in connective tissue even though it might be the site of tip of the needle while injecting the radioactive iron. In the

intra-dermal injection group ~75-85% loss in radioactivity was observed in first two days with concomitant rise and fall in plasma radioactivity and further a slow second rate of loss in radioactivity with a half-life averaged from 54-110 days. Authors concluded that this secondary slow loss of radioactivity might be due to the loss of iron through the sweat and skin shedding.

Later, Beamish *et al* performed a systemic study to measure iron clearance from the skin[100]. ⁵⁹Fe-Ferrous citrate used as iron source was injected into sub-epidermal tissue of the volar aspect of the forearm to healthy volunteers and iron deficient subjects. In normal subjects, ⁵⁹Fe activity at the site of injection showed a rapid decline initially following a slow rate of disappearance thereafter, which is in agreement with earlier report by Weintraub *et al*. When the activity was plotted on a logarithmic scale, three exponential component was identified with an initial half-life about 30 minutes, second half-life of about one day (~19-29 hours) and a slow and third half-life about 60 (47-74) days. In case of sub-dermal injection of radioactive iron to iron deficient patients, the amount of iron cleared in the first rapid phase was less compared to healthy population, confirming the availability of unsaturated transferrin at the site of injection in this patient population group. In one patient, iron was injected after binding it with transferrin *in vitro* and authors reported that very little iron was removed from the site of injection. From these reports, it was concluded that iron injected into the skin was rapidly bound to transferrin till its saturation capacity and rest of the iron was rapidly removed into blood stream. In the same study a dose dependent clearance of iron was also identified confirming the saturation of transferrin at the site of injection. In case of iron that is bound to transferrin in the interstitial pool, approximately two-thirds was cleared with a half-life of about one day and remaining one-third was disappeared slowly with a half-life of 60 days. With all these studies, authors speculated the existence of an intracellular iron pool in the skin.

Later, in their independent studies, Wasserman *et al* (1965) and Pollycove *et al* (1966), suggested the existence of labile iron pools in the physiological system other than the known red cell pool and reticulo-endothelial pools from which iron feedback might occur [106,107]. In further investigations by Cavill and Jacobs *et al* in 1971, they proposed a two compartment model for the transferrin bound iron in the interstitial fluid [103]. From the interstitial iron pool, significant amount of iron bound to transferrin entering into the skin cells (~1 %/ hr) and about 0.1 % of intracellular iron per hour was lost back to the interstitial pool. Iron in the interstitial fluid of the skin was mainly cleared by lymphatic drainage which was confirmed with clearance studies of another protein, albumin from interstitial fluid. From these investigations, it is clear that, when all iron was bound to transferrin, no evidence of rapid clearance of iron from the site of injection and it can leave only through capillary bed or by lymphatic drainage. Based on the findings of intracellular exchangeable iron pool in the skin, authors suggest that there might be other large parenchymal pools existing in the other organs, which are indirectly in equilibrium with the plasma pool.

From all the above investigations regarding the kinetics of iron in the skin that was injected intradermally, it could be inferred that slowest phase of iron clearance from skin was actually from the skin cells, i.e. the slow loss of intracellular iron to the interstitial fluid. The usual turnover time of epithelial cells is ~26 days, but the mean half-life of third phase iron clearance was observed as 67 days. Generally, DNA is conserved in the skin by extrusion from the maturing cells and re-absorption by the basal layers. Cavil *et al* suggested that a similar mechanism might be happening in case of iron that is entering the epithelial cells [104].

In the present study, from SEM experiments the microneedles were dissolved in the skin within 3-4 hours. The FPP retained in the skin in both *in vitro* and *in vivo* conditions (~20-30 %

loaded FPP in the array) suggesting that FPP might be releasing slowly from the microneedle array by maintaining a depot in the skin. In case of cutaneous microdialysis studies, the amount of free iron detected in the interstitial fluid was low, which could be due to the rapid binding of iron by transferrin in the interstitial fluid and clearance of free iron into the systemic circulation to bind transferrin in other metabolic pools.

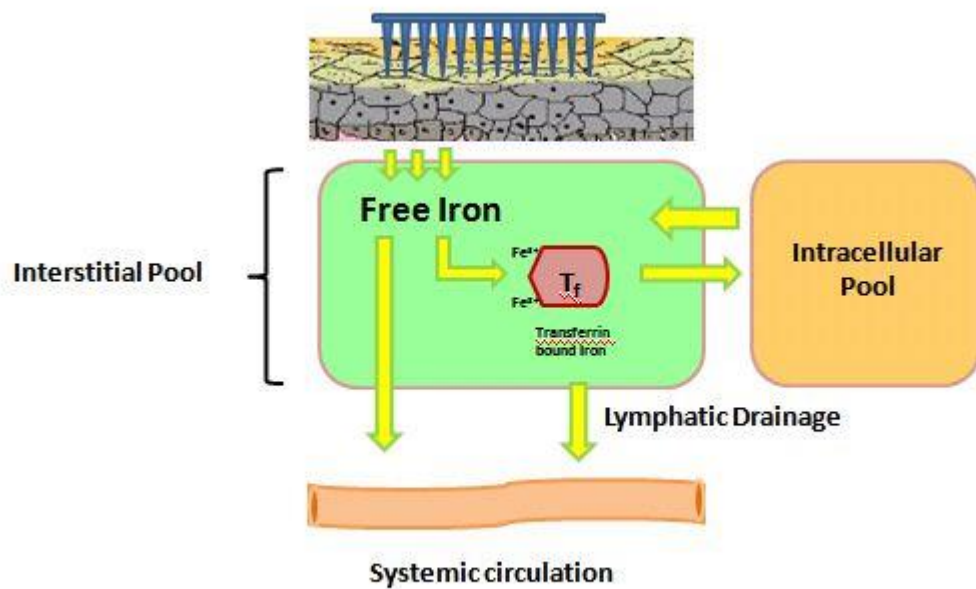


Figure4-6. Iron disposition and expected pathways of iron disappearance from the skin. Most of the iron from soluble microneedles was rapidly cleared as free iron into the systemic circulation to bind transferrin in other metabolic pools and some iron might be bound to transferrin in interstitial fluid. About one-third of transferrin bound iron in interstitial pool was entering into skin cells. From the literature, interstitial fluid in the skin acts as an exchange pool for iron between the skin cells and other metabolic pools.

4.4.8. Safety and toxicity studies in cell lines

4.4.8.1. Cell proliferation assay

The CellTiter 96[®] AQueous ‘one solution’ assay was improvised from previous CellTiter 96[®] AQueous Assay which contains a novel tetrazolium compound [3-(4,5-dimethylthiazol-2-yl)-5-(3-carboxymethoxyphenyl)-2-(4-sulfophenyl)-2H-tetrazolium, inner salt; MTS] and an electron coupling reagent (phenazineethosulfate; PES). PES has enhanced chemical stability, which allows it to be combined with MTS to form a stable solution. This MTS tetrazolium compound (Owen’s reagent) is bio-reduced by cells into a colored formazan product that is soluble in tissue culture medium [107]. Formazan is produced by an amount of NADPH or NADH dehydrogenase enzymes directly proportional to the number of living cells in culture as measured at 490 nm [108].

The decrease in the absorbance indicated the decrease in the mitochondrial activity and the HEK cells treated with FPP at various concentrations showed a dose dependent cell proliferation being least at 250 mg/ml and highest at 7.81 mg/ml. There was a decrease in cell viability at high concentration of FPP, which might be due to the high osmolarity of FPP solution at these concentrations. But the low concentrations (31.2 mg/ml, 15.6 mg/ml and 7.8 mg/ml) of FPP were relatively safe and the amount of FPP that was present in the microneedle arrays were ~5.2 mg and ~9.3 mg only. A similar trend was observed in HDF cell line also. In all these studies cells were treated with serial dilutions of high concentrations of FPP to determine the safe and cytotoxic dose for further evaluations.

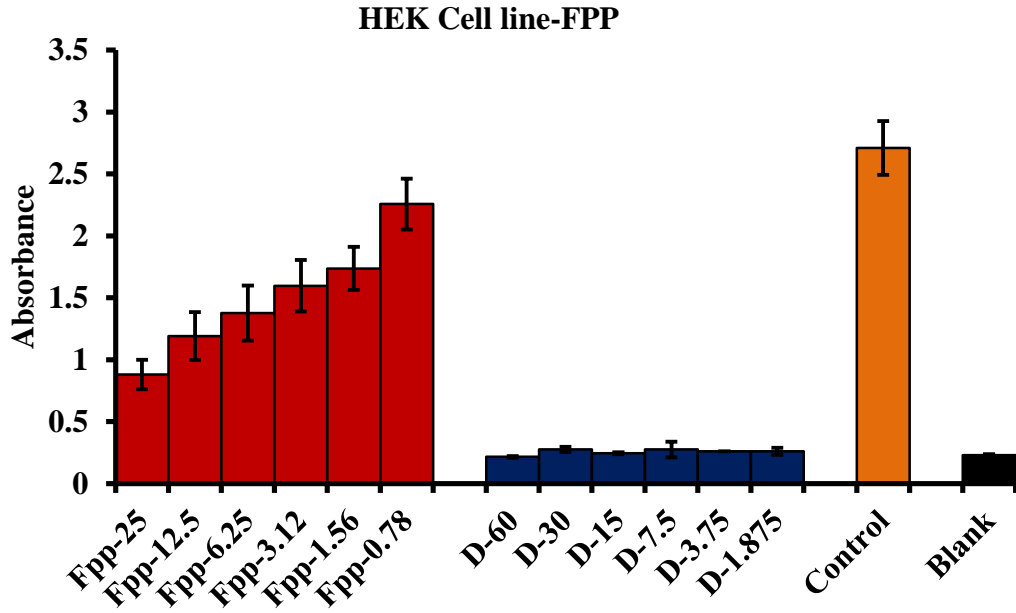


Figure4-7A.

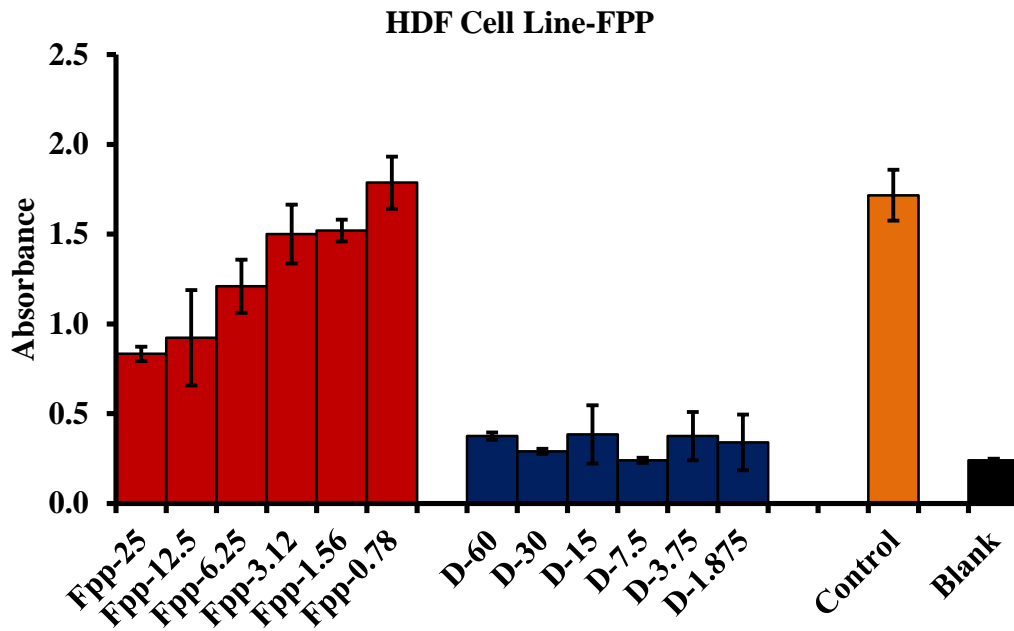


Figure4-7B.

Figure4-7. The mitochondrial activity (MTS activity) of (A) HEK and (B) HDF cells after 24 h exposure to 100 μ l of FPP (250-7.8 mg/ml) and digitonin [D] (60 μ g/ml-1.87 μ g/ml). Results are combined from three independent exposures and expressed as mean (\pm S.D.).

4.4.8.2. ROS assay

OxiselectTM intracellular ROS assay kit measures hydroxyl, peroxy, and other reactive oxygen species activity within a cell. Upon addition to cells, the non-fluorescent DCFH-DA permeates well across the cell membrane and once inside the cell DCFH-DA was rapidly deacetylated by cellular esterases to 2', 7'-dichlorodihydrofluorescein (DCFH), which is also non-fluorescent in nature. DCFH will be rapidly oxidized to fluorescent 2', 7'-dichlorodihydrofluorescein (DCF-green fluorescence) in presence of reactive oxygen species. The fluorescence intensity is proportional to the ROS levels within the cell cytosol. The amount of DCF generated will be compared with the standard calibration curve obtained by using different concentration of DCF using relative fluorescence units (RFU). The DCF detection sensitivity limit of the kit is as low as 10 pM. Hydrogen peroxide used as positive control at different concentrations and it generally crosses cell membranes readily, might be through the aquaporins in the cell [109]. Reactive oxygen species can cause oxidative stress at cellular level and oxidative stress can activate NF- κ B signaling pathway, stress-activated kinases, and such activation could result in cell death by either apoptosis or necrosis [110]. From figure 9, the generation of reactive oxygen species as relative fluorescence units after treating the cells with FPP was compared with standards (H_2O_2). Even at high concentrations of FPP, the amount of DCF generated as a measure of ROS was very low. A similar trend was observed in HDF cell line also with even low levels of ROS generation after treatment with FPP at different concentrations. Low levels of oxidative stress are thought to be beneficial, because it is a necessary prerequisite for a number of normal metabolic pathways, especially those involving signal transductions [111].

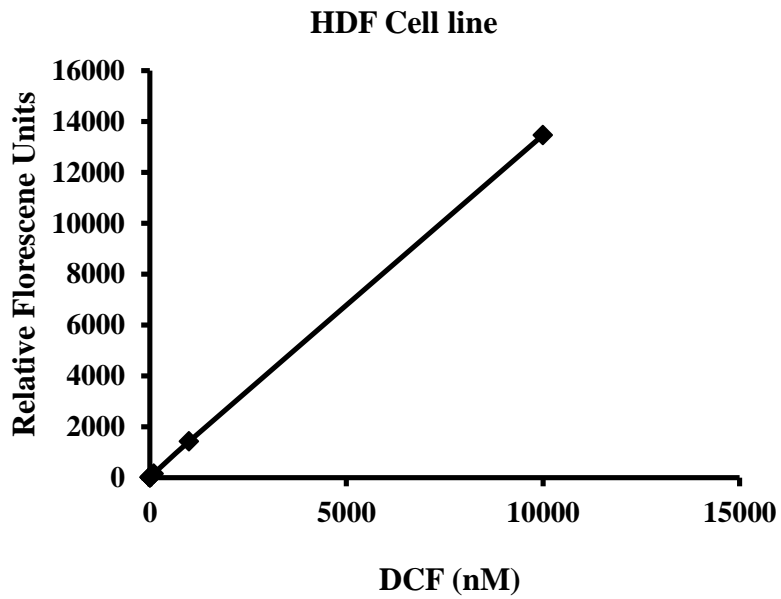
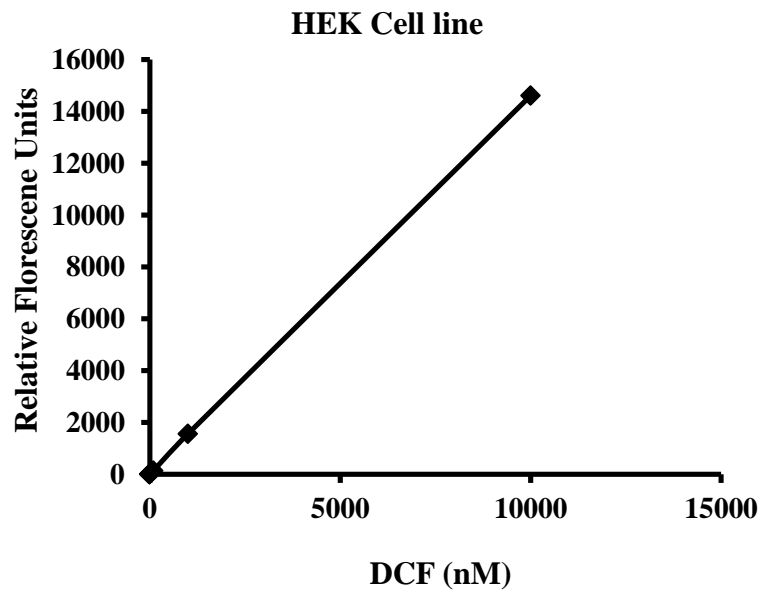


Figure4-8. Standard calibration curve for 2', 7'-dichlorodihydrofluorescein (DCF) assay in HEK and HDF media.

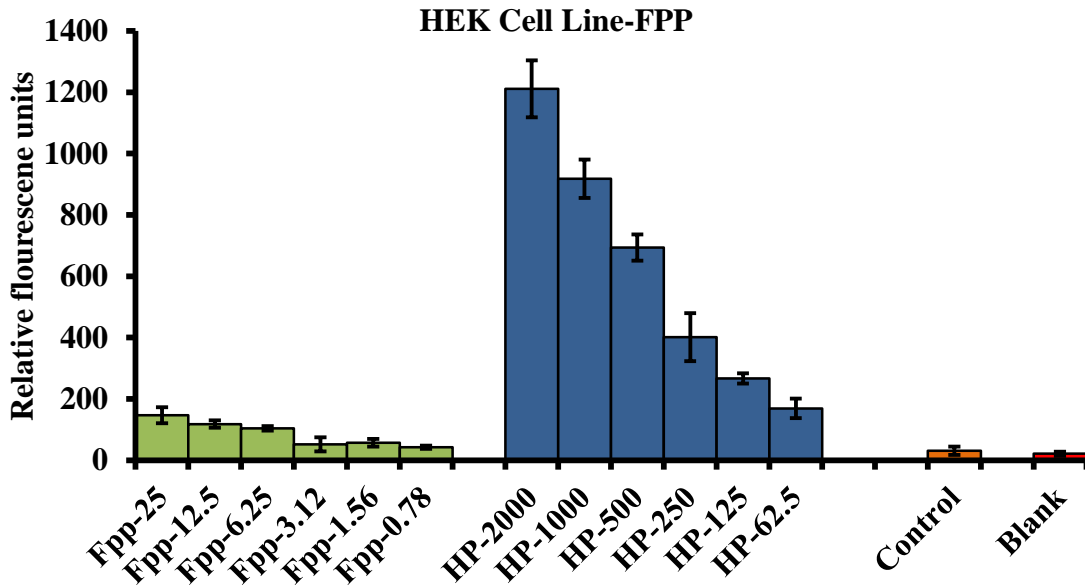


Figure 4-9A

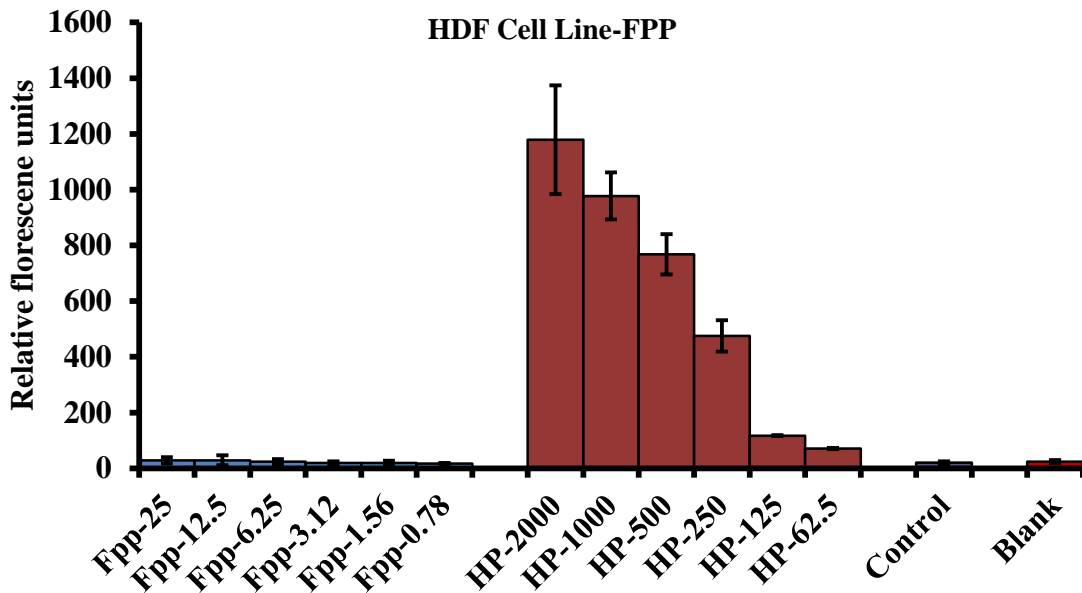


Figure 4-9B

Figure 4-9. Induction of reactive oxygen species (ROS) by FPP (250-7.8 mg/ml) or hydrogen peroxide (HP) in (A) HEK and (B) HDF cells after 24 hours exposure. Results are combined from three independent exposures and expressed as mean (\pm S.D.).

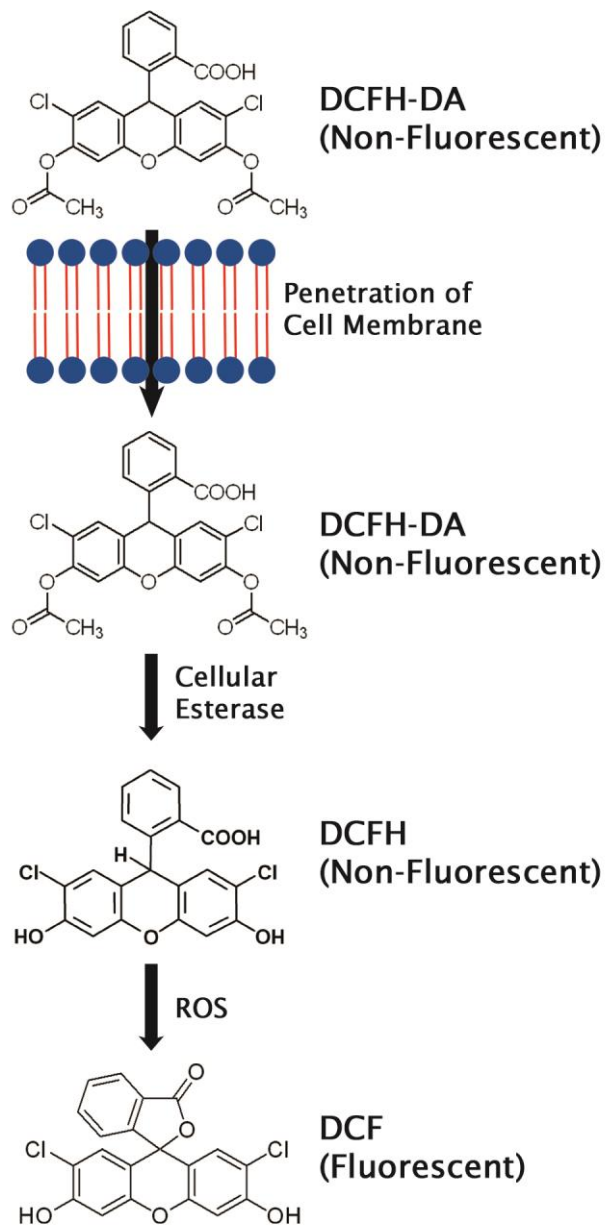


Figure 4-10. Scheme of DCF assay (With kind permission from Cell Biolabs, San Diego, CA).

4.4.8.3. Cytokines measurement

Cytokines are hormone like polypeptides which play a major role in the inflammatory and immunoregulatory responses, apoptosis, cell growth and differentiation. They are involved in interactions between different cell types, cellular responses to environmental conditions, and maintenance of homeostasis. Quantibody[®] array used in this study uses a pair of cytokine specific antibodies for detection, like a traditional sandwich based ELISA. In detail, one standard glass slide is spotted with 16 wells of identical cytokine antibody arrays. Each antibody, together with the positive controls was arrayed in quadruplicate. A capture antibody was first bound to the glass surface. After incubation with the sample, the target cytokine was trapped on the solid surface. A second biotin labeled detection antibody was then added, which recognizes a different isotope of the target cytokine. The cytokine-antibody-biotin complex then visualized through the addition of the streptavidin-labeled Cy3 equivalent dye using a laser scanner. By arraying multiple cytokine specific capture antibodies onto a glass support, multiplex detection of cytokines in one experiment is made possible using this kit. For cytokine quantification, known concentrations of cytokine standards were used to generate a standard curve for each cytokine.

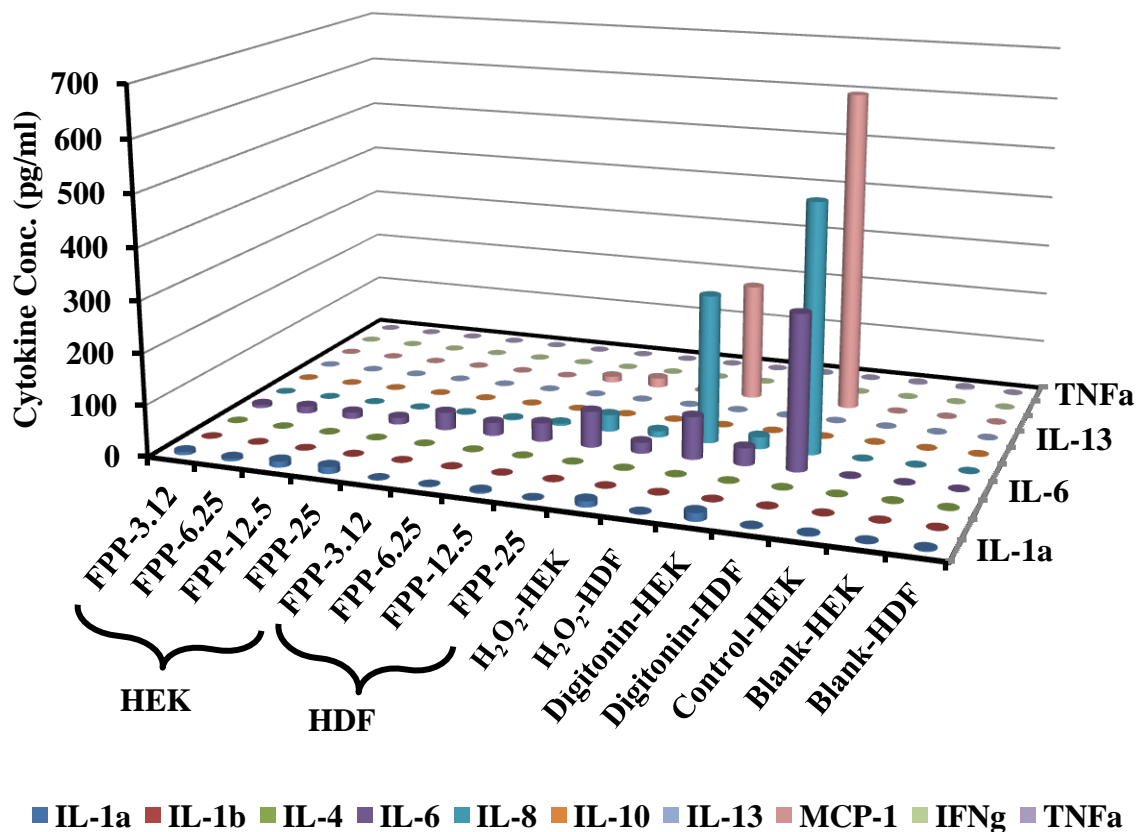


Figure4-11. An overview of the amount of cytokines detected in HEK and HDF cell line after treating them with FPP at different concentrations (31.2-250 mg/ml), H₂O₂ (1000 μM) and digitonin (30 μg/ml). Results are combined from three independent exposures and expressed as mean (± S.D.).

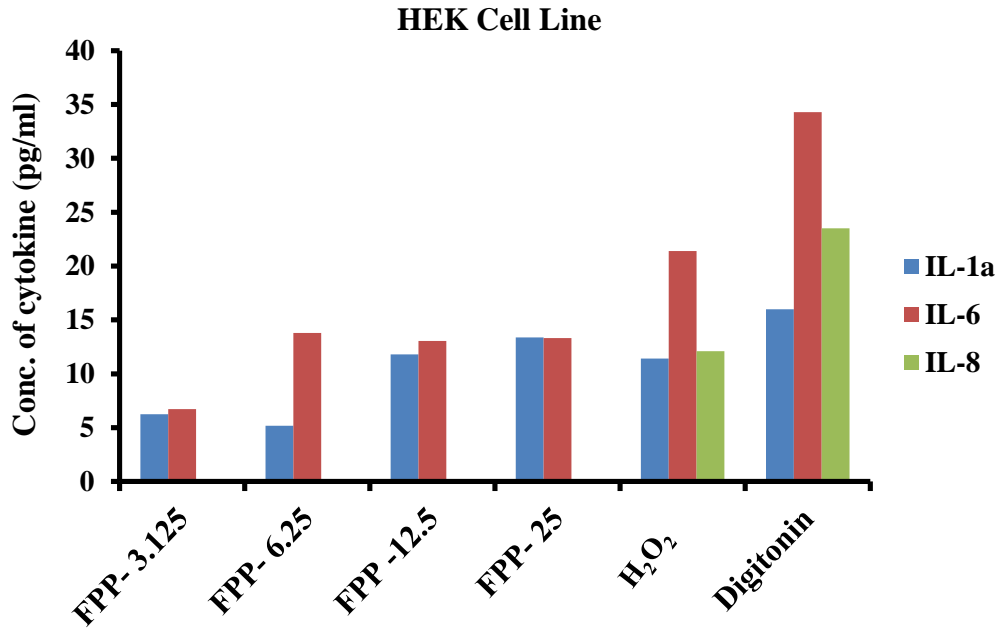


Figure 4-12A

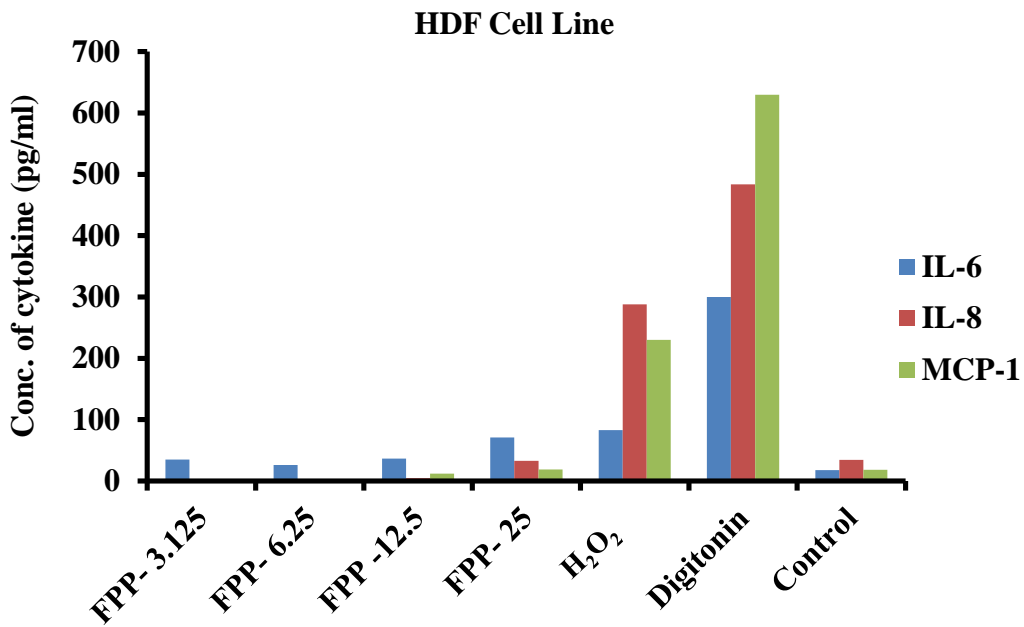


Figure 4-12B

Figure4-12. Presence of cytokines in (A) HEK and (B) HDF cells after 24 h exposure to 100 μ l of FPP (31.25-250 mg/ml) and hydrogen peroxide (1000 μ M) and digitonin (30 μ g/ml). Results are combined from three independent exposures and expressed as mean (\pm S.D.).

Cytokines are hormone like polypeptides which play a major role in the inflammatory and immunoregulatory responses, apoptosis, cell growth and differentiation. They are involved in interactions between different cell types, cellular responses to environmental conditions, and maintenance of homeostasis. Quantibody[®] array used in this study uses a pair of cytokine specific antibodies for detection, like a traditional sandwich based ELISA. In detail, one standard glass slide is spotted with 16 wells of identical cytokine antibody arrays. Each antibody, together with the positive controls is arrayed in quadruplicate. A capture antibody was first bound to the glass surface. After incubation with the sample, the target cytokine was trapped on the solid surface. A second biotin labeled detection antibody was then added, which recognizes a different epitope of the target cytokine. The cytokine-antibody-biotin complex then visualized through the addition of the streptavidin-labeled Cy3 equivalent dye using a laser scanner. By arraying multiple cytokine specific capture antibodies onto a glass support, multiplex detection of cytokines in one experiment is made possible using this kit. For cytokine quantification, known concentrations of cytokine standards were used to generate a standard curve for each cytokine.

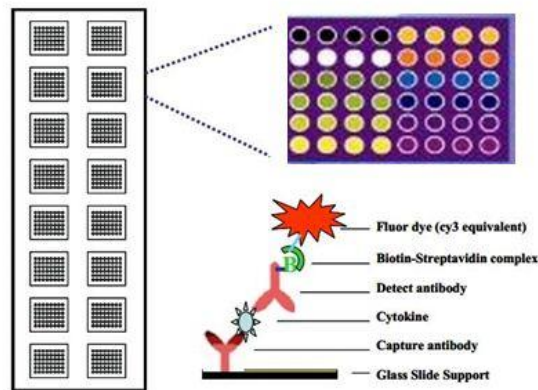


Figure 4-13. Descriptive image to show the floor map of standard glass slide uses in Quantibody[®] array along with the detection mechanism of cytokines (With kind permission from RayBiotech, Atlanta, GA).

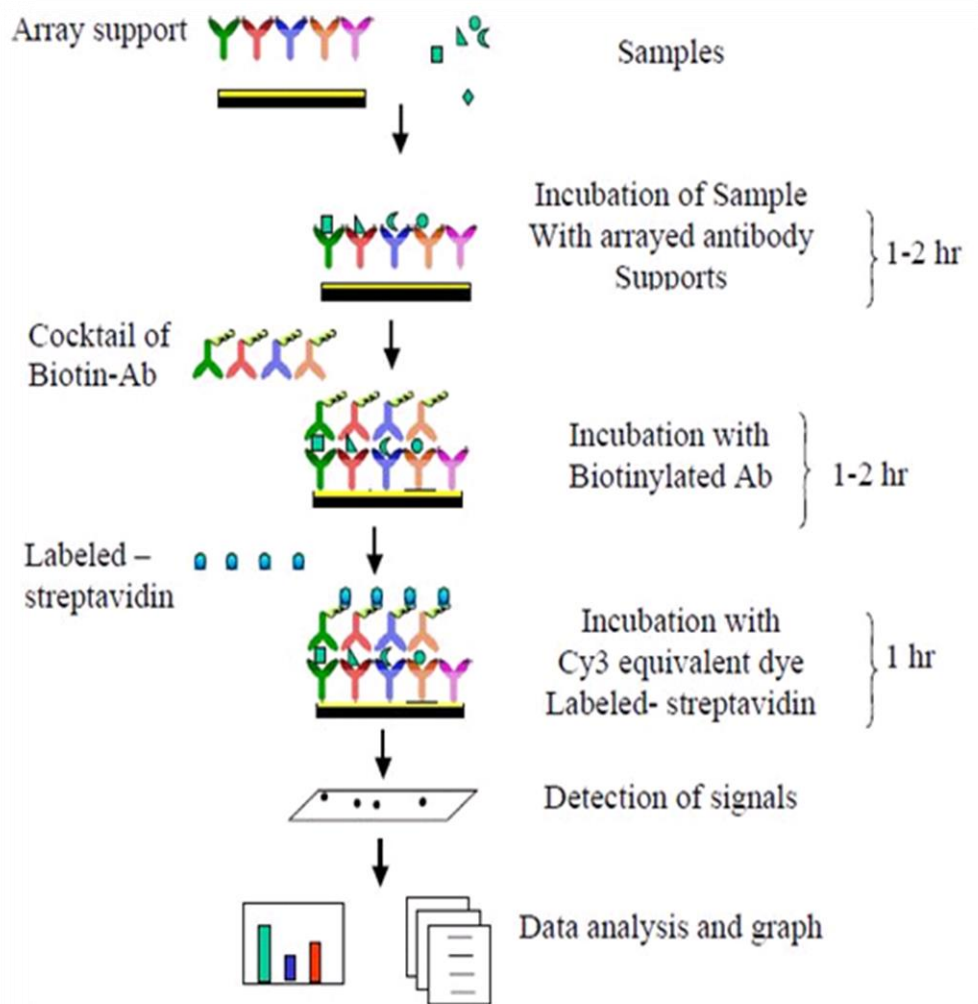


Figure4-14. Experimental procedure (work flow) with Quantibody[®] array for detection of cytokines (With kind permission from RayBiotech, Atlanta, GA).

Among the measured cytokines IL-1 α , IL-6, IL-8 and TNF α are pro-inflammatory cytokines and IL-4, IL-10 and IL-13 are anti-inflammatory cytokines. Keratinocytes produce many cytokines constitutively or by an external stimulus. The pro-inflammatory cytokines expressed by keratinocytes include IL-1 α , IL-6, IL-8, TNF α and IFN γ and keratinocytes have receptors for IL-4, IL-10 and IL-13 cytokines.

Generation of pro-inflammatory mediators like IL-1 α , IL-6, IL-8 and TNF α in human epidermal keratinocytes upon treating these cells with toxic skin irritants was proven in the past [110,111]. Among the 10 cytokines measured, only IL-1 α , IL-6, IL-8 were expressed in detectable quantities above confidence levels in HEK cells. Interleukin 1 is a pro-inflammatory cytokine produced by activated macrophages. It also helps to activate T cells. IL-1 α stimulates further release of secondary mediators, including IL-8. IL-8 promotes dendritic cells migration and recruitment of monocytes and neutrophils as key steps in the initiation phase of cutaneous inflammation [112]. IL-8, a powerful neutrophil attractant and produced by keratinocytes after external stimuli by an irritant. IL-6 promoted keratinocyte cell proliferation and over expression might lead to toxicity in the skin. There was a dose dependent expression of these pro-inflammatory cytokines in HEK cell lines after exposing to FPP at different concentrations. The concentrations of these expressed cytokines in samples were compared with positive standards. With FPP at high concentrations, the production of IL-1 α , IL-6, were observed in HEK cell lines. There was no expression of IL-8 in HEK with FPP but the positive standards expressed IL-8. In HDF cells treated with FPP, there was only IL-6 expression, which is even very low compared to the standards. Only FPP at a concentration of 250 mg/ml expressed detectable quantities of IL-6, IL-8 and MCP-1 in HDF cells. From the above studies it is clear that the FPP at tested concentrations was safe and not eliciting any inflammatory responses.

4.5. CONCLUSIONS

Soluble microneedle system for FPP for treatment of IDA will serve as a potential alternative to oral and parenteral iron formulations. The ease of self-applicability and avoidance of gastrointestinal side effects are the greatest advantages with iron soluble microneedle system. The developed soluble microneedles were found to dissolve in the skin within 3-4 hours and the

dissolved FPP is maintaining a depot in the skin to release the iron slowly over time. The safety and toxicity studies on cell lines proved that the amount of FPP loaded in microneedle arrays was safe and did not show any toxicity in HEK and HDF cell lines. With desired drug loading in the soluble microneedle array system, dose individualization is possible based on the iron status of the patient and carries great potential by avoiding undesired side effects.

CHAPTER 5
MINIMALLY INVASIVE METHOD FOR DELIVERY OF
IRON-DEXTRAN VIA TRANSDERMAL ROUTE

ABSTRACT

Iron dextran colloidal solution is one among the very few US Food and Drug Administration (FDA)-approved iron sources for parenteral administration. Parenteral route does not allow frequent administration because of its invasiveness and other associated complications. The main aim of this project was to investigate the plausibility of transdermal delivery of iron dextran facilitated by microneedles, as an alternative to parenteral iron therapy. In the first part of the project, microneedle pretreatment was explored for iron dextran delivery. *In vitro* permeation studies were carried out using freshly excised hairless rat abdominal skin (after pretreatment with solid microneedles) in a Franz diffusion apparatus. *In vivo* iron repletion studies were carried out in hairless anemic rat model. The hematological and biochemical parameters were measured periodically during treatment in these animals. In the second part of the study, soluble microneedle system was developed by incorporating iron dextran along with poly(methylvinylether/maelic acid) (PMVE/MA) polymers and *in vitro* studies were carried out across hairless rat skin to study the iron dextran release from soluble microneedle arrays. *In vivo* studies were carried out after application of soluble microneedles in healthy hairless rats and biochemical parameters were measured till 24 hours. The results suggest that microneedle-mediated delivery of iron dextran could be developed as a potential treatment method for iron-

deficiency anemia. Finally, the toxicity of iron dextran was evaluated using human skin cell lines.

5.1.INTRODUCTION

Oral iron therapy remains as choice of first line treatment option for iron deficiency despite its high rates of intolerance and non-adherence. Moreover oral iron salts are readily available and inexpensive. Oral iron salts are not able to replenish iron stores rapidly to meet ongoing losses of iron (blood) especially in case of chronic conditions [113, 114]. Intravenous (i.v.) iron formulations are the preferred option for iron replacement therapy to meet greater iron demands especially in patient undergoing routine hemodialysis. Moreover, parenteral iron formulations are the only choice as an adjunct to erythropoietin stimulating agents (ESAs) in patients undergoing dialysis and having nondialysis-associated chronic kidney diseases (CKD), patients with inflammatory bowel syndrome (IBD) and for oncology patients receiving ESAs for chemotherapy-induced anemia [115].

Among all the parenteral iron formulations; Iron dextran (Imferon®-Large molecular weight iron dextran) was the only FDA approved parenteral formulation in US for almost 40 years (1954-1990s). In 1991, Imferon® was discontinued due to its high adverse events and later a low molecular weight iron dextran [InFed (165 kDa) and DexFerrum (267 kDa)] was approved for clinical use in 1992. Sodium ferric gluconate and iron sucrose injection are available from 1999 and 2000 respectively for clinical use as parenteral iron therapy. Ferumoxytol became available from 2009 for iron replacement in patients with IDA and CKD and recently in 2013; ferric carboxymaltose was also approved for use in US [115]. Even though these new formulations were claimed to be safer than earlier formulations in few clinical trials, the complete safety and toxicity profiles are not established to full extent yet.

Iron dextran is a colloidal solution of high molecular weight ferric oxyhydroxide complexed with polymerized low molecular weight dextran. All i.v. iron agents share the same core chemistry; the core of each particle is an iron-oxyhydroxide gel which is surrounded by a shell of carbohydrate that stabilizes the iron-oxyhydroxide; slows the release of bioactive iron and maintains the resulting particles in colloidal suspension [116].

Iron dextran complex was extensively studied clinically for parenteral therapy to treat iron deficiency anemia. Iron dextran is commercially available as stable, clear, viscous and reddish-brown colloidal suspension containing 5% iron and 20% dextran [117]. Iron dextran is the preferred formulation among the all i.v. colloids due to its established safety profile and unlike other parenteral formulations; iron dextran is the only parenteral formulations approved for intramuscular injection, i.v. bolus injection and total dose infusion as well. Total dose infusion has been associated with a higher incidence of adverse events like hypotension, arthralgias, myalgias, abdominal pain, nausea, and vomiting. A test dose is needed for all i.v. iron formulations and patient should be monitored for at least 1 hour for adverse reactions [116]. Parenteral iron dextran administration is also associated with immediate adverse effects such as dyspnea, abdominal or back pain, nausea and vomiting, fever and urticaria [118]. Fatal anaphylactic reactions were also reported with iron dextran therapy [119-120, 45]. Generally, parenteral iron therapy is considered to be safe and efficacious, but repeated administration could potentially results in toxic amounts of free iron in the blood, sometimes even could prove fatal. Slow and prolonged delivery of iron has been suggested as the best suited way to avoid super saturation of iron carrier protein, transferrin, and to control iron stores in the systemic circulation [75].

Transdermal administration is generally intended for delivery of drugs across the skin over long duration simulating slow intravenous infusion [121]. However, transdermal delivery of therapeutic agents is limited due to high molecular weight (> 500 Da) and high hydrophilicity [122]. Chemical enhancers are known to possess limited ability to enhance the permeation of larger molecular weight therapeutic molecules. Use of microneedles is of great interest in recent days due to their unique ability to facilitate the delivery of macromolecules and colloidal drugs across the skin [123, 124]. Microneedles can create micro conduits for transport of drug molecules across the stratum corneum [81]. In the current study, the feasibility of transdermal delivery of iron dextran using microneedles was investigated. Successful delivery of iron dextran via transdermal route could be a potential option for treating iron deficiency anemia.

5.2. MATERIALS AND METHODS

5.2.1 Materials

Iron dextran (50 mg/mL) was purchased from sigma-aldrich (St. Louis, MO). AdminPen 600 device was purchased from nanoBio Sciences LLC, Alameda, CA. Phosphate buffered saline (PBS, pH 7.4) premixed powder was obtained from EMD Chemicals (Gibbstown, NJ). Ferrover® iron reagent was obtained from Hach Company (Loveland, OH). Serum iron & TIBC kit is obtained from Clinia Corporation (San Marcos, CA) and all other chemicals were obtained from Fischer scientific (Fairway, NJ).

5.2.2 Methods

5.2.2.1 Preparation of rat skin

Male hairless rats were used in both *in vitro* and *in vivo* studies, obtained from Charles River, Wilmington, MA, USA. All the animals were of eight weeks old and weighing between 250-300 g. For the preparation of rat skin, animals were asphyxiated with CO₂ and abdominal

skin was excised, subcutaneous fat was removed and the skin pieces were cleaned carefully with normal saline. The rat skin was used on the same day for all *in vitro* experiments. All animal studies were approved by the Institutional Animal Care and Use committee (IACUC) at the University of Mississippi (Protocol # 10-013 & # 11-016).

5.2.2.2 Measurement of hydrodynamic radius of iron dextran

Particle size (hydrodynamic radius) of the iron dextran colloid was measured by dynamic light scattering (DLS) or photon correlation spectroscopy technique using Zetasizer 3000HSA (Malvern Instruments Ltd, Westborough, MA).

5.2.2.3 General *in vitro* experimental setup

In vitro studies were carried out in vertical Franz Diffusion Cell apparatus (Logan Instruments, Boston, MA). The rat skin was sandwiched between the donor and receiver compartment of Franz diffusion cell, with stratum corneum facing the donor compartment of the cell. The active diffusion area was 0.64 cm². The AC electrical resistance of skin was measured with the help of an electric circuit consisting of a digital multimeter and waveform generator (Agilent Technologies, Santa Clara, CA) having a load resistor R_L (100 kΩ) in series with the skin. The voltage drop across the whole circuit (V₀) and across the skin (V_s) was measured and skin resistance was determined by applying a voltage of 100 mV at 10 Hz in the circuit. Skin pieces with a resistance of ≥ 20 kΩ/cm² were considered for permeation studies [125].

5.2.2.4. *In vitro* transdermal permeation studies

5.2.2.4.1 Permeation of iron dextran

After measuring electrical resistance of the skin, the donor compartment was filled with 200μL of 50 mg/mL iron dextran solution and receiver compartment was filled with 5 mL of freshly prepared phosphate buffered saline (pH 7.4). During all *in vitro* permeation studies, the

temperature of receiver compartment was maintained at $37\pm 1^{\circ}\text{C}$ by water circulation. Permeation studies were carried out for 6 hours and one ml samples were collected from the receiver compartment at predetermined time intervals (0, 1, 2, 3, 4, 5 and 6 h). Amount of iron permeated into the receiver compartment across skin was determined with the help of EZ201 UV spectrophotometer (Perkin Elmer, Waltham, MA) using FerroVer® iron reagent at 510 nm.

To study the effect of microneedle pretreatment on the permeation of iron dextran, freshly excised hairless rat skin was pretreated with AdminPen 600 stainless steel microneedles, having an area of 1cm^2 containing 187 microneedles with height of $500\ \mu\text{m}$, for two minutes before mounting on the Franz diffusion apparatus.

5.2.2.4.2. Iron dextran retained in the skin

After *in vitro* permeation study, the active diffusion area ($0.64\ \text{cm}^2$) was excised with biopsy punch and the surface was washed thoroughly with normal saline, to ensure complete removal of any iron dextran adhering to the skin surface. The biopsied skin was then cut into small pieces and homogenized in a vial containing 5mL of 1N sodium hydroxide (NaOH) and incubated at 37°C for 24hrs with intermittent shaking. The solutions were centrifuged to remove any interfering substance and supernatant was collected and analyzed for iron content.

5.2.2.5. Iron repletion studies in anemic rats

5.2.2.5.1. Induction of iron deficiency anemia in rats

In vivo studies were performed in hairless rats. The animals were housed in conventional cages with 12:12 hour day: light cycles maintained in the facility, during the entire study period. Rats (n=18) were on normal diet and were allowed to adapt to the study environment for one week. Initially 200 μl of blood samples were collected in EDTA (ethylenediaminetetraacetic acid) coated Microvette® tubes (Sarstedt, Newton, NC) and 0.5 ml of blood was collected into

1.5 ml centrifuge tubes (Eppendorf, Hauppauge, NY) from all animals by retro orbital bleeding method. Blood samples collected in EDTA coated tubes were analyzed for hematological parameters like hemoglobin (Hb), hematocrit (HCT), red blood cells (RBC), mean corpuscular volume (MCV), mean corpuscular hemoglobin (MCH) and mean corpuscular hemoglobin concentration (MCHC) using VetScanHM2 hematology system (Abaxis, Union city, CA). Serum was separated from blood sample collected in centrifuge tubes and analyzed for biochemical parameters like serum iron (SI), total iron binding capacity (TIBC) and % transferrin saturation (%TS) (Basal values in healthy normal rats). Following initial screening, rats were fed with low iron content diet (~2-6 ppm, Harlan laboratories, Madison, WI) till the end of study. Iron deficiency was induced in rats in 5 weeks since the inception of custom made low iron diet which was further confirmed by measuring the blood hemoglobin and hematocrit values. The anemic rats were divided into intact skin (control), microneedle pretreated, and intraperitoneal (i.p.) groups (n=6) depending on the mode of delivery of iron.

5.2.2.5.2. Delivery of iron dextran, *in vivo*

Animals in the control and microneedle pretreatment group were anesthetized using ketamine + xylazine (80+10 mg/kg) via intra peritoneal route. In case of control group animals, a transdermal patch loaded with 200 μ L of 50 mg/mL iron dextran was placed on the dorsal side of the rat for 6 hrs. For microneedle pretreated group, rats were pretreated with AdminPen 600 microneedles (10 cm^2) on dorsal surface for 2 minutes followed by the application of a transdermal patch, loaded with 200 μ L of 50 mg/mL iron dextran solution for a period of 6 hours. The treatment was continued for 3 weeks on alternate days. The third group (intraperitoneal group) of animals was administered with 100 μ l of iron dextran solution (10 mg/ml) in saline via intraperitoneal route on alternate days for 3 weeks. Blood samples were

drawn from animal in all groups intermittently and at the end of treatment period and hematological and biochemical parameters were evaluated.

5.2.2.5.3. Red blood cell morphology

Blood samples were withdrawn from rats at healthy, anemic and post treatment conditions, from all the three groups and the red blood cells (RBC) were visualized under high resolution optical microscope to study their cell morphology. In brief, a drop of venous blood was collected and smears were prepared by wedge slide method and stained using Wright-Giemsa stain. The RBCs were visualized with oil immersion using high resolution light microscope (Axiolab A1, Carl Zeiss, USA) at 100x magnification. Images of RBCs were captured using Carl Zeiss camera attached to the microscope.

5.2.2.6. Preparation of soluble microneedles

Soluble microneedles containing iron dextran were prepared using water soluble polymers. Aqueous blends containing 15% w/w poly (methylvinylether/maelic acid (PMVE/MA) (Gantrez®AN-139, Ashland, Kidderminster, UK) and the relevant concentration of iron dextran (3 mg and 5 mg of iron in 300 and 600 mg of matrix respectively) were prepared and used to fabricate microneedle arrays using laser engineered silicone micromould templates [98]. The arrays were composed of 121 (11x11) needles perpendicular to the base, of conical shape ranging in height between 450 and 600 μm with base widths about $\sim 300 \mu\text{m}$.

5.2.2.7. Morphology of microneedles

Morphology of microneedles was evaluated with the help of Scanning Electron Microscopy (SEM) studies. Briefly, the microneedle array was fixed on aluminum stubs and using glued carbon tapes and coated with gold using Hummer 6.2 sputter coater (Anatech USA, Union City, California). The sputter coating chamber was supplied with argon gas throughout the

coating process. Photomicrographs of the microneedle arrays were acquired using a model JSM-5600 scanning electron microscopy (JEOL Ltd., Tokyo, Japan).

5.2.2.8. *In vitro* permeation studies of iron dextran

In vitro permeation studies were carried out across hairless rat skin using Franz diffusion cell set up as described earlier in section 2.2.4.1. After insertion of microneedles into the rat skin iron dextran permeation studies were carried out for 24 hours. The amount of iron dextran permeated over time across rat skin was measured using inductively coupled plasma mass spectrometry (ICP-MS) [Thermo Fisher Scientific, Waltham, MA]. The amount of iron retained at the active microneedle array application site was also measured.

5.2.2.9. *In vivo* studies in hairless rats

In vivo studies were carried out in hairless rats (n=6). Only microneedle arrays incorporated with high drug load of iron dextran (~430 µg of elemental iron) was used for *in vivo* studies. Rats were divided into control group and treatment group. In treatment group, the microneedle arrays were applied by firmly pressing them against the rat skin using thumb and the array was secured with the help of a surgical tape. Microneedle array was removed after 12 hours and blood samples were collected from animals every 3 hours, starting from 0 hour till 24 hours. Biochemical parameters like serum iron, total iron binding capacity (TIBC) and % transferrin saturation (%TS) were measured using Serum iron & TIBC kit. A control group was included with transdermal application of iron dextran solution for 12 hours.

5.2.2.10. Evaluation of safety and toxicity of iron dextran in human skin cell lines

The safety studies of iron dextran were carried out using human epidermal keratinocyte (HEK) [HEK001 (ATCC® CRL-2404™)] continuous cell lines and Human Skin Fibroblast (HDF) [CCD1093Sk (ATCC® CRL2115™)] cell lines [ATCC, Manassas, VA].

5.2.2.10.1. Cell culture studies

HEK cells were grown in keratinocyte serum free medium (GIBCO-BRL 17005042) with 5 ng/ml human recombinant epidermal growth factor (EGF) and 2mM L-glutamine (without bovine pituitary extract and serum) in cell culture flasks (75 cm²) to approximately 80% confluence in 5% CO₂ environment incubator maintained at 37 °C. HDF cells were grown in Eagle's Minimum Essential Medium (EMEM) (ATCC-302003) with 10 % FBS in cell culture flasks (75 cm²) to approximately 80% confluence in 5% CO₂ incubator at 37°C. Both the cell media were supplemented with penicillin (10000 units) and streptomycin (10 mg/mL) solution. The cells were seeded into clear/black wall 96-well microplates at a density of 200,000 cells/ml (200 µL) and cell proliferation/viability assay, reactive oxygen species (ROS) measurement assay and cytokines assays were performed. Cell count was obtained with Bio-Rad automatic cell counter (Bio-Rad, Hercules, CA) after staining an aliquot of cell suspension (10 µl) with 10 µl of Trypan blue stain (0.4 %) [Life Technologies, Grand Island, NY]. For HEK cell lines, passage number 78 and for HDF cell lines, passage number 6 were used in all the experiments.

5.2.2.10.2. Cell viability/proliferation assay

Cell proliferation assay was carried out using The CellTiter 96[®] AQueous one solution reagent (Promega, Madison, WI) which can be used to measure the number of viable cells by colorimetric method. After reaching approximately 80% confluence of the cells in microplates, the media in all the wells for both HEK and HDF cell lines was replaced with 100 µL of fresh medium (without serum and penicillin streptomycin solution). Cell lines were exposed to 100 µL of either basal medium (control) or serial dilutions of iron dextran prepared at different

concentrations (10, 5, 2.5, 1.25, 0.62 and 0.31 mg/ml) or digitonin solution (positive control) [Promega, Madison, WI] prepared at different concentrations (60 µg/ml-1.87 µg/ml) with serial dilutions for 24 hours. Iron dextran solutions were prepared in basal medium and digitonin solutions were prepared from a stock of 20 mg/ml using cell culture grade dimethylsulfoxide (DMSO) [ATCC, Manassas, VA]. Untreated cells served as control in this study. The CellTiter 96[®]Aqueous one solution reagent was completely thawed in water bath at 37°C for 10 minutes before use and 40 µl of this reagent was added to each well in the 96 well plate containing the cells and the plate was incubated at 37 °C in a humidified, 5 % CO₂ atmosphere for 4 hours. After incubation the absorbance at 490 nm was recorded using microplate Reader (SpectraMax[®] M5, Molecular Devices, LLC. Sunnyvale, CA). Testing at each concentration of the iron dextran and positive standard was performed in triplicates.

5.2.2.10.3. Measurement of Reactive Oxygen Species (ROS) activity/oxidative stress markers

Possible generation of reactive oxygen species (ROS) and the ROS activity intracellularly upon treating both HEK and HDF cell lines with iron dextran at different concentrations was measured using Oxiselect[™] intracellular ROS assay kit (Cell Biolabs, San Diego, CA). After reaching approximately 80% confluences in 96-well microplates, both the cell lines were treated with cell permeable fluorogenic probe 2', 7'-dichlorodihydrofluorescein diacetate (DCFH-DA). Cells loaded with DCFH-DA were washed gently with Dulbecco's Phosphate-Buffered Saline (DPBS) (Sigma Aldrich, St. Louis, MO) 2-3 times and 100µL of fresh medium was added to all the wells and treated with 100µL of iron dextran prepared at different concentrations (10, 5, 2.5, 1.25, 0.62 and 0.31 mg/ml) or hydrogen peroxide (H₂O₂) (positive control) prepared at different concentrations (2000-62.5 µM) for 24 Hours. Later cells were washed 2-3 times again with

DPBS and 100 μ L of fresh medium and 100 μ L of 2X cell lysis buffer was added. After 5 minutes of incubation, 150 μ L of this medium was transferred to a black wall 96-well microplate and fluorescence was measured. Untreated cells served as control in this study. All the studies were performed in triplicates. The results obtained were compared using a standard calibration curve plotted for 2', 7'-dichlorodihydrofluorescein(DCF) from 0.01 nM to 10 μ M using both media.

5.2.2.10.4. Measurement of cytokines as inflammatory response

Levels of various pro-inflammatory cytokines generated in HEK and HDF cell lines after addition of iron dextran at different concentrations for 24 hours was assayed using Quantibody[®] Human Inflammation Array 1 kit (RayBiotech, Inc. Atlanta, GA). Quantibody[®] array uses the multiplexed sandwich ELISA-based technology which can determine the concentration of multiple cytokines simultaneously and accurately. In the present study, 10 human cytokines, IL-1 α , IL-1 β , IL-4, IL-6, IL-8, IL-10, IL-13, MCP-1, IFN γ and TNF α levels expressed in cell lines were measured after cells were treated with iron dextran for 24 hours. Digitonin (30 μ g/ml) and H₂O₂ (1000 μ M) were used as positive controls. After reaching approximately 80% confluence, the media in all the wells for both HEK and HDF cell lines was replaced with 100 μ L of fresh medium (without serum and penicillin streptomycin solution) and cell lines were exposed to 100 μ L of either basal medium (control) or serial dilutions of iron dextran prepared at different concentrations (10, 5, 2.5, 1.25 mg/ml) for 24 hours. Untreated cells served as control in this study. The standard glass slide provided as Quantibody[®] array was spotted with 16 wells of identical cytokine antibodies arrayed in quadruplicate. Cell supernatant from each well of 96 microplate (samples) or standard were loaded into each spotted well of the glass slide. After proper wash steps with the wash buffers detection antibody cocktail was added to each

spottedwell and incubated for overnight. Later, detection antibody cocktail was discarded and after proper wash steps Cy3 equivalent dye-conjugated streptavidin was added to each well and the glass slide was incubated in dark for overnight again. After incubation, glass slide was washed again and completely air dried and the signals were visualized through use of a laser scanner equipped with a Cy3 wavelength (Axon GenePix) and data was extracted. Quantitative data analysis was performed using Quantibody® Q-Analyzer software (RayBiotech, Inc. Atlanta, GA).

5.2.3 Statistical analysis

GraphPadInStat 3 software was used for statistical analysis. One-way ANOVA was used to determine the level of significance for correlation between parameters and $P < 0.05$ was considered as the significant difference. Unpaired t-test was used to determine the level of significance for correlations in absorbance and florescence values observed in cell studies between iron dextran and positive controls. A significance level of $p < 0.05$ was considered as statistically significant.

5.3. RESULTS AND DISCUSSION

Skin is known to be a formidable barrier to the penetration of large molecular size therapeutic agents [122]. However, certain studies have demonstrated permeation of macromolecular substrates across the skin [126]. Some reports even demonstrated the penetration of particulate drug delivery systems ranging from nanometer to micrometer size [127, 128] into the skin. Recently, Sonavane and co-workers have demonstrated the *in vitro* delivery of gold nanoparticles of various sizes across rat abdominal skin. The authors reported that, nanoparticles with average size of 15nm permeated across rat abdominal skin in significantly higher amounts than those of 102nm and 198nm at the end of 12h. The X-ray

spectroscopy studies revealed deeper localization of 15nm size particles than the larger particles [129].

The hydrodynamic diameter of iron dextran was measured using DLS technique and found to be ~ 14 nm. In the present study even at the end of 12 h (data shown up to 6 h) there was no iron dextran detected in the receiver compartment indicating practically no permeation across the rat skin. Moreover, there was no iron dextran detected in the skin either. Despite all the *in vitro* experimental conditions being similar, it is still unknown at this stage, the reasons for conflicting observation between our studies and the studies by Sonavane and co-workers.

Recently, iontophoresis has been shown to enhance the dermal penetration and permeation of particulate substances even up to the size of ~100 nm [130, 131]. In the present study, even application of a constant electrical current (both anodal and cathodal) at 0.5 mA/cm² could not enhance the permeation of colloidal iron dextran across the abdominal rat skin (data not shown). It is likely that at this current density, the electrophoretic driving force is not strong enough to drive the colloidal particles of huge mass.

So far, many research groups have studied the effect of microneedles on the transdermal delivery of a wide range of molecules with different physico-chemical properties [132-135]. Microneedles are micron sized needles and have the potential to deliver micro and macro molecules across the skin without causing significant pain [136]. The effect of microneedles on delivering both small and large molecules including proteins, peptides and genes into the skin was explored in the past [81, 132, 135&137]. Several reports exist on the delivery of particulate systems utilizing microneedles via transdermal route. Kohli and Alpar demonstrated that, nanoparticles of 50 nm or less in size can penetrate into the skin layers [138]. Therefore, the

effect of microneedle pretreatment of skin on the permeation of iron dextran was investigated in this study.

5.3.1 *In vitro* permeation of iron dextran

In vitro permeation studies of iron dextran were carried out for 6 hours after pretreating the rat skin with AdminPen 600 microneedles for 2 minutes. The cumulative amount of iron dextran permeated at the end of 6th hour was found to be $10.28 \pm 0.45 \mu\text{g}/\text{cm}^2$ (Figure5-1). After the completion of *in vitro* permeation studies for 6 hours, $2.48 \mu\text{g}/\text{mg}$ of iron dextran was found to have retained in the skin. *In vitro* permeation studies concluded that microneedle pretreatment could lead to delivery of substantial amount of iron-dextran across the skin.

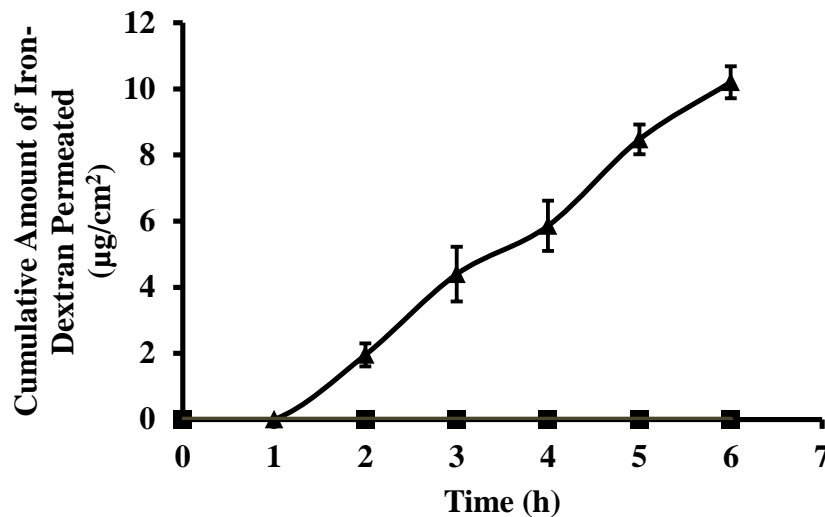


Figure5-1. *In vitro* permeation studies of Iron dextran across the (■) intact hairless rat skin (control) and (▲) skin pretreated with microneedles.

5.3.2. Iron repletion studies in anemic rats

Initially, healthy animals were checked for all hematological and biochemical parameters and recorded as basal values. Iron deficiency anemia was induced in all animals (n=18) by feeding low iron diet for five weeks. There was a significant change in the hematological

parameters, indicating successful induction of anemia. The first step in the typical diagnosis of iron deficiency anemia includes measuring the hemoglobin levels in the blood. Along with hemoglobin levels, measurement of MCV, HCT and other red blood cell indices are critical in assessing the status of iron deficiency anemia. Hematocrit measures the percent volume of red blood cells in unit volume of whole blood. MCV gives the average volume and size of red blood cell and in case of iron deficiency condition; microcytic and hypochromic erythrocytes are usually observed. The RBC morphology in iron deficient rat clearly shows the presence of microcytic RBC (figure 5-3b). MCH is the average mass of hemoglobin in red blood cell and MCHC is the measure of concentration of hemoglobin in a given volume of packed red blood cells. The red cell distribution width is a measure of the variation of red blood cell width and is used in combination with the mean corpuscular volume in differential diagnosis of various other anemic conditions. In this study, the mean hemoglobin and RBC values at healthy condition was 14.43 ± 0.81 g/dL and $8.59 \pm 0.44 \times 10^{12}$ /L respectively were found to decrease to 10.06 ± 1.05 g/dL and $6.32 \pm 0.59 \times 10^{12}$ /L when the rats were induced anemic condition.

Serum samples were analyzed for biochemical parameters. The average values of serum iron before and after inducing anemia were found to be 187.96 ± 3.04 μ g/dL and 91.20 ± 10.58 μ g/dL, respectively. The TIBC values increased from 351.60 ± 16.64 μ g/dL to 556.90 ± 58.39 μ g/dL. There was a decrease in mean % TS from 42.43 ± 3.12 to 16.01 ± 0.76 after inducing anemia compared to healthy state. Serum iron and %TS decreased significantly, while the TIBC values increased after inducing anemia. Serum iron measures the transferrin bound iron in blood and TIBC measure the amount of transferrin that is still available to bind and transport iron. %TS gives the ratio of SI to TIBC which is an accurate measurement compared to individual

measurements of SI and TIBC. Mean values of other hematological parameter of healthy and anemic condition of all the rats (n=18) are shown in table 5-1.

5.3.2.1 Transdermal delivery of iron dextran, *in vivo*

The anemic rats were divided into three groups and were treated with iron dextran using different modes of delivery. Polyolefin foam patch of area 10 cm² was loaded with 200 µL of iron dextran solution and placed on the dorsal surface of the rats in case of control group. Whereas, in case of microneedle pretreatment group, the dorsal surface of the rat was pretreated with AdminPen 600 microneedles for 2 minutes and then the patch was placed on the treated surface for six hours.

The treatment was continued for 3 weeks on alternate days. Blood samples were collected by retro-orbital bleeding and all hematological and biochemical parameters were evaluated at the end of 2nd and 3rd week. In case of control group, the hematological or biochemical parameters turned out to be severely poor at the end of 2nd week. This indicates that, there is no feasibility of delivery of iron dextran via passive transdermal delivery without microneedle pretreatment. Therefore, the passive transdermal delivery treatment was not continued to prevent endangering the lives of rats. However, in case of microneedle pretreated group, there was a significant improvement in all the parameters at the end of 3rd week. The mean biochemical parameter values, prior to inducing anemia, after inducing anemia, after treatment with iron dextran in case of microneedle pretreated group and intraperitoneal injection group are shown in figure 5-2.

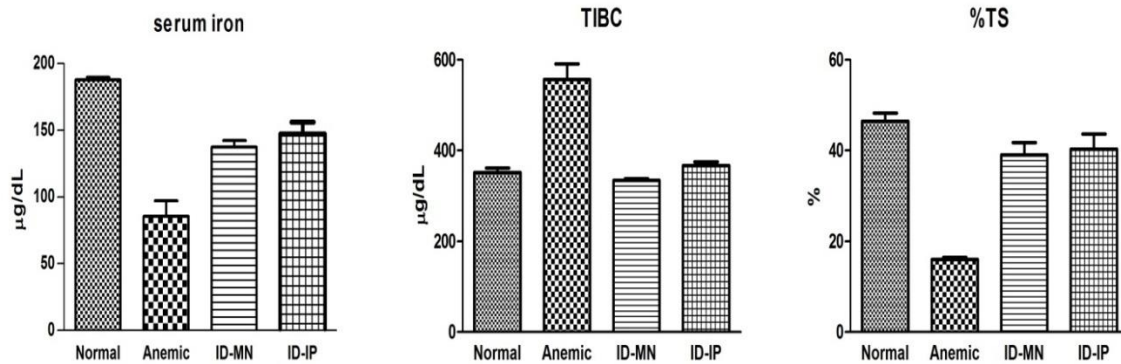


Figure 5-2. The mean values of all biochemical parameters, prior to inducing anemia (Normal), after inducing anemia (Anemic), after treating with iron dextran (microneedle pretreatment (ID-MN)) and treatment with intraperitoneal injection of iron dextran (ID-IP).

The mean hemoglobin value of 10.36 ± 0.57 g/dL at anemic condition increased to 13.96 ± 0.51 g/dL in microneedle pretreated group. An increase in the hemoglobin level of 1 g per dL for every two to three weeks is considered as an effective iron replacement therapy [139, 14]. The mean SI, TIBC and %TS at the end of study in case of microneedle treated group were found to be 137.63 ± 8.07 µg/dL, 334.23 ± 6.14 µg/dL and 39.03 ± 4.75 %, respectively (figure 5-2). Mean values of all hematological parameters are shown in table 5-1. There was significant improvement in the morphology of RBCs in microneedle treatment group of rats compared to anemic condition (Figure 5-3c).

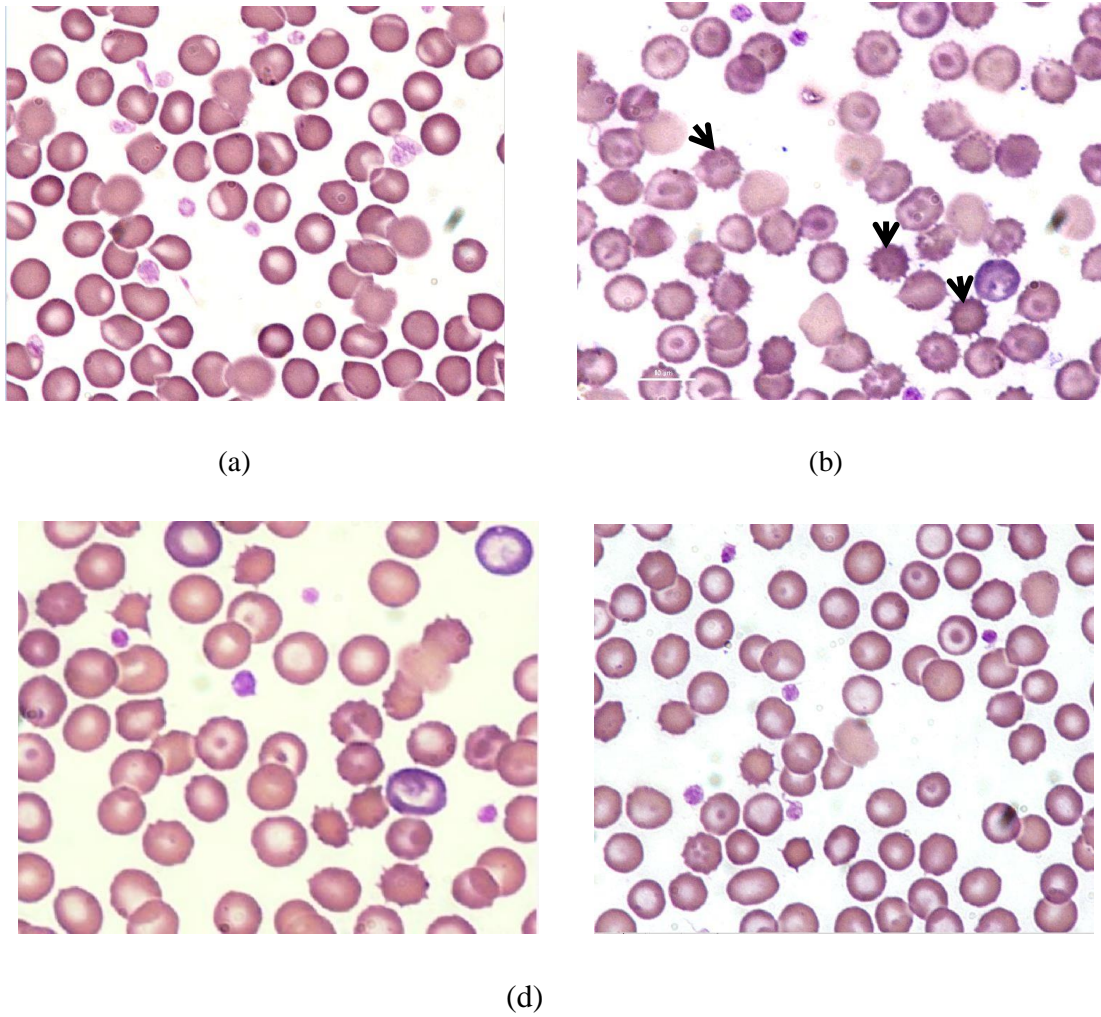


Figure 5-3. Representative pictures of morphology of RBCs (a) RBCs in healthy rats (b) RBCs of anemic rats (arrow marks point the microcytic and hypochromic RBC) (c) RBCs of rats treated with iron dextran following microneedle pretreatment and (d) RBC of rats received iron dextran through intraperitoneal injection.

5.3.2.2. Intraperitoneal delivery of iron dextran

Iron dextran was administered via intraperitoneal route on alternate days to one of the groups to serve as positive control. There was statistically significant improvement in all the biochemical and hematological parameters in the positive control group. The mean SI, TIBC and %TS values at the end of study was found to be $147.30 \pm 15.56 \mu\text{g/dL}$, 366.90 ± 14.07

$\mu\text{g/dL}$ and $40.29 \pm 5.78 \%$ followed by IP injection of iron dextran (Figure 5-2). All other hematological parameters are shown in the table 5-1.

Hematological Parameter	Healthy rats	Anemic condition	After microneedle pretreatment	Intraperitoneal group
Hemoglobin (g/dL)	14.43 ± 0.81	10.06 ± 1.05	13.96 ± 0.51	14.5 ± 0.22
RBC ($\ast 10^{12}/\text{L}$)	8.59 ± 0.44	6.32 ± 0.59	10.25 ± 0.95	10.32 ± 0.25
Hematocrit (%)	42.65 ± 1.28	33.24 ± 3.37	41.87 ± 4.98	41.48 ± 0.91
Mean Corpuscular Volume (fL)	55.33 ± 4.12	45.31 ± 3.07	41.33 ± 2.25	46.03 ± 2.02
Mean Corpuscular hemoglobin (pg)	19.30 ± 1.58	14.93 ± 0.68	14.86 ± 0.68	18.30 ± 0.75
Mean Corpuscular hemoglobin concentration (g/dL)	35.39 ± 0.87	30.00 ± 1.83	32.03 ± 2.21	34.01 ± 0.73
Red blood cell distribution width (%)	16.47 ± 0.81	15.47 ± 3.87	16.73 ± 1.50	17.73 ± 0.73

Table 5-1. The mean values of hematological parameters, prior to inducing anemia (healthy), after inducing anemia, after treating with iron dextran in case of microneedle pretreatment and after treating with iron dextran via intraperitoneal route.

Iron dextran is known to be readily uptaken by the reticuloendothelial system from the intravascular fluid compartments and processed to make the iron available to the body for different biochemical and physiological needs [115]. Treatment of iron deficiency with iron dextran solution via intravenous route is well established [140]. In the present study, the levels of hemoglobin and other parameters were close to that of normal condition (baseline values) at the end of 2nd week in case of positive control group (IP). On the other hand, in case of

microneedletreated group biochemical and hematological parameters were statistically significant from its basal levels at the end of third week after treatment initiation.

5.3.3. Soluble iron dextran microneedles

Soluble microneedle arrays incorporating two different iron dextran loads (with 3 mg and 5 mg of initial drug loads) were prepared successfully using aqueous blends of 15% w/w poly (methylvinylether/maelic acid) (PMVE/MA) via laser-engineered silicone micromould templates as described by Donnelly *et al* (2011) previously [98]. In case of microneedle arrays with 3 mg drug load, final amount of elemental iron presented in the arrays was estimated to be $\sim 260 \mu\text{g}$ and for microneedle arrays with 5 mg drug load, final amount of elemental iron presented in the arrays was $\sim 430 \mu\text{g}$.

5.3.4 Morphology of soluble microneedles

The prepared microneedles have an average height of $\sim 550 \pm 60 \mu\text{m}$ with an average base radius of $250 \pm 10 \mu\text{m}$ and an average tip radius of $25 \pm 5 \mu\text{m}$.

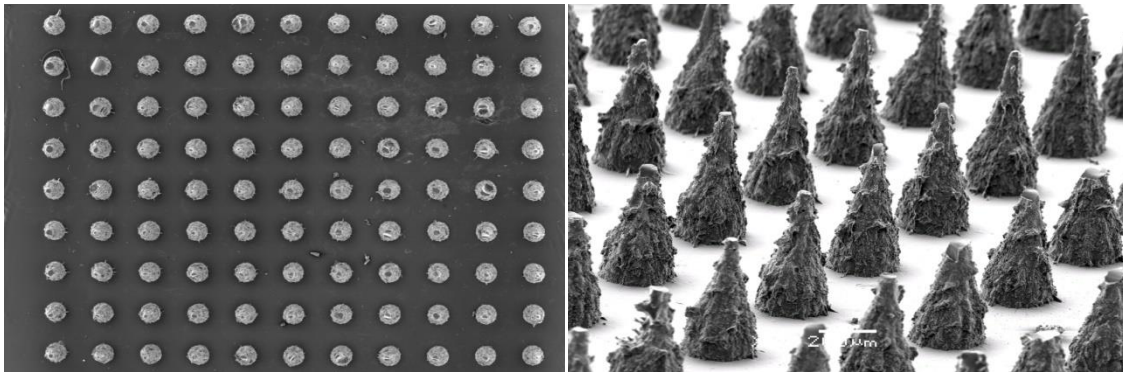


Figure5-4. SEM images of iron dextran soluble microneedle arrays. (a) microneedles array containing 121 microneedles (18X magnification) (b) microneedles array visualized at 75X magnification.

5.3.5. *In vitro* permeation studies of iron dextran from soluble microneedles

From the *in vitro* transport studies after insertion of microneedles in hairless rat skin, there was a lag time of 2 hours was observed. A cumulative amount of $15.66 \pm 0.87 \mu\text{g}/\text{cm}^2$ was

permeated in 24 hours from microneedle array with $\sim 260 \mu\text{g}$ iron and $20.64 \pm 1.84 \mu\text{g}/\text{cm}^2$ was permeated from arrays having $\sim 430 \mu\text{g}$ respectively. The amount of iron retained in the skin at the active array application site was $\sim 0.32 \pm 0.04 \mu\text{g}/\text{mg}$ with microneedle array containing $\sim 260 \mu\text{g}$ iron and $\sim 0.45 \pm 0.07 \mu\text{g}/\text{mg}$ with microneedle array containing $\sim 430 \mu\text{g}$ iron.

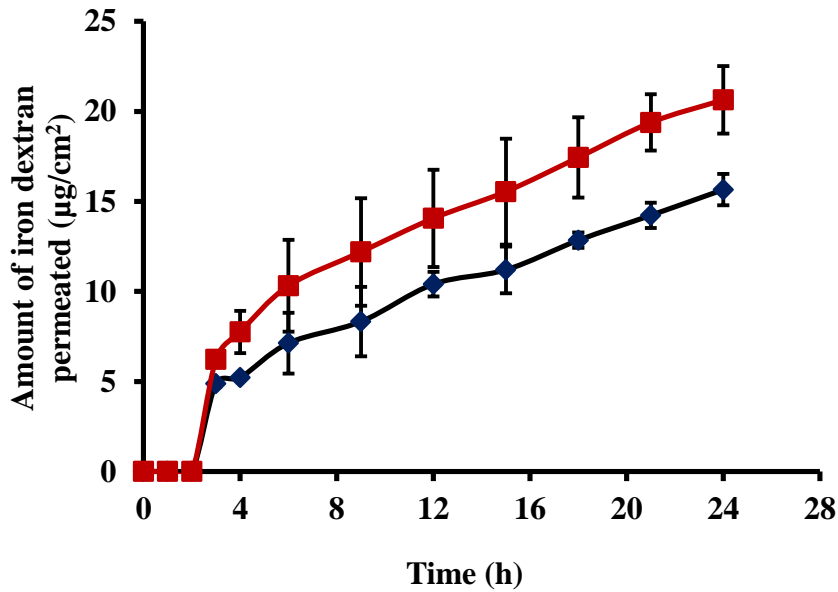


Figure 5-5. The cumulative amount of iron dextran permeated across rat skin from soluble microneedles with $\sim 260 \mu\text{g}$ of iron (◆) and with $\sim 430 \mu\text{g}$ of iron (■). The data points represented are the average of $n= 6 \pm \text{S.D.}$

5.3.6. *In vivo* studies using soluble microneedles

There was a significant increase in the serum iron and % TS after 12 hours of application of the soluble microneedle array to rats compared to the control group. The microneedle array was applied for 12 hours and blood samples were collected for 24 hours. From *in vitro* studies there was a 2 hour lag time for the drug release into the receiver fluid. In case of *in vivo* studies the microneedle array was applied for 12 hours and the total serum iron concentration started improving after 6 hours with a maximum concentration of $208.45 \pm 18.46 (\mu\text{g}/\text{dl})$ detected at 24

hours. The %TS was increased from 48.60 ± 6.77 (at 6 hours) to 65.20 ± 8.7 (at 24 hours). The iron dextran retained in the biopsied section of rat skin after in vivo studies was $\sim 0.36 \pm 0.08$ $\mu\text{g}/\text{mg}$ (with an absolute amount of $\sim 103.5 \pm 8.3$ μg in the tissue).

Iron carbohydrate complexes that are administered into the systemic circulation enters into plasma and phagocytosed within reticuloendothelial system (RES). In RES, iron and carbohydrate complex gets cleaved to generate free iron and stored as ferritin in reticuloendothelial iron pool or transported away by iron export protein ferroportin, and iron gets exchanges with transferrin [115]. The circulating transferrin carries iron to various metabolic pools and bone marrow for erythropoiesis. From a previous study by Henderson *et al*, after intravenous infusions of radiolabelled iron dextran at different dose strengths (100-2000 mg), iron was detected in the RES within few hours and the administered iron getting cleared from plasma into RES in 4-10 days based on the dose strength administered [141]. In the present study, the iron dextran might be releasing slowly from the soluble microneedles and entering into the systemic circulation which might be eventually picked up by RES to release iron from the iron dextran complex.

Biochemical parameters	Time (h)					
	Basal values	3	6	12	18	24
Serum Iron($\mu\text{g}/\text{dl}$)	156.15 ± 27.30	162.05 ± 3.36	161.2 ± 18.95	179.45 ± 8.27	190.9 ± 10.87	208.45 ± 18.46
TIBC ($\mu\text{g}/\text{dl}$)	320.39 ± 11.51	349.55 ± 5.28	347.75 ± 12.52	313.35 ± 6.86	306.55 ± 8.27	319.02 ± 17.82
%TS	48.60 ± 6.77	46.79 ± 8.55	46.48 ± 7.12	57.31 ± 3.89	62.24 ± 1.87	65.20 ± 8.7

Table 5-2. The mean biochemical parameters measured at different time points. Iron dextran soluble microneedle array (430 μg of iron) was inserted into the rat abdominal skin for 12 hours and blood sample were collected till 24 hours. The values represented are the average of $n= 3 \pm$ S.D.

5.3.7. Cell culture studies

5.3.7.1. Cell proliferation assay

MTS [(3-(4,5-dimethylthiazol-2-yl)-5-(3-carboxymethoxyphenyl)-2-(4-sulfophenyl)-2H-tetrazolium)] assay was performed to measure the mitochondrial activity of the cells after treating the cells with iron dextran at different concentrations (10-0.31 mg/ml) and digitonin (60-1.87 µg/ml) (positive control) prepared at different concentration. The absorbance due to the formation of colored formazan by the reduction of tetrazolium compound in presence of the cells was measured at 490 nm. Cell proliferation studies were performed both in HEK and HDF cell lines. In both the cell lines; cells treated with different concentrations of iron dextran exhibited very high absorption. In a different study, the absorbance of iron dextran with basal media without cells was measured in presence of MTS reagent and a background absorbance was observed with iron dextran which might be due to the intense color of iron dextran. Due to the interference of iron dextran at formazan absorption wavelength, MTS assay was not conclusive to determine the cell viability in both the cell lines.

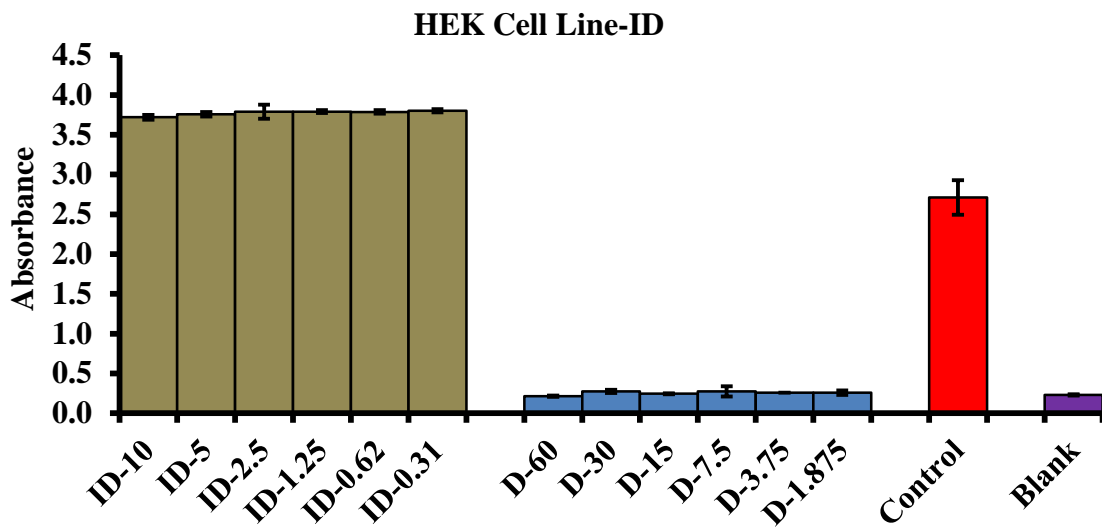


Figure5-6A.

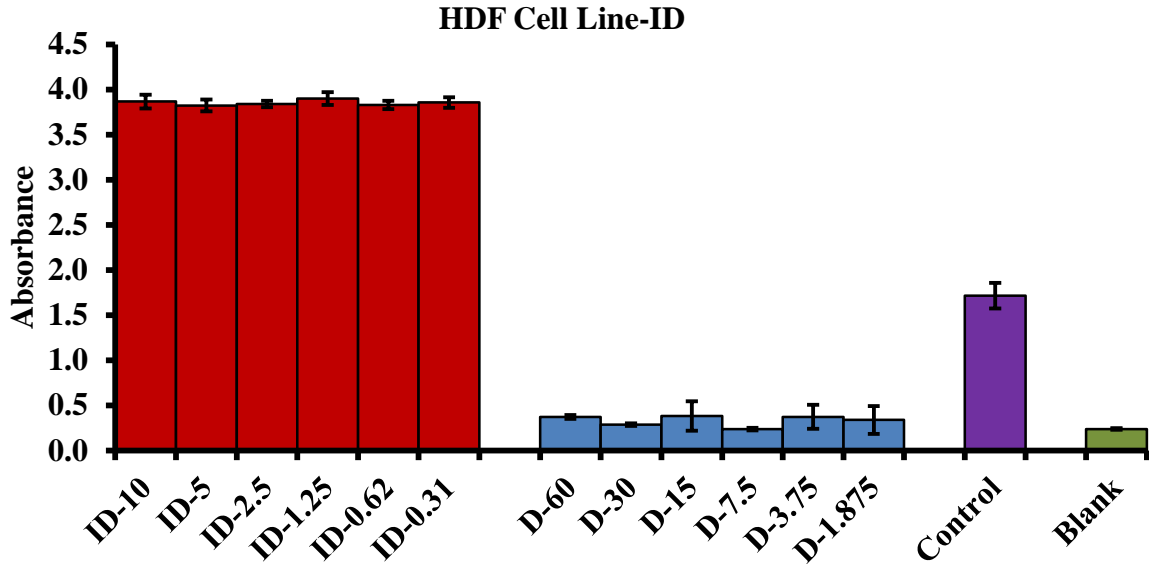


Figure5-6B.

Figure5-6. The mitochondrial activity (MTS activity) of (A) HEK and (B) HDF cells after 24 h exposure to 100 μ l of iron dextran (10-0.31 mg/ml) and digitonin (60 μ g/ml-1.87 μ g/ml). Results are combined from three independent exposures and expressed as mean (\pm S.D.).

5.3.7.2. ROS assay

From figure 5-7, the amount of DCF generated (in florescence units) was very low, indicating that there was no ROS production after treating the cells with iron dextran at different concentrations. In case of cells treated with hydrogen peroxide at different concentrations the amount of DCF produced was high indicating the toxicity in these cell lines.

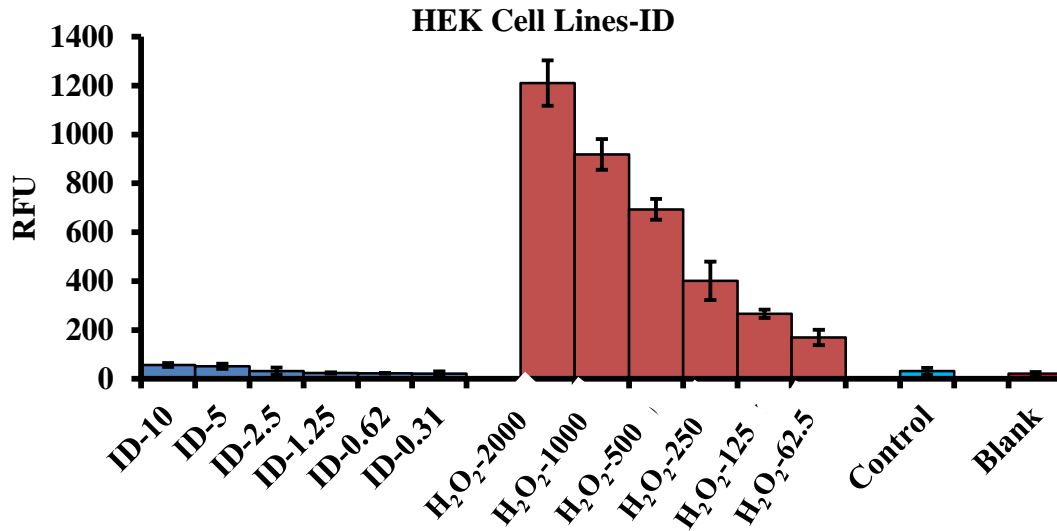


Figure5-7A.

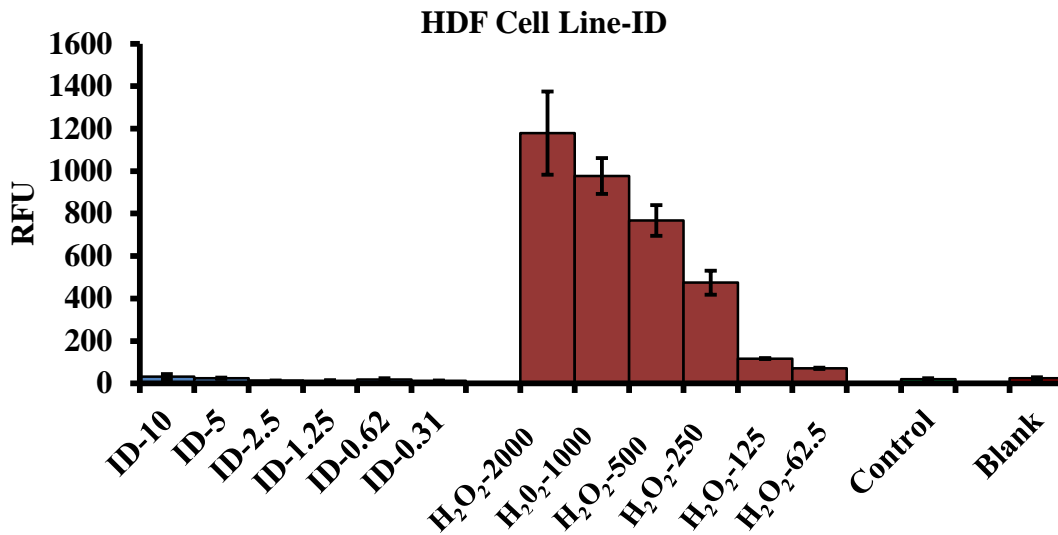


Figure 5-7B.

Figure5-7. Induction of reactive oxygen species (ROS) by iron dextran (10-0.31 mg/ml) or hydrogen peroxide in (A) HEK and (B) HDF cells after 24 h exposure. Results are combined from three independent exposures and expressed as mean (\pm S.D.).

5.3.7.3. Cytokines measurement

All the measured cytokines in this study were excretory proteins and any cytotoxic effect of iron dextran on the cells can be detected by measuring and quantifying these cytokines. In HEK cell lines, a dose dependent expression of IL-1 α , IL-6 levels were observed after exposing the cells to different concentrations of iron dextran. These observed cytokine concentrations were very low compared to cytokines concentrations expressed with positive controls, hydrogen peroxide and digitonin. In HDF cell lines, only a small concentration of IL-6 and MCP-1 were observed with high concentrations of iron dextran (10 mg/ml and 5 mg/ml). From the observed results, iron dextran at these concentrations might be safe to both HEK and HDF cells with no sign of excessive up-regulation of inflammatory markers.

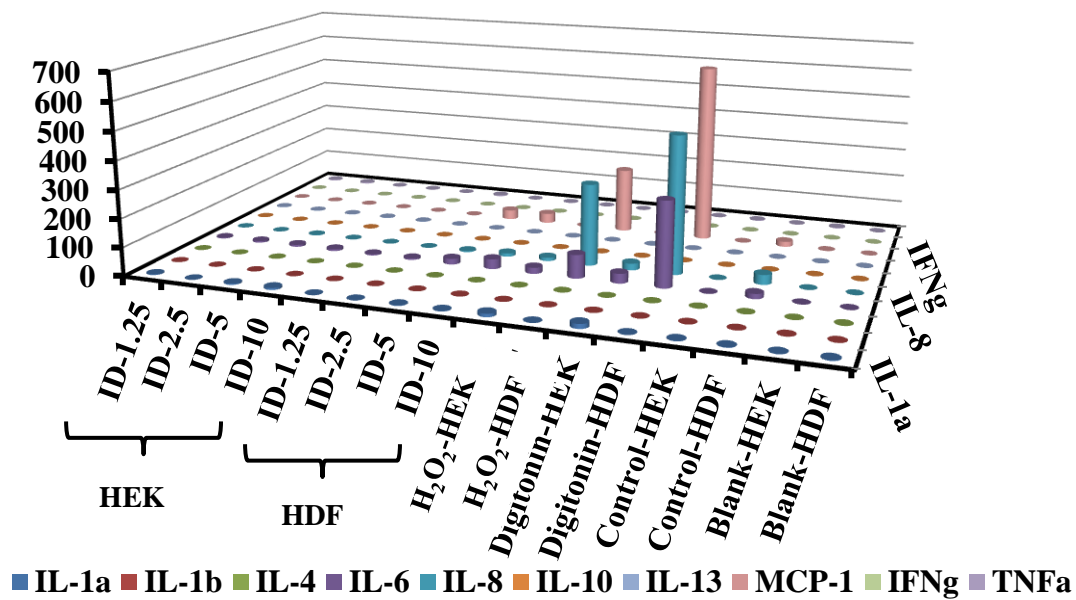


Figure5-8. An overview of the amount of cytokines detected in HEK and HDF cell line after treating them with iron dextran at different concentrations (1.25-10 mg/ml), H₂O₂ (1000 μ M) and digitonin (30 μ g/ml). Results are combined from three independent exposures and expressed as mean (\pm S.D.).

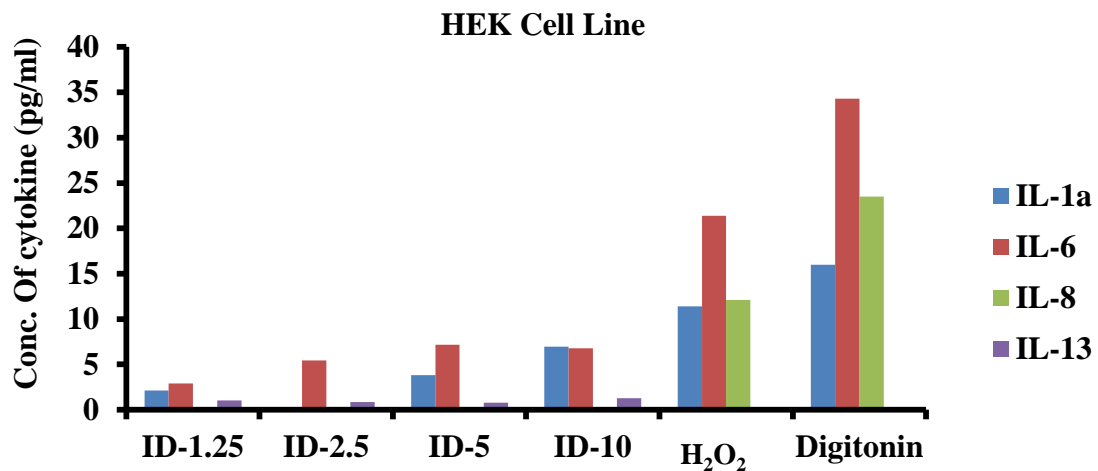


Figure5-9A.

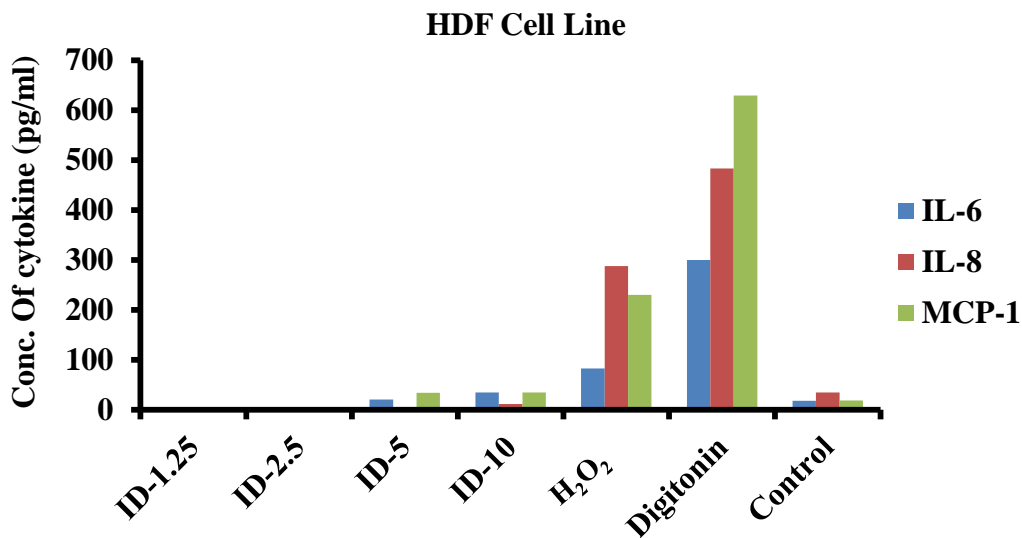


Figure5-9B.

Figure5-9. Presence of cytokines in (A) HEK and (B) HDF cells after 24 h exposure to 100 μ l of iron dextran (1.25-10 mg/ml) and hydrogen peroxide (1000 μ M) and digitonin (30 μ g/ml). Results are combined from three independent exposures and expressed as mean (\pm S.D.).

5.3. CONCLUSIONS

Transdermal delivery of therapeutic agents allows slow and prolonged delivery, which is essential for delivering iron to avoid the saturation of transferrin and to control the free iron stores in the systemic circulation. This study demonstrates the feasibility of microneedle based transdermal delivery of iron dextran as one of the potential routes for iron replenishment. In the preliminary studies the iron dextran delivered transdermally in the form of Poke and Patch proved to be successful to treat iron deficiency anemia in anemic animal models. Further studies with soluble microneedle system is likely to overcome the limitations of parenteral delivery of iron dextran and is believed to be relatively more patient compliant due to minimal invasive nature of the mode of delivery.

BIBLIOGRAPHY

1. Wächtershäuser, G. (1990). Evolution of the first metabolic cycles. *Proceedings of the National Academy of Sciences of the United States of America*, 87(1), 200-204.
2. Wächtershäuser, G. (2000). Origin of life. Life as we don't know it. *Science (New York, N.Y.)*, 289(5483), 1307-1308.
3. Sheftel, A. D., Mason, A. B., & Ponka, P. (2012). The long history of iron in the universe and in health and disease. *Biochimica et Biophysica Acta*, 1820(3), 161-187. doi:10.1016/j.bbagen.2011.08.002; 10.1016/j.bbagen.2011.08.002
4. Santiago, P. (2012). Ferrous versus ferric oral iron formulations for the treatment of iron deficiency: A clinical overview. *The scientific world journal*, 2012, 846824. doi:10.1100/2012/846824; 10.1100/2012/846824
5. Alleyne M, Horne, M.K. & Miller J.L. (2008). Individualized treatment for iron-deficiency anemia in adults. *Am J Med*. 121:943–948.
6. Hercberg, S., Preziosi, P., Briancon, S., Galan, P., Triol, I., and Malvy, D. (1998). A primary prevention trial using nutritional doses of antioxidant vitamins and minerals in cardiovascular diseases and cancers in a general population: The SU.VI.MAX study-- design, methods, and participant characteristics. *Supplementation en Vitamines et minéraux Antioxydants. Controlled Clinical Trials*, 19(4), 336-351.
7. Hostynek, J. J., Hinz, R. S., Lorence, C. R., Price, M., & Guy, R. H. (1993). Metals and the skin. *Critical Reviews in Toxicology*, 23(2), 171-235. doi:10.3109/10408449309117116
8. Cherayil, B. J. (2011). The role of iron in the immune response to bacterial infection. *Immunologic Research*, 50(1), 1-9. doi:10.1007/s12026-010-8199-1; 10.1007/s12026-010-8199-1

9. Chitambar, C. R. (2005). Cellular iron metabolism: Mitochondria in the spotlight. *Blood*, *105*(5), 1844-1845.
10. Recommendations to prevent and control iron deficiency in the United States. Centers for disease control and prevention (1998). *MMWR.Recommendations and Reports: Morbidity and Mortality Weekly Report. Recommendations and Reports / Centers for Disease Control*, *47*(RR-3), 1-29.
11. Trumbo, P., Yates, A. A., Schlicker, S., & Poos, M. (2001). Dietary reference intakes: Vitamin A, vitamin K, arsenic, boron, chromium, copper, iodine, iron, manganese, molybdenum, nickel, silicon, vanadium, and zinc. *Journal of the American Dietetic Association*, *101*(3), 294-301. doi:10.1016/S0002-8223(01)00078-5
12. Al-Sayes, F., Gari, M., Qusti, S., Bagatian, N., & Abuzenada, A. (2011). Prevalence of iron deficiency and iron deficiency anemia among females at university stage. *Journal of Medical Laboratory and Diagnosis*, *2*(1), 5-11.
13. World Health Organization. (2001). *Iron deficiency anaemia: Assessment, prevention and control. A guide for programme managers*. No. WHO/NHD/01.3)World Health organization.
14. Pasricha, S. R., Flecknoe-Brown, S. C., Allen, K. J., Gibson, P. R., McMahon, L. P., Olynyk, J. K., *et al.* (2010). Diagnosis and management of iron deficiency anaemia: A clinical update. *The Medical Journal of Australia*, *193*(9), 525-532.
15. Nissenson, A. R., Goodnough, L. T., & Dubois, R. W. (2003). Anemia: Not just an innocent bystander? *Archives of Internal Medicine*, *163*(12), 1400-1404. doi:10.1001/archinte.163.12.1400

16. Pasricha, S. R., Drakesmith, H., Black, J., Hipgrave, D., & Biggs, B. A. (2013). Control of iron deficiency anemia in low- and middle-income countries. *Blood*, *121*(14), 2607-2617. doi:10.1182/blood-2012-09-453522; 10.1182/blood-2012-09-453522
17. Chen, M. H., Su, T. P., Chen, Y. S., Hsu, J. W., Huang, K. L., Chang, W. H., et al. (2013). Association between psychiatric disorders and iron deficiency anemia among children and adolescents: A nationwide population-based study. *BMC Psychiatry*, *13*, 161-244X-13-161. doi:10.1186/1471-244X-13-161; 10.1186/1471-244X-13-161
18. Ekiz, C., Agaoglu, L., Karakas, Z., Gurel, N., & Yalcin, I. (2005). The effect of iron deficiency anemia on the function of the immune system. *The Hematology Journal : The Official Journal of the European Haematology Association / EHA*, *5*(7), 579-583.
19. Afzal, M., Qureshi, S. M., Lutafullah, M., Iqbal, M., Sultan, M., & Khan, S. A. (2009). Comparative study of efficacy, tolerability and compliance of oral iron preparations (iron edetae, iron polymatose complex) and intramuscular iron sorbitol in iron deficiency anaemia in children. *JPMA. The Journal of the Pakistan Medical Association*, *59*(11), 764-768.
20. Hoen, B., Kessler, M., Hestin, D., & Mayeux, D. (1995). Risk factors for bacterial infections in chronic haemodialysis adult patients: A multicenter prospective survey. *Nephrology, Dialysis, Transplantation: Official Publication of the European Dialysis and Transplant Association - European Renal Association*, *10*(3), 377-381.
21. al-Momen, A. K., al-Meshari, A., al-Nuaim, L., Saddique, A., Abotalib, Z., Khashogji, T., et al. (1996). Intravenous iron sucrose complex in the treatment of iron deficiency anemia during pregnancy. *European Journal of Obstetrics, Gynecology, and Reproductive Biology*, *69*(2), 121-124.

22. Cook, J. D., Finch, C. A., & Smith, N. J. (1976). Evaluation of the iron status of a population. *Blood*, 48(3), 449-455.
23. Breyman, C. (2002). Iron deficiency and anaemia in pregnancy: Modern aspects of diagnosis and therapy. *Blood Cells, Molecules & Diseases*, 29(3), 506-16; discussion 517-21.
24. Besarab, A. (2006). Resolving the paradigm crisis in intravenous iron and erythropoietin management. *Kidney International.Supplement*, (101)(101), S13-8.
25. Neven, E., De Schutter, T. M., Behets, G. J., Gupta, A., & D'Haese, P. C. (2011). Iron and vascular calcification. is there a link? *Nephrology, Dialysis, Transplantation: Official Publication of the European Dialysis and Transplant Association - European Renal Association*, 26(4), 1137-1145. doi:10.1093/ndt/gfq858; 10.1093/ndt/gfq858
26. Wilson, A., Reyes, E., & Ofman, J. (2004). Prevalence and outcomes of anemia in inflammatory bowel disease: A systematic review of the literature. *The American Journal of Medicine*, 116 Suppl 7A, 44S-49S. doi:10.1016/j.amjmed.2003.12.011
27. Kulnigg, S., & Gasche, C. (2006). Systematic review: Managing anaemia in crohn's disease. *Alimentary Pharmacology & Therapeutics*, 24(11-12), 1507-1523. doi:10.1111/j.1365-2036.2006.03146.x
28. Ye, H., & Rouault, T. A. (2010). Human iron-sulfur cluster assembly, cellular iron homeostasis, and disease. *Biochemistry*, 49(24), 4945-4956. doi:10.1021/bi1004798; 10.1021/bi1004798
29. Schultz, I. J., Chen, C., Paw, B. H., & Hamza, I. (2010). Iron and porphyrin trafficking in heme biogenesis. *The Journal of Biological Chemistry*, 285(35), 26753-26759. doi:10.1074/jbc.R110.119503; 10.1074/jbc.R110.119503

30. Richardson, D. R., Lane, D. J., Becker, E. M., Huang, M. L., Whitnall, M., Suryo Rahmanto, Y., et al. (2010). Mitochondrial iron trafficking and the integration of iron metabolism between the mitochondrion and cytosol. *Proceedings of the National Academy of Sciences of the United States of America*, 107(24), 10775-10782. doi:10.1073/pnas.0912925107; 10.1073/pnas.0912925107
31. Ebner, N., & von Haehling, S. (2013). Iron deficiency in heart failure: A practical guide. *Nutrients*, 5(9), 3730-3739. doi:10.3390/nu5093730; 10.3390/nu5093730 doi:10.1038/sj.thj.6200574
32. Groenveld, H. F., Januzzi, J. L., Damman, K., van Wijngaarden, J., Hillege, H. L., van Veldhuisen, D. J., et al. (2008). Anemia and mortality in heart failure patients a systematic review and meta-analysis. *Journal of the American College of Cardiology*, 52(10), 818-827. doi:10.1016/j.jacc.2008.04.061; 10.1016/j.jacc.2008.04.061
33. Ben-Ishay, O., Peled, Z., Othman, A., Brauner, E., & Kluger, Y. (2013). Clinical presentation predicts the outcome of patients with colon cancer. *World Journal of Gastrointestinal Surgery*, 5(4), 104-109. doi:10.4240/wjgs.v5.i4.104; 10.4240/wjgs.v5.i4.104
34. Gupta, R., Lahan, V., & Goel, D. (2012). Primary headaches in restless legs syndrome patients. *Annals of Indian Academy of Neurology*, 15(Suppl 1), S104-8. doi:10.4103/0972-2327.100031
35. Vukovic-Cvetkovic, V., Plavec, D., Lovrencic-Huzjan, A., Galinovic, I., Seric, V., & Demarin, V. (2010). Is iron deficiency anemia related to menstrual migraine? post hoc analysis of an observational study evaluating clinical characteristics of patients with menstrual migraine. *Acta Clinica Croatica*, 49(4), 389-394.

36. Hughes, E. R. (1978). Iron in model and natural compounds. *Human iron metabolism* (pp. 351-373). New York: Marcel Dekker.
37. Beutler, E. (2002). History of iron in medicine. *Blood Cells, Molecules & Diseases*, 29(3), 297-308.
38. Busacchi, V. (1958). Vincenzo menghini and the discovery of iron in the blood. [Vincenzo Menghini e la scoperta del ferro nel sangue] *Bullettino Delle Scienze Mediche*, 130(2), 202-205.
39. Tapiero, H., Gate, L., & Tew, K. D. (2001). Iron: Deficiencies and requirements. *Biomedicine & Pharmacotherapy*, 55(6), 324-332.
40. Silverstein, S. B., & Rodgers, G. M. (2004). Parenteral iron therapy options. *American Journal of Hematology*, 76(1), 74-78. doi:10.1002/ajh.20056
41. Laurence, L. B., John, S. L., & Keith, L. P. (2006). *Goodman & Gilman's the pharmacological basis of therapeutics* (11th ed.). USA: McGraw-Hill.
42. Dennis, L. K., Eugene, B., Anthony, S. F., & et al. (2005). *Harrison's principles of internal medicine* (16th ed.). USA: McGraw-Hill.
43. Rimon, E., Kagansky, N., Kagansky, M., Mechnick, L., Mashiah, T., Namir, M., et al. (2005). Are we giving too much iron? low-dose iron therapy is effective in octogenarians. *The American Journal of Medicine*, 118(10), 1142-1147. doi:10.1016/j.amjmed.2005.01.065
44. Johnson-Wimbley, T. D., & Graham, D. Y. (2011). Diagnosis and management of iron deficiency anemia in the 21st century. *Therapeutic Advances in Gastroenterology*, 4(3), 177-184. doi:10.1177/1756283X11398736; 10.1177/1756283X11398736

45. Hamstra, R. D., Block, M. H., & Schocket, A. L. (1980). Intravenous iron dextran in clinical medicine. *JAMA: The Journal of the American Medical Association*, 243(17), 1726-1731.
46. Zanen, A. L., Adriaansen, H. J., van Bommel, E. F., Posthuma, R., & Th de Jong, G. M. (1996). 'Oversaturation' of transferrin after intravenous ferric gluconate (ferrlecit(R)) in haemodialysis patients. *Nephrology, Dialysis, Transplantation: Official Publication of the European Dialysis and Transplant Association - European Renal Association*, 11(5), 820-824.
47. Schaefer, R. M., & Schaefer, L. (1995). The hypochromic red cell: A new parameter for monitoring of iron supplementation during rhEPO therapy. *Journal of Perinatal Medicine*, 23(1-2), 83-88.
48. Schaefer, R. M., & Schaefer, L. (1998). Iron monitoring and supplementation: How do we achieve the best results? *Nephrology, Dialysis, Transplantation: Official Publication of the European Dialysis and Transplant Association - European Renal Association*, 13 Suppl 2, 9-12.
49. Brown M.B., Martin G.P., Jones S.A. & Akomeah FK. (2006). Dermal and transdermal drug delivery systems: current and future prospects. *Drug Deliv.* 13(3):175-87.
50. Williams, A. C., & Barry, B. W. (2004). Penetration enhancers. *Advanced Drug Delivery Reviews*, 56(5), 603-618. doi:10.1016/j.addr.2003.10.025
51. Benson, H. A. (2005). Transdermal drug delivery: Penetration enhancement techniques. *Current Drug Delivery*, 2(1), 23-33.

52. Gupta, A., & Crumbliss, A. L. (2000). Treatment of iron deficiency anemia: Are monomeric iron compounds suitable for parenteral administration? *The Journal of Laboratory and Clinical Medicine*, 136(5), 371-378. doi:10.1067/mlc.2000.110368
53. Kosch, M., Bahner, U., Bettger, H., Matzkies, F., Teschner, M., & Schaefer, R. M. (2001). A randomized, controlled parallel-group trial on efficacy and safety of iron sucrose (venofer) vs iron gluconate (ferrlecit) in haemodialysis patients treated with rHuEpo. *Nephrology, Dialysis, Transplantation: Official Publication of the European Dialysis and Transplant Association - European Renal Association*, 16(6), 1239-1244.
54. Gupta, A., Amin, N. B., Besarab, A., Vogel, S. E., Divine, G. W., Yee, J., & Anandan, J. V. (1999). Dialysate iron therapy: Infusion of soluble ferric pyrophosphate via the dialysate during hemodialysis. *Kidney International*, 55(5), 1891-1898. doi:10.1046/j.1523-1755.1999.00436.x
55. Ringbom A. Complexation in analytical chemistry: A guide for the critical selection of analytical methods based on complexation reactions. In: *Chemical analysis: A Series of Monographs on Analytical Chemistry and its Applications* (16). Elving PJ and Kolthoff IM (Editors), Interscience Publishers, New York, 1963.
56. Gupta A, Yocum R, Holberg W et al. (2009). Fe (III) transfer from soluble ferric pyrophosphate (SFP) to human apotransferrin. *J Am Soc Nephrol*; 20: 668A–669A.
57. Morgan EH. (1977). Iron exchange between transferring molecules mediated by phosphate compounds and other cell metabolites. *Biochim Biophys Acta*, 499:169–177.
58. Cervato, G., Viani, P., Gatti, P., Cazzola, R., & Cestaro, B. (1993). Further studies on the antioxidant role of pyrophosphate in model membranes. *Chemistry and Physics of Lipids*, 66(1-2), 87-92.

59. Sammeta S.M., Vaka S.R., Murthy S.N. (2009). Transcutaneous sampling of ciprofloxacin and 8-methoxypsoralen by electroporation (ETS technique). *Int J Pharm.*;369(1-2):24-9.
60. Walters, K. A. (1990). Surfactants and percutaneous absorption. . In R. C. Scott, R. H. Guy & J. Hadgraft (Eds.), *Predictions of percutaneous penetration* (pp. 148-162). London: IBC Technical Services.
61. Junginger, H. E., Bodde, H. E., & De Haan, F. H. N. (1994). Visualization of drug transport across human skin and the influence of penetration enhancers'. In D. S. Hsieh (Ed.) (Ed.), *Drug permeation enhancement, theory and applications* (1st ed., pp. 59-90). New York, Honk Kong, Basel: Marcel Dekker Inc.
62. Knutson, K., Krill, S. L., Lambert, W. J., & Higuchi, W. I. (1987). Physico-chemical aspects of transdermal permeation. *Journal of Controlled Release*, 6, 59-74.
63. Marjukka Suhonen, T., Bouwstra, J. A., & Urtti, A. (1999). Chemical enhancement of percutaneous absorption in relation to stratum corneum structural alterations. *Journal of Controlled Release: Official Journal of the Controlled Release Society*, 59(2), 149-161.
64. Harrison, J. E., Watkinson, A. C., Green, D. M., Hadgraft, J., & Brain, K. (1996). The relative effect of azone and transcutol on permeant diffusivity and solubility in human stratum corneum. *Pharmaceutical Research*, 13(4), 542-546.
65. Hadgraft, J. (1999). Passive enhancement strategies in topical and transdermal drug delivery. *International Journal of Pharmaceutics*, 184(1), 1-6.
66. Pathan, I. B., & Setty, C. M. (2009). Chemical penetration enhancers for transdermal drug delivery systems. *Tropical Journal of Pharmaceutical Research*, 8(2), 173-179.

67. Singh, P. B., & Choudhury, P. K. (2007). Penetration enhancers for transdermal drug delivery of systemic agents. *Journal of Pharmacy Research*, 6, 44-50.
68. Chowhan, Z. T., & Pritchard, R. (1978). Effect of surfactants on percutaneous absorption of naproxen I: Comparisons of rabbit, rat, and human excised skin. *Journal of Pharmaceutical Sciences*, 67(9), 1272-1274.
69. Aungst, B. J., Rogers, N. J., & Shefter, E. (1986). Enhancement of naloxone penetration through human skin *in vitro* using fatty acids, fatty alcohols, surfactants, sulfoxides and amines. *International Journal of Pharmaceutics*. 33, 225-234.
70. Seki, T., Kawaguchi, T., Sugibayashi, K., Juni, K., & Morimoto, Y. (1989). Percutaneous absorption of azidothymidine in rats. . *International Journal of Pharmaceutics*, 57, 73-75.
71. Bennett, S. L., Barry, B. W., & Woodford, R. (1985). Optimization of bioavailability of topical steroids: Non-occluded penetration enhancers under thermodynamic control. *The Journal of Pharmacy and Pharmacology*, 37(5), 298-304.
72. Songkro, S. (2009). An overview of skin penetration enhancers: Penetration enhancing activity, skin irritation potential and mechanism of action. *Songklanakarin Journal of Science and Technology*, 31(3), 299-321.
73. Guy, R. H., Kalia, Y. N., Delgado-Charro, M. B., Merino, V., Lopez, A., & Marro, D. (2000). Iontophoresis: Electrorepulsion and electroosmosis. *Journal of Controlled Release: Official Journal of the Controlled Release Society*, 64(1-3), 129-132.
74. Higuchi, W. I., Li, S. K., Ghanem, A. H., Zhu, H., & Song, Y. (1999). Mechanistic aspects of iontophoresis in human epidermal membrane. *Journal of Controlled Release: Official Journal of the Controlled Release Society*, 62(1-2), 13-23.

75. Murthy S.N., Vaka S.R.(2009). Iontophoresis: transdermal delivery of iron by iontophoresis. *J Pharma Sci.* 98(8):2670–6.
76. Hirvonen, J., Kontturi, K., Murtomaki, L., Paronen, P., Urtti, A., 1993. Transdermal iontophoresis of sotalol and salicylate —the effect of skin charge and penetration enhancers. *J. Control. Release.*26, 109–117.
77. Hager, D.F., Laubach, M.J., Sharkey, J.W., Siverly, J.R., (1993). In vitro iontophoretic delivery of CQA 206–291— influence of ethanol. *J. Control. Release.* 23, 175–182.
78. Fang, J.Y., Fang, C.L., Huang, Y.B., Tsai, Y.H., (1997). Transdermal iontophoresis of sodium nonivamide acetate. III. Combined effect of pretreatment by penetration enhancers. *Int. J. Pharm.* 149, 183–193.
79. Vemulapalli V, Yang Y, Friden PM, Banga AK. Synergistic effect of iontophoresis and soluble microneedles for transdermal delivery of methotrexate. *J Pharm Pharmacol.* 2008;60(1):27–33.
80. Wu XM, Todo H, Sugibayashi K. (2007). Enhancement of skin permeation of high molecular compounds by a combination of microneedle pretreatment and iontophoresis. *J Control Release.*118(2):189–95.
81. Prausnitz MR. (2004) Microneedles for transdermal drug delivery. *Adv Drug Deliv Rev.*;56(5):581-587.
82. Kalluri H and Banga A.K. (2011).Formation and Closure of Microchannels in Skin Following Microporation, *Pharm Res.* 28:82–94.
83. Gupta J, Gill H.S, Andrews S.N and Prausnitz M.R. (2011). Kinetics of skin resealing after insertion of microneedles in human. *J Control Release.*154: 148–155.

84. CDC. Recommendations to prevent and control iron deficiency in the United States. *MMWR*. 1998;47:1-29.
85. Carley A. (2003). Anemia: when is it iron deficiency? *Pediatr Nurs*.29(2):127-133.
86. Soliman GZA, Mahfouz MH, Emara IA. (2010). Effect of Different Types of Oral Iron Therapy Used for the Treatment of Iron Deficiency Anemia and Their Effects on Some Hormones and Minerals in Anemic Rats. *J Am Sci*.6(6):109-118.
87. Kurtoglu E, Ugur A, Baltaci AK, Undar L. (2003). Effect of iron supplementation on oxidative stress and antioxidant status in iron-deficiency anemia. *Biol Trace Elem Res*.96(1-3):117-123.
88. Sundaram RC, Selvaraj N, Vijayan G, Bobby Z, Hamide A, Rattina Dasse N. (2007). Increased plasma malondialdehyde and fructosamine in iron deficiency anemia: effect of treatment. *Biomed Pharmacother*.61(10):682-685.
89. Knutson MD, Walter PB, Ames BN, Viteri FE. (2000). Both iron deficiency and daily iron supplements increase lipid peroxidation in rats. *J Nutr*.130(3):621-628.
90. Masini A, Trenti T, Caramazza I, Predieri G, Gallesi D, Ceccarelli D. (1994). Dietary iron deficiency in the rat. II. Recovery from energy metabolism derangement of the hepatic tissue by iron therapy. *Biochim Biophys Acta*.1188(1-2):53-57.
91. Uehara M, Chiba H, Mogi H, Suzuki K, Goto S. (1997). Induction of increased phosphatidylcholine hydroperoxide by an iron-deficient diet in rats. *J Nutr Biochem*.8(7):385-391.
92. Sherman AR, Moran PE. (1984). Copper metabolism in iron-deficient maternal and neonatal rats. *J Nutr*.114(2):298-306.

93. Bremner I. Manifestations of copper excess. *Am J Clin Nutr.*(1998) ;67 (5 Suppl):1069S-1073S.
94. Balagopalakrishna C, Manoharan PT, Abugo OO, Rifkind JM. Production of superoxide from hemoglobin-bound oxygen under hypoxic conditions. *Biochemistry.*1996;35(20):6393-6398.
95. Nagababu E, Gulyani S, Earley CJ, Cutler RG, Mattson MP, Rifkind JM. Iron-deficiency anaemia enhances red blood cell oxidative stress. *Free Radic Res.* 2008;42(9):824-829.
96. Forbes A. Iron and parenteral nutrition. *Gastroenterology.* 2009;137(5 Suppl):S47-54.
97. Modepalli N, Jo S, Repka MA & Murthy SN. (2013). Microporation and 'Iron'tophoresis for Treating Iron Deficiency Anemia. *Phar Res.* 30, 889–98.
98. Donnelly RF, Majithiya R, Singh TR, Morrow DI, Garland MJ, Demir YK, Migalska K, Ryan E, Gillen D, Scott CJ and Woolfson AD. (2011). Design, optimization and characterization of polymeric microneedle arrays prepared by a novel laser-based micromolding technique, *Pharm.Res.* 28: 41-57.
99. Weintraub, L. R., Demis, D. J., conrad, M. E., & Crosby, W. H. (1965). Iron excretion by the skin. Selective localization of iron-59 in epithelial cells. *The American Journal of Pathology*, 46, 121-127.
100. Beamish, M. R., & Jacobs, A. (1968). The measurement of iron clearance from the skin. *British Journal of Haematology*, 15(3), 231-235.
101. Beamish, M. R., Jobbins, K., & Cavill, I. (1971). The cellular distribution of transferrin-bound iron in the skin. *The British Journal of Dermatology*, 85(1), 49-51.
102. Cavill, I., & Jacobs, A. (1970). Skin clearance of iron in normal and iron deficient subjects. *The British Journal of Dermatology*, 82(2), 152-156.

103. Cavill, I., & Jacobs, A. (1971). Iron kinetics in the skin. *British Journal of Haematology*, 20(2), 145-153.
104. Cavill, I., Jacobs, A., Beamish, M., & Owen, G. (1969). Iron turnover in the skin. *Nature*, 222(5189), 167-168.
105. Pollycove, M. (1966). Iron metabolism and kinetics. *Seminars in Hematology*, 3(4), 235-298.
106. Wasserman L.R., Sharney L, Gevirtz N.R., Schwartz L., weintraub L.R., Tendler D., Dumont A.E., Dreiling D. and witte M. (1965). Studies in iron kinetics. I. Intrepretation of ferrokinetic data in man. *J Mt Sinai Hosp.*, 32, 262.
107. Berridge, M. V., & Tan, A. S. (1993). Characterization of the cellular reduction of 3-(4,5-dimethylthiazol-2-yl)-2,5-diphenyltetrazolium bromide (MTT): Subcellular localization, substrate dependence, and involvement of mitochondrial electron transport in MTT reduction. *Archives of Biochemistry and Biophysics*, 303(2), 474-482. doi:10.1006/abbi.1993.1311
108. Wilson, J. R., Mills, J. G., Prather, I. D., & Dimitrijevič, S. D. (2005). A toxicity index of skin and wound cleansers used on in vitro fibroblasts and keratinocytes. *Advances in Skin & Wound Care*, 18(7), 373-378.
109. Henzler, T., & Steudle, E. (2000). Transport and metabolic degradation of hydrogen peroxide in chara corallina: Model calculations and measurements with the pressure probe suggest transport of H₂O₂ across water channels. *Journal of Experimental Botany*, 51(353), 2053-2066.
110. Manna, S. K., Sarkar, S., Barr, J., Wise, K., Barrera, E. V., Jejelowo, O., Ramesh, G. T. (2005). Single-walled carbon nanotube induces oxidative stress and activates nuclear

- transcription factor-kappaB in human keratinocytes. *Nano Letters*, 5(9), 1676-1684.
doi:10.1021/nl0507966
111. Shvedova, A. A., Tyurina, J. Y., Kawai, K., Tyurin, V. A., Kommineni, C., Castranova, V., Kagan, V. E. (2002). Selective peroxidation and externalization of phosphatidylserine in normal human epidermal keratinocytes during oxidative stress induced by cumene hydroperoxide. *The Journal of Investigative Dermatology*, 118(6), 1008-1018. doi:10.1046/j.1523-1747.2002.01759.x
112. Barker, J. N., Jones, M. L., Mitra, R. S., Crockett-Torabe, E., Fantone, J. C., Kunkel, S. L., Nickoloff, B. J. (1991). Modulation of keratinocyte-derived interleukin-8 which is chemotactic for neutrophils and T lymphocytes. *The American Journal of Pathology*, 139(4), 869-876.
113. Auerbach M, Pappadakis JA, Bahrain H, Auerbach SA, Ballard H and Dahl NV. (2011). Safety and efficacy of rapidly administered (one hour) one gram of low molecular weight iron dextran (INFeD) for the treatment of iron deficient anemia. *Am J Hematol*. 86 (10) 860-62.
114. Barton JC, Baron EH, Bertoli LF, et al. (2000). Intravenous iron dextran therapy in patients with iron deficiency and normal renal function who failed to response to or did not tolerate oral iron supplementation. *Am J Med* 109: 27–32.
115. Auerbach M and Ballard H. (2010). Clinical use of intravenous iron: administration, efficacy, and safety. *Hematology Am Soc Hematol Educ Program*. 2010:338-47
116. Danielson BG. (2004). Structure, chemistry, and pharmacokinetics of intravenous iron agents. *J Am Soc Nephrol*. 15(Suppl 2):S93–S98.
117. Report on Carcinogens. Iron Dextran Complex. 2011. Twelfth Edition. 246-247.

118. David LB and James JP. 1999. Toxicity of parenteral iron dextran therapy. *Kidney Int.* 55(69):S-119-S-124.
119. Auerbach M, Witt D, Toler W, Fierstein M, Lerner RG and Ballard H. (1988). Clinical use of the total dose iv infusion of iron dextran. *J Lab Clin Med.* 111:566-570.
120. Blake DR, Lunec J, Ahern M, Ring EF, Bradfield J and Gutteridge IM. (1985). Effect of intravenous iron dextran on rheumatoid synovitis. *Ann Rheum Dis.* 44:183-188.
121. Lawrence AH. (2009). Transdermal Pharmaceuticals: Unique Aspects of Clinical Development. *Transdermal Magazine.* 1(1) 14-18.
122. Potts RO and Guy RH. (1992). Predicting Skin Permeability. *Pharm Res.* 9(5):663-669.
123. Coulman SA, Barrow D, Anstey A, Gateley C, Morrissey A, Wilke N, Allender C, Brain K and Birchall JC. 2006. Minimally invasive cutaneous delivery of macromolecules and plasmid DNA via microneedles. *Curr Drug Deliv.* 3(1):65-75.
124. Sachdeva V and Banga AK. (2011). Microneedles and their applications. *Recent Pat Drug Deliv Formul.* 5(2):95-132.
125. Sammeta SM, Vaka SRK and Murthy SN. (2010). Transcutaneous electroporation mediated delivery of doxepin-HPCD compels: A sustained release approach for treatment of postherpetic neuralgia. *J Cont Rel.* 142:361-367.
126. Prausnitz MR. (1997). Transdermal delivery of macromolecules: Recent advances by modification of skin's barrier properties. *Therapeutic protein and peptide formulation and delivery.* 675:124-153.
127. Prow TW, Grice JE, Linn LL, Faye R, Butler M, Becker W, Wurm EM, Yoong C, Robertson TA, Soyer HP, Roberts MS. (2011). Nanoparticles and microparticle for skin drug delivery. *Adv Drug Deliv Rev.* 63(6):470-91.

128. Cappel MJ and Kreuter J. (1991). Effect of nanoparticles on transdermal drug delivery. *J Microencapsul.* 8(3):369-74.
129. Sonavane G, Tomoda K, Sano A, Oshima H, Terada H and Makino K. (2008). *In vitro* permeation of gold nanoparticles through rat skin and rat intestine: Effect of particle size. *Colloids Surf B Biointerfaces.* 65(1):1-10.
130. Liu W, Yang X, Zhu Y, Chem H and Xu H. (2005). Nanostructured lipid carriers as vehicles for transdermal iontophoretic drug delivery. *Conf Proc IEEE Eng Med Biol Soc.* 2:1236-9.
131. Keishiro T, Hiroto T, Kenichi S, Toshio I, Hiroshi T and Kimiko M. 2011. Enhanced transdermal delivery of indomethacin-loaded PLGA nanoparticles by iontophoresis. *Colloids Surf B Biointerfaces.* 88(2):706-10.
132. Martanto W, Davis SP, Nicholas RH, Wang J, Gill HS and Prausnitz MR. (2004). Transdermal delivery of insulin using microneedles *in vivo*. *Pharm Res.* 21:947-52.
133. Ding Z, Verbaan FH, Bivas BM, Bungener L, Huckriede A, Van den Berg DJ, Kersten G and Bouwstra JA. (2009). Microneedle arrays for the transcutaneous immunization of diphtheria and influenza in BALB/c mice. *J Contr Rel.* 136:71-8.
134. Donnelly RF, Morrow DI, McCarron PA, Woolfson AD, Morrissey A, Juzenas P, Juzeniene A, Iani V, McCarthy HO and Moan J. (2008). Microneedle mediated intradermal delivery of 5-aminolevulinic acid: Potential for enhanced topical photodynamic therapy. *J Contr Rel.* 129:154-62.
135. Badran MM, Kuntsche J, Fahr A. (2009). Skin penetration enhancement by a microneedle device (Dermaroller[®]) *in vitro*: dependency on needle size and applied formulation. *Eur J Pharm Sci.* 36: 511-23.

136. Kaushik S, Hord A.H, Denson D.D, Mcallister D.V, Smitra S, Allen M.G, and Prausnitz, M.R. (2001). Lack of pain associated with microfabricated microneedles. *Anesth. Analg.* 92:502-504.
137. Chang RI, Moon SK, Lee HB, Han KI, John MR and Gilson K. (2007). The effect of molecular weight of drugs on transdermal delivery system using microneedle device. *Key Eng Mater.* 342(3):945-8.
138. Kohli AK and Alpar HO. (2004). Potential use of nanoparticles for transcutaneous vaccine delivery: effect of particle size and charge. *Int. J. Pharm.* 275:13–17.
139. Provan D. (1999). Mechanisms and management of iron deficiency anemia. *Br J Haematol.* 105(Supplement 1):19-26
140. Dheerendra KR, Harold LM, Jeong HL, Rajiv S, Karl DN, Ramesh K and Zbylut JT. (2001). Chronic peritoneal dialysis in iron-deficient rats with solutions containing iron dextran. *Kidney International.* 59: 764-773.
141. Henderson PA and Hillman RS. (1969). Characteristics of Iron Dextran Utilization in Man. *Blood.* 34: 357-375.

VITA

Naresh Modepalli was born on July 18, 1985 in Amaravathi, AP, India. He completed his B.Pharmacy in 2007 from KVSR Siddhartha College of Pharmaceutical Sciences, Acharya Nagarjuna University, Guntur, India and M.S. in Pharmaceutical chemistry in 2009 from Fairleigh Dickinson University, Madison, NJ. Modepalli joined Department of Pharmaceutics and drug delivery, The University of Mississippi as a graduate student in Spring 2010. Modepalli has published 3 research papers and 2 review articles in peer reviewed international journals and presented more than 15 research posters at scientific conferences. He received CORE-NPN Fellowship in 2010 and Graduate Student Council Research Grant in 2012. Modepalli was inducted into Phi Kappa Phi scholastic honor society in 2011. He was also inducted into Rho Chi Honor society in 2012 and Gamma Beta Phi honor society in 2014. He also received Travelship award for AAPS-SRDG meeting in 2013 and best research poster award at American Chemical Society-OleMiss section meeting in 2013. Modepalli was awarded with outstanding oral presentation award at AAPS-SRDG meeting in 2013. He was Chair-Elect of AAPS-UM Student chapter during 2012 and served as Chair in 2013 during which he played a key role in the organizing several guest lectures and talks from industry and academic experts in pharmaceutics. Modepalli served in several student organizations in different roles at The University of Mississippi. Modepalli is also a recipient of dissertation fellowship from The University of Mississippi. Modepalli is a member of AAPS Dermatopharmaceutics Focus Group and Formulation Design and Development section.